Self-assembling Peptide for HIV-1 Vaccine Design

by

Yong Ding

A thesis
presented to the University of Waterloo
in fulfillment of the
thesis requirement of the degree of
Doctor of Philosophy
in
Chemical Engineering

Waterloo, Ontario, Canada, 2015

Author's Declaration

I hereby declare that I am the sole author of this thesis. This is a true copy of the thesis, including any required final revisions, as accepted by my examiners. I understand that my thesis may be made electronically available to the public.

Abstract

Human immunodeficiency virus-1 (HIV-1) is a worldwide epidemic, which cannot be eliminated by any current therapeutics, even with highly active antiretroviral therapy, which only can control virus replication. A safe and effective vaccine against HIV-1 that can elicit both potent humoral and cellular responses has been considered a best solution to prevent the infection or to reduce the viral load. However, despite the fact that over 250 clinical trials have been conducted based on different concepts, no vaccine has been successfully developed. The extraordinary diversity of HIV-1, the capability of the virus to escape from the adaptive immunity, the difficulty in inducing broadly neutralizing antibodies, and the lack of clear immune correlates of protection represent the major challenges obstructing the development of HIV-1 vaccines. Designing a peptide-based vaccine that stimulates cytotoxic T lymphocytes (CTLs) specifically against the highly conserved epitopes in HIV-1 has been considered a promising strategy. This can provide two theoretical advantages: maximizing the immunological coverage and minimizing the viral escape from recognition of T cells. However, owning to the short sequence (normally 8-10 amino acids for CTL epitopes), these conserved epitopes are weakly immunogenic, requiring potent adjuvants to boost the efficiency. Some novel strategies have been reported to achieve an efficient adjuvant without causing any side effect. Among them, nanoparticle based delivery systems that can provide targeted delivery to immune cells and/or self-adjuvant effect, are emerging as a promising approach.

In this thesis, we present a self-assembling peptide based delivery platform efficiently integrating antigenic peptides and immune potentiators in the formulation of a

nanoparticle vaccine, and evaluate the immunogenicity in vitro and in vivo. Three parts are involved in this work: (1) feasibility study of the delivery of HIV-1 CTL epitope with the self-assembling peptide EAK16-II (sequence: AEAEAKAKAEAEAKAK) and the cross-presentation efficiency by dendritic cells (DCs); (2) co-delivery of an antigenic peptide and a toll like receptor (TLR) agonist within one nanoparticle to target and maturate DCs, leading to enhanced CTL response; (3) formulating a prophylactic peptide vaccine against HIV-1 by the combination of CD4 epitope-conjugated EAK16-II, CD8 epitope-conjugated EAK16-II, and a TLR agonist R848, which was subsequently assessed the immunogenicity in the transgenic mice.

The peptide EAK16-II could self-assemble into nanofibers, which were stable in the acidic environment and in the presence of proteases. We hypothesized that by directly conjugating HIV-1 CD8 epitope with EAK16-II, the fibrillar structures of the conjugate would enhance the stability of epitope and thus improve the immunogenicity. To verify this, the CD8 epitope SL9 was conjugated with EAK16-II to obtain the epitope-loading peptide SL9-EAK16-II. Physicochemical characterizations revealed SL9-EAK16-II spontaneously assembled to short nanofibers in PBS, which were more stable in serum or oligopeptidase than unstructured SL9. Ex-vivo generated DCs that were pulsed with SL9-EAK16-II and activated by maturation cytokines, stimulated more poly-functional CD8+ T cells. This augment was explained by the evidence that SL9-EAK16-II was degraded more slowly than SL9 within DCs, therefore prolonging the stimulation to CD8 T cells. Moreover, the results from confocal microscopy suggested the cytosolic pathway for the cross-presentation of SL9-EAK16-II.

However, SL9-EAK16-II itself failed to maturate DCs after internalization, which might cause antigen tolerance. To avoid the induction of tolerance and further enhance the antigenicity of epitope SL9, TLR agonist R837 or R848 was incorporated into the nanofiber formulation. The data from fluorescence spectra and calorimetric titration suggested the co-assembly between SL9-loaded nanofibers and TLR agonist was mainly driven by hydrogen bonding and hydrophobic interactions. The SL9-EAK16-II/R848 co-assemblies strongly facilitated the activation of DCs, and stimulated significantly more epitope specific CTLs when assessed in the form of DC based vaccine.

The in vitro studies implied the potential of the self-assembling peptide EAK16-II as a nanocarrier in the formulation of vaccine. We further determined the applicability of this formulation in vivo. Since the activation of CD4+T cells plays a critical role in the generation of functional memory CTLs, we incorporated an additional CD4 epitope TL13 into the vaccine formulation, via conjugating with EAK16-II. The new formulation of antigen was characterized as nanofibers with average size of approximately 220 nm. The transgenic mice that were subcutaneously injected with these nanofibers produced as much as 1 fold increase in frequencies of SL9 specific CTLs, when compared with the mice vaccinated with either the mixture of epitopes and R848, or R848 alone. Moreover, almost 90% of the SL9 specific CTLs primed by the nanofibers were central memory CD8+ T cells (CD44+, CD62L+), which was the hallmark of the acquired immune response. The in-vivo study suggested not only enhanced magnitude, but also higher quality of T cell response was induced by the nanoparticle-based vaccine. Our findings demonstrated the self-assembling peptide had considerable promise as a delivery platform to integrate the principal components for cellular response-focusing vaccines.

Acknowledgements

I would firstly express appreciate to my supervisor, Dr. Pu Chen, who has provided me this invaluable opportunity to join this innovative research in the cutting-edge area. Without his infinite support, valuable advisory, and critical guidance during my study in the lab, this work could not be accomplished.

Next, I would like to thank M.D. Mario Ostrowski, at clinical science division in University of Toronto. He provides not only expert advisory in immunology and HIV-1 vaccine design, but also perfect collaborations on the *in vitro* and *in vivo* studies. The deep appreciate is extended to my direct collaborator M.D. Jun Liu, who is knowledgeable in vaccine design and excellent in molecular biotechnology. He gives me huge support in the experiment design and teaches me the techniques in the research, such as dendritic cell culture, intracellular staining, and flow cytometry. In addition, he helped finish the animal work.

I am also thankful to my advisory committee members who monitored my work and took effort in reading and providing critical advice on this thesis: Dr. William A. Anderson, Dr. Frank Gu from Chemical Engineering department, Dr. Shawn Wettig from School of Pharmacy.

My acknowledgements are extended to many individuals who helped me in experimental work or daily life during PhD study. Thanks to Dale Weber and Mishi Savulescu for their help with TEM at biology department. Appreciate Feng Xu at Toronto general hospital for his help and training in confocal microscopy. I would like to give my special thanks to

my current and previous group members; they provide me with a happy and friendly working environment. I got huge help and valuable advice from the anticancer drug delivery group members, Dr. Sadatmousavi Parisa, Dr. Mohammad Ali Sheikholeslam, Dr. Sheng Lu, Lei Zhang, Mohammad Mohammadi, as well as siRNA delivery group members, Dr. Mousa Jafari, Dr. Dafeng Chu, Dr. Wen Xu, Dr. Baolin Chen, Dr. Ran Pan. Deeply appreciate all of you.

Lastly, and also most importantly, I would like to thank my friends and families for give me infinite support and enormous encouragements. My deep love to my parents, my wife Lu Hong and my newborn daughter Chris.

Table of Contents

List of Figures

Appendix:

List of Tables

List of Abbreviations

Acronym	Full name
5-FAM	5-carboxyfluorescein
AAP	amino acid pairing
ADSA-P	Axisymmetric drop shape analysis-profile
AFM	Atomic Force Microscopy
APCs	antigen presenting cells
AuNPs	gold nanoparticles
BMDCs	bone marrow derived DCs
CD	Circular Dichroism
CTLs	cytotoxic T lymphocytes
DCs	dendritic cells
DLS	dynamic light scattering
DMF	N, N-dimethylformamide
ER	endoplasmic reticulum
FBS	fetal bovine serum
HAAT	highly active antiretroviral therapy
HBcAg	hepatitis B core antigen
HIV-1	Human immunodeficiency virus-1
IFN	Interferon
IL	Interleukin
ISCOMS	immunostimulating complexes
ITC	Isothermal Titration Calorimetry
LPS	lipopolysaccharide
mDCs	myeloid DCs
MDDCs	monocyte-derived dendritic cells
MHC	major histocompatibility complex
MPLA	monophospholipid A

MyD88	myeloid differentiation primary response protein 88
PAMPs	pathogen associated molecular patterns
PCL	poly (ε-caprolactone)
pDCs	plasmacytoid DCs
PEG	poly (ethylene glycol)
PGA	poly (glycolic acid)
PLA	poly (lactic acid)
PLGA	poly (lactide-co-glycolide)
PMBCs	peripheral blood mononuclear cells
PRR	pattern recognition receptor
SIV	simian immunodeficiency virus
TCA	trichloroacetic acid
TEM	Transmission Electron Microscopy
Th	T helper
TIR	Toll/interleukin-1 receptor
TLR	toll like receptor
TOP	thimet oligopeptidase
TRIF	TIR-domain-containing adapter protein-inducing IFN-β
VLPs	virus like particles
w/o/w	water-in-oil-in-water

Chapter 1 Introduction

1.1 Overview

Since first discovered in 1983, human immunodeficiency virus (HIV) has become a global pandemic, threatening the lives of human beings. This type of retrovirus can infect several human cells, especially some important immune cells, such as CD4+ T helper (Th) cells, or dendritic cells (DCs), and consequently destroy the immune system. As shown in Fig.1-1, it is believed that the infection process starts from the binding of glycoprotein 120 (gp120) on the surface of HIV, with CD4 protein expressed on Th cell, which is followed by the fusing of virus and the Th cell membrane, allowing the capsid of the virus entering the cells. Inside the Th cell, the capsid releases the genetic material-RNA and uses reverse transcription to convert RNA to DNA, which is further integrated into DNA sequence of the host Th cell. Then HIV can use the host cell's machinery to synthesize viral proteins as the building blocks to assemble into more viruses. These newly formed viruses leave the host cell through a "budding" process, and then maturate. Targeting the different stages during the virus life cycle, various inhibitors have been developed, the combination of which can efficiently suppress the virus replication and reduce the viral load to an undetectable level. However, this so-called "highly active antiretroviral therapy (HAAT)" strategy cannot eliminate the virus. Moreover, latent HIV-1 reservoir established during acute infection in memory CD4+ T cells has a remarkably long half-life and is resistant to HAAT, resulting in the viral rebound in HIV-1 infected patients who even receive HAAT treatment[1]. A safe and effective vaccine is

undoubtedly the best solution to eradicate the virus and end HIV-1 pandemic. Ideally, such a vaccine should elicit humoral response to produce neutralizing antibodies for preventing infection by HIV-1, as well as potent cellular response in order to eliminate the formation of latent viral reservoir[2]. Since the first phase-I human trial of AIDS vaccine started in 1986, more than 250 clinical trials have been carried out, with only three vaccine concepts completing clinical efficacy studies, including monomeric HIV-1 Env gp120 protein[3], RV144 (a recombinant canarypox vector prime, gp120 protein boost vaccine regimen), and "STEP" trial (a trivalent mixture of rAd5 vectors expressing HIV-1 clade B protein Gag, Pol, and Nef)[4]. However, currently no ideal vaccine that can offer the clinical benefit for the protective purpose has been achieved. Thus far, the development of an HIV-1 vaccine remains elusive.

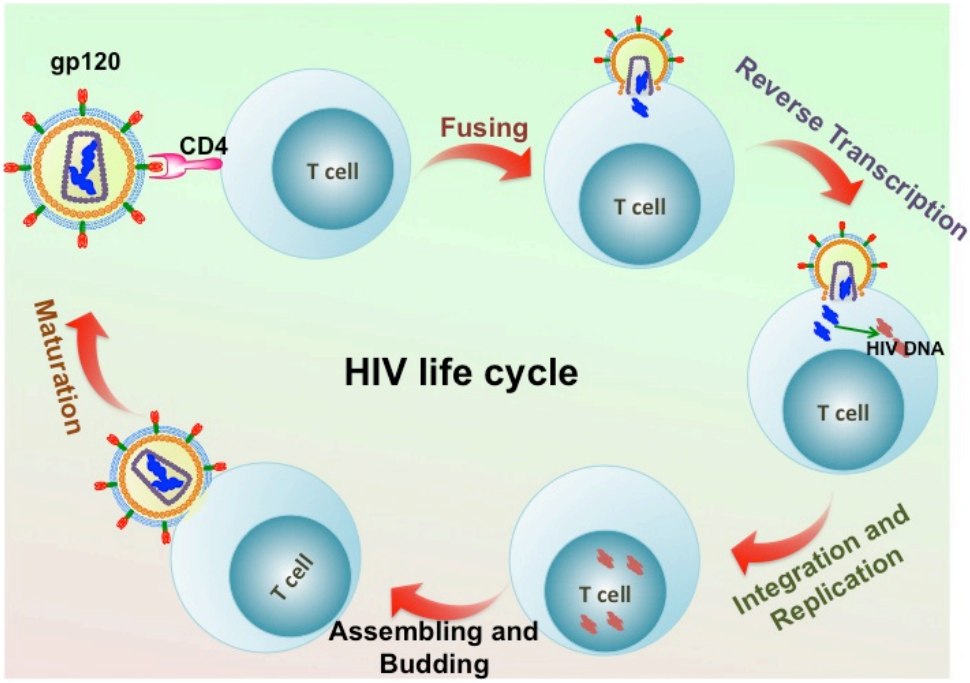

Figure 1-1 Schematic illustration of HIV life cycle. The infection against CD4+ T cell includes: 1) Binding between gp120 and CD4; 2) Fusing; 3) Reverse transcription; 4) Integration and replication; 5) Assembling and budding; 6) Maturation.

Learning from the past clinical trials, several key challenges in the design of HIV-1 vaccine are summarized, including the extensive viral clade and sequence diversity, early establishment of latent viral reservoirs, unclear immune correlates of protection (what sort of immune response the vaccine should stimulate), and lack of proper animal model, *etc*.[5] The main obstacle is ascribed to the extraordinary HIV-1 protein diversity. Owning to the "error-prone" property of HIV reverse transcriptase, the virus populations that constantly evolve could be generated within the infected individuals. This extraordinary mutability of virus results in the ease of escape from the recognition by the immune system. Broadly neutralizing antibodies that are found in ~20% HIV-1 positive long-term non-progressors, potentially provide complete protection against infection, however, no candidate immunogen can do this so far. The conserved regions to which these antibodies are directed, are effectively shielded or only formed after Env protein of virus binding with CD4, thus requiring extensive somatic hypermutaion of antibody gene[6].

The failure of an antibody-eliciting vaccine against HIV-1 has promoted a shift in the focus of the vaccine development. The vaccine that stimulates HIV-1 specific cytotoxic T lymphocytes (CTLs) response has been considered as a possible alternative. CTLs cannot eliminate the virus directly, but rather it can control the infected cells by recognizing the HIV epitope/ MHC (major histocompatibility complex) class I on the surface of cells via their T cell receptor and subsequently destroying the infected cells. Recent studies in which a rhesus monkey cytomegalovirus vector with recombinant SIV (simian immunodeficiency virus) genes as the immunogen induced potent effector memory CTL response and cleared the virus soon after the peak of acute infection[7], demonstrated the feasibility of this strategy in the control of HIV-1.

However, a major difference between SIV and HIV is the higher variability of HIV proteins, as highlighted above. For CTL epitopes, a difference of a single amino acid in an sequence (~10% variance) results in a 30-50% chance of negating recognition by T cells[8]. To overcome this hurdle, focusing the CTL response on the highly conserved epitopes identified in very large patient cohorts is suggested as a promising approach[8]. This strategy offers two theoretical virtues, including maximizing immunologic coverage of HIV-1 diversity, and minimizing the viral escape from recognition by CTLs. Furthermore, compared with the traditional vaccines utilizing killed, inactivated or attenuated microorganisms as the immunogen, antigenic peptide based vaccines provide several advantages, particularly with regards to safety and ease of production.

Nevertheless, owning to the small size of these conserved CTL epitopes (normally comprised of 8-10 amino acids), they are poorly immunogenic. Additionally, short epitopes can be directly loaded onto MHC molecules, also on non-professional antigen presenting cells (APCs), causing the induction of immune tolerance. Thus, to elicit a potent and durable antigen specific cellular response, an efficient adjuvant is normally necessary for formulating a peptide-based vaccine. The adjuvant effect can be divided into two principle components, including delivery system and immune potentiator[9]. The delivery system can provide the antigenic peptides with the protection against proteolytic degradation, and deliver the cargos into the targeted cells, such as DCs. Meanwhile, the immune potentiator can activate innate immune cells to provide pro-inflammatory environment for the induction of acquired immune response. However, currently only few adjuvants are licensed for the use in humans, MF59 (an oil-in-water adjuvant) and aluminum salt in Europe, while only aluminum salt in US. In addition, most adjuvants

including alum or Incomplete Freund's Adjuvant (IFA) have been developed for the induction of humoral response, but are weak at eliciting T cell mediated immune response. Moreover, many adjuvants use structurally heterogeneous materials, which make it challenging to understand their mechanisms[10]. Thus, the development of a simple, yet potent and safe adjuvant is of great importance.

Nanoparticles, such as liposomes[11,12], polymeric nanoparticles[13,14], and virus-like particles[15,16] have been intensively investigated as delivery platforms and/or immune potentiators in formulating subunit vaccines. In addition, self-assembling peptides, which have been widely developed for application in regenerative medicine[17], tissue engineering[18], also attract considerable attention for vaccine design, owning to their biocompatibility, safety, ease of manufacturing, and control over size, shape and surface properties. Moreover, when conjugating with an exogenous B cell epitope, self-assembling peptides are reported to act as self-adjuvant nano-carriers, enhancing the antigen specific humoral response[10,19]. Compared with other biomaterials, self-assembling peptide based delivery system can provide a number of advantages. First, any identified epitope can be easily conjugated with the self-assembling sequence using solid phase peptide synthesis. And the conjugation by the peptide bond can also provide higher antigen loading efficiency and stability, compared to other loading strategies, such as encapsulation, simply mixing, or surface absorption. Moreover, the nanoscale vaccine formulations can be directly produced from the self-assembling process, without using organic reagents or applying complex preparation procedures. However, whether self-assembling peptide could stimulate innate immunity and be applied for enhancing the

immunogenicity of T cell epitope, especially HIV-1 protein derived epitope remains unclear.

Thus, in this work we investigated the potential of self-assembling peptide based delivery system for the formulation of CTL response-stimulating vaccine towards HIV-1. EAK16-II, a typical ionic-complementary self-assembled peptide, which is resistant to acidic environments and/or the presence of proteases, as well as induced no detectable immune response in animal[20], was conjugated with an HIV-1 CTL epitope SL9. Physicochemical characterizations were carried out to study the self-assembly process of the epitope-bearing peptide SL9-EAK16-II, including the critical assembling concentration (CAC), morphology and hydrodynamic size, as well as the stability of the particles in physiological environment. The cross-presentation efficiency of the conjugating peptide was then evaluated in the form of DC-based vaccine *in-vitro* using HIV-1 specific CTL recall response as readout. In the next step, the feasibility of the self-assembling peptide for co-delivery of epitope and TLR (toll-like receptor) agonist was further assessed. Two hydrophobic small organic molecules Resiquimod (R848) and Imiquimod (R837), which can activate TLR7/8, were incorporated into the SL9-EAK16-II system to enhance the maturation activity towards DCs. Afterwards, an integrated formulation of nanoparticle-based vaccine consisting of one CD4 epitope, one CD8 epitope, and a TLR agonist (R848), was prepared and administrated in transgenic mice to determine the antigen specific CTL response by prime-boost strategy. The mice vaccinated with the nano-formed vaccine generated significantly more antigen specific central memory CTLs. According to the results reported in this work, the self-assembling peptide was suggested

as an efficient matrix for delivering both antigenic peptide and immune potentiator (TLR agonist) to potently induce HIV-1 specific memory CTLs.

1.2 Research objectives

The goal of this research is to develop an efficient and safe delivery platform for formulating peptide vaccine to elicit potent HIV-1 specific CTL response. To achieve this, direct conjugation and non-covalent encapsulation have been applied to incorporate the antigen and the immune potentiator within the formulation respectively, to enhance the immunogenicity of CTL epitope *in vitro* and *in vivo*. The specific objectives of this thesis are listed as following:

1) Synthesis and characterization of epitope-bearing self-assembling peptides to protect the degradation of epitope from extra/intra-cellular proteases, as well as determining the cross-presentation efficiency by DCs *in-vitro*.
2) Incorporation of the TLR agonist within epitope-loaded nanoparticles, and evaluation of antigen specific CTL response in the form of DC-based vaccine *in vitro*.
3) Formulating an efficient nanoparticle based vaccine consisting of CD4+ and CD8+ T cell epitopes as well as the TLR7/8 agonist to generate more HIV-1 specific memory CTLs *in vivo*.

1.3 Outline of the thesis

The thesis consists of six chapters, of which the scopes are listed in following:

Chapter 1 introduces the overview of the thesis, including HIV infection mechanism, the development of HIV-1 vaccines with the challenges and new strategies, the importance and potential of CTL response in the design of HIV-1 vaccines, and the feasibility of the self-assembling peptides-based nanoparticles as delivery platforms in the formulation of epitope-based vaccines. Additionally, the objectives and scopes of the thesis are given as well.

Chapter 2 provides a review on peptide based vaccines, in which TLR agonists based adjuvants, the existing nanoparticle based delivery system, as well as the cross-presentation of exogenously administrated peptides by DCs are included. The rational design principle for the self-assembling peptides and their biological applications, particularly in drug delivery and vaccine design are also reviewed.

Chapter 3 focuses on the assessment of the cross-presentation efficiency of HIV-1 CTL epitope-loaded self-assembling peptide by DCs *in vitro*. Physicochemical characterizations were conducted, and the stabilities of the peptides with the presence of serum or oligopeptidase were determined with HPLC. Flow cytometry and confocal microscopy were employed to study the persistence and intracellular distributions of the peptides within DCs.

Driven by the fact that the epitope-loaded self-assembling peptide did not show self-adjuvant capacity, enhancing the immunogenicity, in Chapter 4, the TLR7/8 agonists were incorporated into nanoparticles, via non-covalent interactions. The results from fluorescence spectra and calorimetric titration demonstrated the co-existence of the antigen and the TLR agonist within the nanostructures, which enhanced the DCs

maturation, as well as stimulated more antigen-specific poly-functional CD8+ T cells *in vitro.*

In Chapter 5, to study the immunogenicity of the peptide/agonist co-assemblies *in vivo*, a CD4+ T cell epitope was conjugated with the self-assembling peptide as the same method we did for the CD8 + T cell epitope. The morphology of the tripartite nanovaccine was characterized as cross-linked nanofibers, of which the immunogenicity was assessed in HLA-A2 transgenic mice. From the *in vivo* results, the mice subcutaneously administrated with the nanovaccine produced significantly more HIV-1 specific central memory CTLs.

Chapter 6 presents the conclusions of the studies in the thesis, and the recommendations for the future work.

Chapter 2 Literature review

2.1 Peptide vaccine

Vaccination has been considered as one of the most successful innovations for public health in preventing and eradicating the danger from various diseases, such as smallpox and poliomyelitis. The general principle for a traditional prophylactic vaccine is to provoke a response from the immune system (humoral and cellular immunity) and create a memory within the immune system so that the next exposure to the disease agent will be eliminated by primed immune response. In the last two decades, with the knowledge about the human immune system better established, the therapeutic vaccine that cures chronic infectious patients by inducing or augmenting antibody and/or cellular response is also intensively studied. Traditionally, vaccines are developed consisting of dead or inactivated pathogenic microorganisms, or purified products derived from the microorganisms as the immunogens. These vaccines can induce both humoral and cellular immune responses potently, usually requiring only one boost[21], however, several drawbacks limit the development and application of these vaccines, such as a serious risk of reverting back to the virulent form, the possibility of inducing an autoimmune response, the intrinsic instability making them hard to administrate, and the complicated compositions perplexing the mechanism of the induced immune response[22]. Moreover, many pathogens are difficult to culture in *vitro*, making the large-scaled manufacturing impractical[23]. Therefore, the new generations of vaccine, which only adopt the specific antigenic fractions from pathogens to stimulate appropriate immune response have been placed great expectation. So far, protein-, DNA-, or peptide-based subunit vaccines have

been intensively examined either in pre-clinical or clinical stages. Benefiting from the removal of the unnecessary components, these subunit vaccines offer higher stability and safety. Among them, the most precise selection of antigen can be achieved from peptide-based vaccine, which is the subject of this project.

Peptide-based vaccines usually incorporate a pool of short or long peptides, which are termed as epitopes (antigenic determinant parts of antigens that can be recognized by immune system, especially antibodies, B cells or T cells), to induce an adaptive immune response, but avoiding allergenic and / or reactogenic response. With the rapid development of solid phase peptide synthesis, peptide-based vaccines can be easily and economically produced in large scale, with high purity and guaranteed quantity. Additionally, peptide vaccines can be designed to induce a broad-spectrum immune response against multiple serological variants or strains of a pathogen by formulating various non-continued epitopes, or epitopes highly conserved in different strains[24]. For example, a major hurdle in the development of HIV-1 vaccines is the high variability of HIV-1, which might be overcome by focusing CD8+ T cell response on multiple conserved epitopes derived from HIV-1 proteins[8]. However, because of the relatively small size, the epitopes are easily degraded in body fluid, leading to weak immunogenicity when they are administrated alone, and therefore require adjuvants.

Broadly, adjuvants could be defined as either immune potentiators that can activate innate immune cells or delivery systems that are able to stabilize antigens and increase their cellular uptake, trafficking and presentation. To date, many adjuvant strategies have been developed for peptide-based immunotherapies, such as particulate[25,26], oil emulsions[27], toll-like receptor (TLR) agonists[28], immunostimulating complexes (ISCOMS)[29], and

other biologically degradable materials[13]. However, currently very few vaccine adjuvants are licensed for use in humans, MF 59 and aluminum salts in Europe, while only aluminum salts in US. In addition, most adjuvants, including alum, are optimized for the effective induction of high antibody serum titers (humoral response), but weak at eliciting a cellular, T cell mediated immune response, which is essential for eliminating intracellular pathogen associated diseases, such as HIV-1, malaria, cancer, *etc*. Therefore, the development of more efficient and safer adjuvants and delivery systems eliciting both humoral and cellular responses is of primary importance.

2.1.1 TLR (Toll-like receptor) agonists as adjuvant

An adjuvant is broadly defined as anything that can increase the immunogenicity of antigens, which functions though a number of ways, including providing an antigen depot for increased uptake by DCs, or shielding peptide from degradation. The TLR agonist is a kind of emerging adjuvant that offers higher safety and efficiency. TLRs are a family of pattern recognition receptors (PRRs) that play a critical role in activating both innate and adaptive immune response. They are mainly expressed on innate immune cells, such as B cells, macrophages, or dendritic cells (DCs). To date, in humans there have been 10 TLRs identified, which locate in different compartments of cells: TLR1, 2, 4, 5, 6 are mainly expressed on the cell surface, while TLR3, 7, 8, 9 are located in the endosomal compartments with their ligand-binding domains facing the lumen of the vesicle[30]. From the structure, they are type I membrane proteins, consisting of a leucine-rich ectodomain, and a cytoplasmic domain, termed as Toll/interleukin-1 receptor (TIR) domain. Each TLR can recognize particular structures, usually referred to as "PAMPs" (pathogen associated molecular patterns) in bacteria, virus, fungi and other pathogens. Natural

ligands binding to TLRs 1-9 have been identified, but not to TLR10. For example, TLR2 forms heterodimers with TLR1 or TLR6 to recognize multiple lipopeptides, TLR 4 recognizes lipopolysaccharide (LPS), and TLR7/8 form homodimers to bind with single stranded RNA[31]. In addition to natural ligands, synthetic agonists have been developed for some of the TLRs, such as imidazoquinoline derivatives for TLR7, 8 or 7/8.

The binding of TLRs with natural or synthetic ligands initiates complicated intracellular pathways, and results in the secretion of cytokines from immune cells, as well as increased phagocytosis by macrophages. Furthermore, TLR activation plays a key role in bridging innate and adaptive immunity through their presence in professional antigen presenting cells, DCs particularly. Via up-regulating the expression of major histocompatibility complex (MHC) or co-stimulatory proteins (CD80 and CD86) on DCs, it enhances the antigen presentation to T lymphocytes, eliciting potent immune response. However, persistent signaling can be of risk and all TLRs are involved in the pathogenesis of acute and chronic inflammation, autoimmunity, cancer, and other diverse disease[32]. Therefore, understanding the way that the ligand stimulates the corresponding TLR is necessary to avoid undesirable side effect. TLR signaling is distinguished to two pathways, MyD88 (myeloid differentiation primary response protein 88) dependent and MyD88-independent pathway. MyD88 is involved in all TLRs signaling with the exception of TLR3, which needs to bind with TRIF (TIR-domain-containing adapter protein-inducing IFN-β) for stimulation. The other TLR that uses TRIF adapter is TLR4, which is the first TLR described using TRIF to activate MyD88-dependent pathway.

Although the regulation of TLRs is involved in the pathogenesis of various diseases, its application as a new therapeutic strategy is of great interest, as vaccine adjuvant

particularly. The type of immune responses elicited by various TLR ligands, specially the efficacy and safety of these agents are well reviewed [33]. TLR7 and 8 that can be activated by synthetic imidazoquinoline derived compounds, such as imiquimod (R837) or resiquimod (R848) are focused here, since they have the advantage of activating both myeloid DCs (mDCs) and plasmacytoid DCs (pDCs), which augments the expression of co-stimulatory molecules (e.g. CD80, CD86), as well as triggers the production of IFN-α (Interferon-α) preferentially by TLR-7 on pDCs, and IL-12 by TLR-8 activation towards mDCs[34]. Moreover, type I IFN produced by pDCs can facilitate the direct priming of CTLs. In addition to targeting DCs, TLR7 or 8 activates nature killer (NK) cells to secret IFN-γ, and triggers B cells to produce Ig and cytokines. To date, most pre-clinical studies on TLR7/8 activation utilized R837 or R848 as the agonist. Though these two imidazoquinoline derivatives exhibit a similar molecular structure, only R848 can stimulate TLR7 and TLR8 simultaneously, making it more potent than R837.

Pre-clinical studies demonstrate both agonists can enhance antigen specific T cell and B cell response, not only the magnitude but also the quality. Both in mice and non-human primate models, the delivery of R837 or R848 with HIV-1 Gag protein or plasmid enhanced T helper 1 (Th1) biases immune response, specially when the agonists were conjugated with protein[35–37]. Imiquimod alone or in the combination with HSV glycoprotein vaccine, significantly reduced the recurrence of HSV in guinea pig model, mostly correlated to the increased Interleukin-2 (IL-2) and antibody response[38]. The adjuvant potential of Resiquimod was also tested in chicken model, in which Resiquimod was found to augment both humoral and cellular response, by up-regulating the gene expressing of IFN (interferon)- α, IFN-β, IFN-γ, IL-1β, IL-4, and MHC II[39]. Beside the

direct injection of TLR7/8 agonists, the topical application of Imiquimod or Resiquimod at the injection site of peptide-based vaccine could also enhance antibody response, as well as CD4+ T cell response[40,41]. Furthermore, both Imiquimod and Resiquimod have been tested in the combination with cancer antigen NY-ESO-1 protein vaccine in patients with malignant melanoma, eliciting potent humoral and cellular responses in a significant fraction[42,43]. In general, TLR7/8 have been demonstrated as potent adjuvant for vaccine consisting of different immunogen, such as protein, DNA, peptide, and even DCs based vaccine.

2.1.2 Nanoparticle based delivery system for vaccine design

Nanoparticles, which are defined as the particles with the size ranging from 1nm to 1000nm[44] , have been intensively studied in the development of subunit vaccines. In both prophylactic and therapeutic strategies, nanoparticles can efficiently deliver the antigens to specific immune cells, and /or act as immunostimulatant adjuvants to activate innate immunity. Based on the type of material, nanoparticles can be classified as liposomes (Fig.2-1A), polymeric nanoparticles (Fig.2-1B), inorganic nanoparticles (Fig.2-1C), and virus like particles (Fig.2-1D), self-assembling peptides and so on.

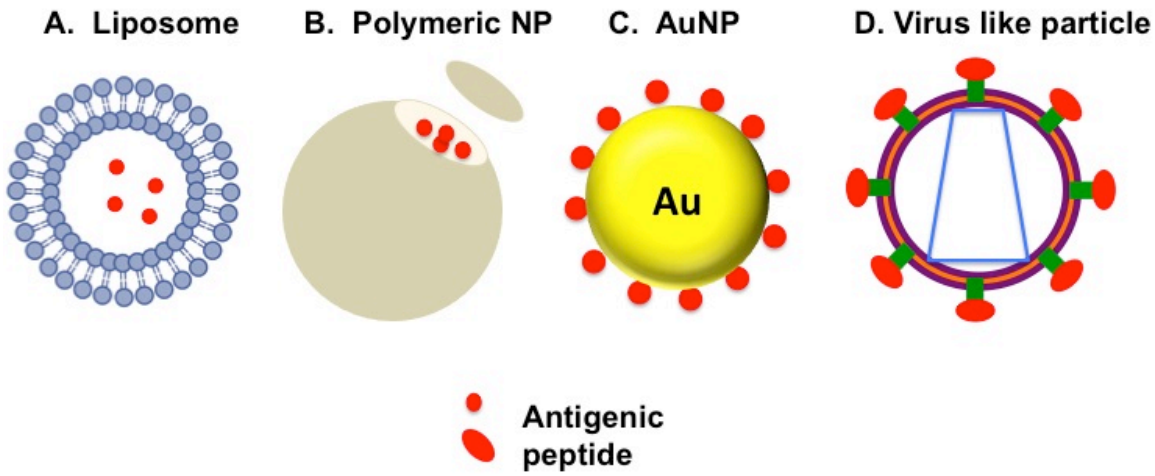

Figure 2-1 Schematic representation of different nanoparticles for antigen delivery (A) Liposome, (B) nanoparticles prepared from polymer, (C) gold nanoparticle, (D) virus like particle

2.1.2.1 Liposomes:

Liposomes are artificially prepared vesicles composed of a phospholipid bilayer shell with an aqueous core. As vaccine carries, liposomes have been used extensively to induce either CTLs response (cytotoxic T lymphocytes) or antibody titers (humoral immunity)[45–47] in *vitro* and in *vivo* [48,49]. For vaccine formulation, an antigen (or adjuvant) may be encapsulated in the core of the liposome, buried within the lipid bilayers or adsorbed as well as chemically coupled on the surface [11,50].

Based on the fact that the delivery efficacy of liposomes is affected by such factors as surface charge, vesicle size, phospholipid composition, lamellar structure [51], a large number of different approaches have been made to improve the immunoadjuvant activity of liposomes. The approaches include the modification of the liposome structures, the combination with other molecules such as immune potentiators, or conjugating with surface ligands for targeting to the DCs, a typical professional antigen presenting cells (APCs). Nakanishi *et al.* demonstrated that cationic liposomes were much more potent than anionic or neutral ones for generating cell-mediated immune response [52]. An

interesting preclinical study done by Guan *et al*. revealed that liposome-associated (either encapsulated or surface-exposed) MUC1 peptide (BP25) produced a strong specific CTL response; however, a humoral response was only observed for the surface-absorbed BP25 formulation [53]. This suggests the strategy that is adopted for antigen loading has an impact on what sort of immune response is induced.

Akira et al. demonstrated a highly efficient antiviral CD8+ T- cell induction by peptide epitopes chemically coupled to the surface of liposomes [54]. This form of vaccination with a single epitope elicited antigen specific memory CD8+ T cell in the absence of CD4+ T cell help, which might had a potential advantage for the induction of antiviral immunity.

As of 2008, there are two liposome-based vaccines in market, Epaxal for Hepatitis A, Inflexal V for influenza, which are both from Berna Biotech Company. Additionally, several liposome-based vaccines are under clinical study currently, for the intracellular infectious diseases, such as cancer and HIV-1.

2.1.2.2 Polymeric nanoparticles:

Biodegradable polymeric nanoparticles have attracted much attention for biomedical applications, such as drug, gene, or vaccine delivery. The commonly used biodegradable polymers are aliphatic polyesters, including poly (lactic acid) (PLA), poly (glycolic acid) (PGA), poly (ε-caprolactone) (PCL), poly (lactide-co-glycolide) (PLGA). In particular, microsphere vaccine delivery systems based on PLA and PLGA [26,55,56] have been extensively investigated due to their long-term safety in humans, biodegradability, and the commercial availability of a variety of polymers of different molecular weights and monomer ratios [57,58]. Similarly to liposomes, there are two main methods for antigen loading with polymeric nanoparticles, encapsulation and surface adsorption. The

encapsulation of antigens into PLGA NPs can be carried out by mainly three ways: the water-in-oil-in-water (w/o/w) emulsion technique[59,60], the phase separation, and spray drying.

To date, there have been many promising studies on different vaccine antigens encapsulated into PLGA nanoparticles shown to induce broad and potent immune response. For example, Chong et al. used PLGA nanoparticles (300nm) to load the hepatitis B core antigen (HBcAg) with or without monophospholipid A (MPLA) adjuvant [61]. A single immunization with HBcAg encapsulating NPs containing MPLA induced a stronger cellular immune response, compared with those induced by HBcAg alone or by physical mixture of HBcAg with MPLA. Moreover, PLGA/antigenic peptide complex administrated by various routes, including oral, nasal and subcutaneous delivery, have all successfully generated potent CTL response, which suggests that PLGA particles can be taken up in vivo and cross-presented by resident APC[62–64]. In addition to the enhanced uptake, PLGA based delivery system is also observed to facilitate the endosomal escape of exogenous antigen and sustain the antigen level in cytosol of DCs to augment the cross-presentation efficiency[65].

However, these kinds of polymeric nanoparticles have some drawbacks, resulting from their hydrophobic nature, which would lower antigen encapsulation efficacy and higher burst effect of antigen release from NPs [66]. To overcome these, a second hydrophilic component poly (ethylene glycol) (PEG) is introduced to form an ABA poly-D, L-lactide-PEG [67,68].

Beside of the modification of PLGA, recently, many studies have been focused on self-assembled biodegradable nanoparticles fabricated by the amphiphilic block and graft

copolymers based on poly (amino acid) s, such as poly (α-L-glutamic acid) [69], poly (L-lysine) [70], poly (γ-glutamic acid) [71], poly (ε-lysine) [72], poly (L-aspartic acid) [73], poly (L-arginine) [74] and poly (L-asparagine) [75] as hydrophilic segments, with poly (β-benzyl-L-aspartate) [76], poly (γ-benzyl-L-glutamate) [77], or poly (L-histidine) [78] as hydrophobic segments. Poly (γ-glutamic acid) (γ-PGA) is a naturally occurring poly (amino acid) synthesized by certain strain of Bacillus, which itself is poorly immunogenic [79–81], but has good resistance against many proteases. Nanoparticles composed of hydrophobically modified γ-PGA, in which γ-PGA acts as the hydrophilic backbone with L-phenylalanice (Phe) as the hydrophobic segment, are prepared as antigenic protein or peptide delivery system [14]. Antigen-loaded γ-PGA-Phe based nanoparticles show an exciting strategy for the enhancement of antigen-specific humoral and cellular immune response through selective targeting of the antigen to APCs [82,83]. It has been observed that the γ-PGA NPs are also effective for vaccines against human immunodeficiency virus (HIV-1) [84], influenza virus [85], Japanese encephalitis virus [86], or cancer [87,88].

2.1.2.3 Inorganic nanoparticles:

Many inorganic materials, such as gold nanoparticles (AuNPs), or silica based nanoparticles (SiNPs) have also been used as vehicles for antigen delivery, offering the advantages of rigid structure and controllability over the synthesis, including size, shape, and surface properties. As vaccine delivery platform, AuNPs have been studied for the antigens derived from respiratory syncytial virus[89], foot-and-mouth disease[90], or DNA vaccine for HIV-1[91]. By coating West Nile virus on AuNPs with different shapes (spherical, rod, cubic) and size range (2-150nm), the influence of shape and size of AuNPs on immune response *in vitro* and *in vivo* was investigated, in which 40nm sphere

was found optimal for antibody production[92]. For the development of cancer vaccines, AuNPs are found to promote significant antigen specific response without additional adjuvants, leading to subsequent anti-tumor activity and prolonged survival in both prophylactic and therapeutic *in vivo* tumor models[93,94].

The other promising inorganic material for vaccine design is silica. Despite the tunable particle size and shape, the abundant silanol group on the particle surface can contribute to the further modification with antigens, targeting moieties. Compared with solid SiNPs, mesoporous SiNPs (such as SBA-15 or MCM-41) with uniform pore size and ordered pore structures have higher loading capacity owning to their larger surface area, and perform better in control release of the cargos[44]. Furthermore, up to 30mg unfunctionalized mesoporous SiNPs were nontoxic when administrated subcutaneously, and only trace amount of mesoporous silicates were detected after 2 months[95]. Benefiting from these attributes, mesoporous SiNPs with the size ranging of 50-200nm have been applied as nanocarriers for protein based antigen via encapsulation and/or absorption[96–100]. It is also reported that SBA-15 can induce potent antibody response, independently of immune cell committed, while OVA loaded MCM-41 elicits both antibody and cellular response, with the latter one as dose-dependent[98,99].

2.1.2.4 Virus like particles (VLPs):

VLPs that resemble viruses, but do not contain any viral genetic materials, are prepared from the self-assembly of viral structure proteins, such as Envelope, or Capsid. Benefiting from the ideal particle size and repetitive display of virus surface proteins that present conformational viral epitopes, VLPs can induce both B cell and T cell immune response in the absence of adjuvant[101]. VLPs based vaccine is the first nanoparticle based

vaccine class in market, with the first product (hepatitis B vaccine) commercialized at 1986. In 2006 and 2011, another two VLPs based vaccines were licensed for human use, for papillomavirus and Hepatitis E, respectively. In addition to the direct use of VLPs as immunogen, they are ideal carriers for the delivery of epitopes[16,102], DNA targeting other diseases, with potency in stimulating humoral and cellular response. For epitope delivery, the particular VLPs structure is readily taken up into APCs, and thus prime long lasting CTL response, as well as potent antibody response. Remarkable work has been done with the hepatitis B core particles, human papillomavirus VLPs and parvovirus VLPs displaying T cell specific epitopes from other proteins on their capsid[103–105]. It is demonstrated that VLPs are efficient stimulators of MHC class I and class II responses[106]. Though the antigenic peptide can be exposed on the surface of VLPs by rational design of vaccine, the requirement of capsid to self-assemble often limit length of the foreign sequences incorporated into VLPs[106].

2.1.3 Cross-presentation of exogenous antigen by DCs

Based on the presentation pathway, antigens can be classified as endogenous ones, which can be presented on the surface of all nucleated cells in the complex with MHC (major histocompatibility complex)-I molecules, and exogenous antigens processed and presented through MHC-II pathway. To prime CD8+ T cell response that is critical in the immunological control of tumor and infectious diseases, exogenous antigens need to be internalized from extracellular environment and presented as MHC-I bounded peptide, which process is termed “cross-presentation”. The principal cells that have this capacity, are dendritic cells and macrophages[107,108], although in some circumstances various other cells, e.g. B cells[109], neutrophils[110] as well as endothelial cells[111]. Most studies indicate

that DCs are the most important cross-presentation APCs (antigen presenting cells) *in vivo* even though it is not unclear which DC subtypes can or cannot cross-present antigens.

The phenomenon of cross-presentation was firstly found by Bevan[112] that in animals immunized with fully allogenic cells, part of the CTLs were generated specifically for minor antigens from the graft presented on MHC-I molecules of the host. The cross-presented antigens can be acquired in several different forms, including DNA or RNA[113,114], peptides, peptide-HSP (heat-shock proteins) complexes[113,114], or as protein [107,115,116], and, most importantly, cellular antigens[117–119]. Different forms of antigens would be internalized and cross-presented by APCs under distinct mechanisms. To date, two main intracellular pathways for cross-presentation have been reported, "cytosolic" and "vacuolar" pathways[120].

The "cytosolic" pathway is sensitive to proteasome inhibitors, indicating the internalized antigens access the cytosol, where they are degraded into oligopeptides, which can then feed into endoplasmic reticulum (ER) by transporter associated with antigen processing 1 (TAP1) and TAP2, through the classical MHC-I mediated presentation pathway. In ER, proteasome generated oligopeptides are further trimmed by ER aminopeptidase-1 (ERAP1) and endosomal insulin-responsive aminopeptidase (IRAP) to 8-mer or 9-mer peptides, for complex with MHC-I molecules and transporting to the cell surface for display. By contrast, the "vacuolar" mechanism for cross-presentation is resistant to proteasome inhibitors and generally independent of TAP, but is sensitive to inhibitors of lysosomal proteolysis[120]. This suggests both antigen processing and binding with MHC class I molecules take place in endocytic compartments in this pathway.

The capacity of DCs to cross-present antigen is not only dictated by the characteristics of DC subtypes, but also influenced by additional factors, including mode of antigen internalization, formulation of antigens, as well as DCs' maturation status[121]. Antigens can be internalized by DCs via various mechanisms, including non-specific, receptor-independent pathway, such as pinocytosis and phagocytosis, as well as specific, receptor-dependent processes, like uptake through C-type lectin receptors (CLRs), Fc receptors, and scavenger receptors, among which CLRs are considered as ideal candidate for the targeting of antigens to DCs. Dendritic cell-specific intracellular adhesion molecule-3-grabbing non-integrin (DC-SIGN) is a paradigmatic example of CLRs expressed on human mucosal and dermal DCs, which facilitates rapid antigen uptake and processing for efficient cross-presentation. In most of recent studies, monoclonal antibody[122] and natural CLR ligands (glycan)[123] are intensively applied as targeting agents against DC-SIGN. In addition, as another important CLR, mannose receptor (MR) targeting by two glycan ligands of MR, 3-sulfo-Lewis ^{A} and N-acetylglucosamine conjugated OVA antigen shows improved uptake by bone marrow derived DCs (BMDCs), resulting in enhanced cross-presentation in vivo[124]. With different receptor mediated internalizations, antigens would be routed to distinct endocytic compartments, determining cross-presentation efficiency, possibly by influencing antigen translocation to cytosol. Mellman group compared the internalization and endosomal degradation of receptor bounded antigen by human DCs, by conjugating antibodies against different DCs receptors that were targeted to early or late endosomes, with CD40 and mannose receptor against early endosome, whereas DEC205 for late compartments[125]. Their results showed, the peptide conjugated with the antibody targeting CD40 had the highest cross-presentation

efficiency, even though this antigen was least internalized by DCs. Additionally, inhibiting the antigen degradation in the late endosome rescued the DEC205 targeted cross-presentation, suggesting the internalization of antigen into the late compartments would impair the cross-presentation. The understanding of cross-presentation is crucial for the design of vaccine that aims to prime protective immunity against infectious diseases.

2.1.4 Rational design for formulating peptide based vaccine

A primary goal of vaccine design is to find an optimal formulation to induce potent and long memory humoral and cellular responses to protect against specific diseases. There are a variety of considerations that need to be made during the incorporation of the three components for peptide-based vaccine: antigenic epitope, adjuvants (immune potentiator) and delivery platform (as shown in Fig.2-2).

First and foremost among them is the selection of epitopes in terms of antibody response and/or cellular response from targeted pathogen. Though the humoral responses in sufficient quantity are predominant protective correlate, the cellular immunity is critical in the protection against intracellular infections, and in most diseases, the help from CD4+ T cells is necessary for the generation of effector B cells[126]. A vaccine that stimulates CD8+ T cells has been considered as a promising strategy to prevent infections with HIV-1[8]. Moreover, the stimulation of CD4+ T cells is required to generate memory CTLs, even though some adjuvants such as TLR agonist can provide inflammatory cytokines to prime potent CTL response[127]. Thus, the epitope selection for broad-spectrum HIV-1 vaccine may have to be directed towards not only highly conserved CTL

epitopes, but also helper T cell epitopes from the same protein.

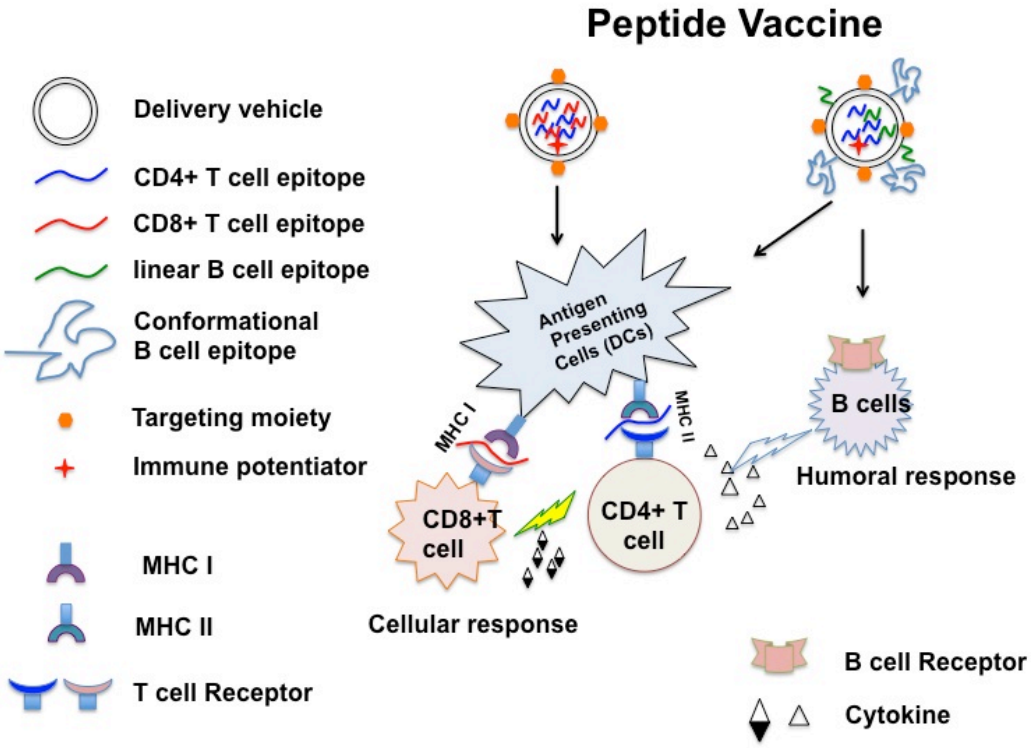

Figure 2-2 Ideal formulations of peptide based vaccine, depending on the expected immune response: cellular or humoral response.

The formulation strategy for the association of antigens to the carriers is another factor that will affect the efficiency of artificial vaccines. The association has been achieved mainly through adsorption, encapsulation, and conjugation. Adsorption of antigen to the surface of inorganic particle-based delivery system is generally driven by electrostatic or hydrophobic forces[26,128,129]. However, this kind of interaction between antigens and carries is relatively weak, which may lead to the rapid dissociation of cargoes from nanoparticles *in vivo*. By contrast, encapsulation or conjugation with chemical bond can provide stronger interaction, which are widely applied in the attachment of antigen to the delivery vehicles based on VLPs[106], polymeric nanoparticles[13], or liposomes[51]. In encapsulation, antigens are added to the nanoparticle precursor solutions before assembly

process and located in the interior of particles, in which a fraction of antigens might be lost causing relatively low loading efficacy. The complete and stable association of antigenic peptides to nanocarriers can be easily achieved by direct conjugation, which usually utilizes cleavable chemical bonds for the release of epitopes at the targeting location, such as peptide bond[10], disulfide bond[130].

Besides, the size of vaccine particle can influence the biodistribution and the uptake mechanism, which subsequently affects the type or the level of resulting immune response. All particle used in vaccine formulations usually have a comparable size (<5μm) to the pathogens recognized by immune system, and internalized by APCs with different mechanisms depending on the respective size. When vaccine particles are administrated subcutaneously, small particles (20-200nm) can take free-drainage to the lymph node (LN), to be internalized by either LN-resident DCs, or macrophages, while larger particles (500-2000nm) need DCs or macrophages at the inject site to transport them to LN[131]. By using model polystyrene particles ranging from 20 to 2000nm, it is found that smaller particles (<500nm), in particular 40-50nm are preferentially taken up by DCs, and are significantly more able to promote CD8 and CD4 type I cellular responses, while large particles (>500nm) are mainly internalized by macrophages to induce a considerable antibody response[132]. No consensus exits about a specific size range for all vaccine formulations, but controlling the size of particles can be one promising means to passively target APCs, especially LN resident DCs, or to bias the immune response.

Aside from size, the incorporation of an additional immune potentiator into the system, can further enhance the immunogenicity of the antigen, though some nanoparticle based delivery systems themselves already have the capacity of stimulating immunity[133–136]. It

is also suggested that for an efficient vaccine, the antigen and adjuvant should be processed by the same APC simultaneously[137]. In fact, the antigen and TLR agonist should co-localize in the same phagosome for the efficient MHC II antigen presentation[138].

Furthermore, as the primary APCs processing and cross-presenting exogenous antigens to prime CTL response, targeting antigen to DCs is an intensively explored concept to reduce the required antigen dose and improve the cellular immunity. Thus it appears logical to combine DCs targeting with the co-delivery strategy to provide particular DC subtypes with both antigen and TLR agonist. Despite the passive targeting strategy by tuning the precise size of the vaccine formulation, active receptor-dependent targeting has also been intensively investigated, as discussed above. Additionally, since most nanoparticle based vaccines are internalized by DCs within the endosomal compartments, where the antigens are degraded impairing the cross-presentation efficiency, the endosomal escape of antigens to cytosol of DCs is another concern to enhance the CTL response. To achieve efficient cytosolic delivery of antigen, nanoparticle based delivery system is further harnessed with the moiety capable of membrane interruption, such as cell penetrating peptide[139–141], pH-responsive polymers[134].

Combining the factors discussed above, the optimal formulation of peptide-based vaccine is illustrated as shown in Fig. 1, though there is no exactly ideal strategy for the design of all vaccines, which vary in the type of targeting diseases, the defined immune responses, and the administration routes. To date, the main challenge is the peptide-based vaccines have been slow to reach commercialization, largely due to safety concerns regarding the adjuvants and insufficient efficiency causing low clinical benefit rate. The new adjuvants

or delivery system is on demand, which should be evaluated more comprehensively and systematically.

2.2 Self-assembling peptide

Self-assembly is defined as the autonomous organization of components into ordered patterns or structures[142]. In the past decades, variable biocompatible and bioactive small molecules have been used as building blocks for self-assembling materials, such as nucleic acids, carbohydrates, or amino acids. Among them, amino acids that are the molecular units for proteins or peptides provide the widest feasibility of functionalization and modification, as well as cell signaling capacity. Inspired from the basic conformational structures (α helix, β sheet and turn, or coiled coils) existing in natural proteins, small peptides can be rationally designed to assemble to different kinds of supramolecular structures as fibers[143–145], rods[146,147], tubes[148], micelles[149], and globules[150,151].

2.2.1 De novo design principles for self-assembling peptide

Though each artificially synthesized self-assembling peptide has its unique design strategy, the general rules underlying their design can be summarized as one of the combinations of the following factors: molecular amphiphilicity, structural compatibility, and environmental responsiveness. Large research efforts have been targeted on the *de novo* design principles for predicting structures from primary sequence[152,153]. Frederix *et al*. applied computational approach to screen all possible combinations (8,000 in total) of amino acids in tri-peptides and subsequently identified those with the best-predicted properties for experimental characterizations, demonstrating a methodology to predict the

self-assembling properties of tri-peptides[152]. Our group presents a systematic and simple design principle of amino acid pairing (AAP) for constructing functional supermolecules with peptide as the building block. In the principle, three main side chain interactions, including hydrophobic interaction, electrostatic attraction, and hydrogen bonding were discussed[154]. Based on this principle, our group designed and synthesized various self-assembling peptides, for the delivery of either hydrophobic drug[154] or hydrophilic small interferon RNA (siRNA)[155]. Both the computational and empirical principles provide a "bottom-up" engineering route for the design of artificial self-assembling peptides with predictable nanostructures for various applications.

2.2.2 The application of self-assembling peptide

Combining with biocompatibility as well as the ease of synthesis and functionality, the flexible construction of nanostructures makes the self-assembling peptide as an attractive biomaterial in the applications of regenerative medicine[17], tissue engineering[18,156,157] , drug delivery[158], and vaccine design[10,159], which are further reviewed in the following subsections.

2.2.2.1 Drug delivery

In the delivery of biological molecules, such as DNA, siRNA, or hydrophobic drugs etc., self-assembling peptide acts as a promising approach, by encapsulation or co-assembly. Yang *et al*. developed a novel class of self-assembling peptide that formed core-shell structured nanoparticles (sequence: cholesterol-G3R6YGRKKRRQRRR). This peptide exhibited a broad-spectrum of antimicrobial activities against a variety of wild or drug-resistant Gram-positive bacteria, fungi and yeast at low inhibitory concentration[160]. They

also synthesized an oligopeptide amphiphile containing three blocks of amino acids (Ac-$(AF)_6$-H_5-K_{15}, termed as FA32) that self-assembled into cationic core-shell micelles with the average diameter of 102nm, and evaluated its potential as a carrier for the co-delivery of Doxrubicin (DOX) and p53 gene. FA32 was found to encapsulate DOX at the loading capacity up to 22%, which further efficiently condensed p53 to small complex with net positive charge on the surface. A synergistic effort in end point cytotoxicity was observed by the sustained release of hydrophobic DOX and negatively charged p53[161]. For nuclei acid delivery, Zhang and coworkers designed a series of surfactant like peptides, in which there are repetitive hydrophobic amino acids, such as Alanine (A) or Leucine (L) as the tail, and positively charged amino acids at the terminal. These peptides self-assembled to nanovesicles or nanotubes, showing potential application for DNA delivery[162]. Moreover, the drug release concerns can also be beneficial from harnessing the self-assembling peptide with the stimuli-responsive properties, such as pH[163], temperature[154], ant other factors[164].

2.2.2.2 Vaccine design

During the application of self-assembling peptides as the scaffolds for regenerative medicine, or drug delivery, they have been found to be minimally immunogenic in animal models, even conjugating with the sequences derived endogenous proteins[165–168]. This feature is clearly an advantage as delivery platform for the application of vaccine design, especially for the peptide based vaccines, since either solid phase peptide synthesis or recombinant protein expression can easily conjugate the selected epitopes with self-assembling sequence. Thus, nanoparticles based on self-assembling peptides have attracted considerable attentions in the design of peptide vaccines.

Burkhard and his group designed a novel type of nanoparticles (synthetic virus like particles) with regular icosahedral symmetry and with a diameter at about 16nm, which were formed by a polypeptide chain consisting of a pentameric coiled coil and a trimeric-coiled coil. They extended the C-terminus of the trimeric coiled coil with either *Pseudomonas* [159]or Severe acute respiratory syndrome (SARS) epitope[19], and evaluated the immunogenicity in rabbit or mice, which demonstrated that protective antibodies were elicited without the use of adjuvant and the immune response was conformation-specific. The formation of SARS epitope (red labeled) loaded peptide nanoparticle was simulated by computer model as shown in Fig.2-3. Similarly, a self-assembling coiled-coil lipopeptide was developed to form synthetic virus-like particles, which induced potent humoral response in rabbit as well[169]. Besides of the coiled-coil peptide as the building block for self-assembly, a simpler method that conjugating a di-alkyl tail with a CTL epitope at the N-terminal was presented and the formed cylindrical micelles offered *in-vivo* protection from tumors by stimulating the antigen specific CTLs[165].

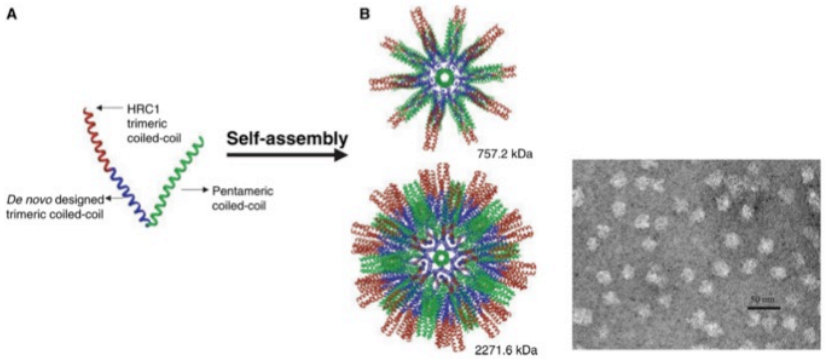

Figure 2-3 (A) 3D monomeric building block of P6HRC1 composed of a pentameric coiled coil domain from COMP (green) and trimeric *de novo* designed coiled-coil domain (blue) that is extended by a sequence of SARS HRC1 epitope (red). (B) Computer models of the peptide nanoparticle and the calculated molecular weight. TEM of the nanoparticles was shown. (Adapted from reference[19] with permission from the journal)

Moreover, a short fibrillization peptide, Q11 (Ac-QQKFQFQFEQQ-Am) that self-assembled in salt-containing aqueous environment and formed networks of β-sheet rich nanofibers was designed and intensively investigated for displaying functional amino acid sequences or chemical groups by Collier and coworkers[170,171]. As shown in Fig.2-4, when Q11 was conjugated with a model epitope $OVA_{323-339}$ containing bother T cell and B cell epitopes, the formed nanofibers displayed the epitopes on the surface and elicited antibody response in a comparable level to the epitope delivered in complete Freund's adjuvant (CFA)[10]. They found this augmented antibody response was long-lived with the duration up to 40 weeks, and T cell- and MyD88-dependent, but self-assembling peptide type-independent[172,173].

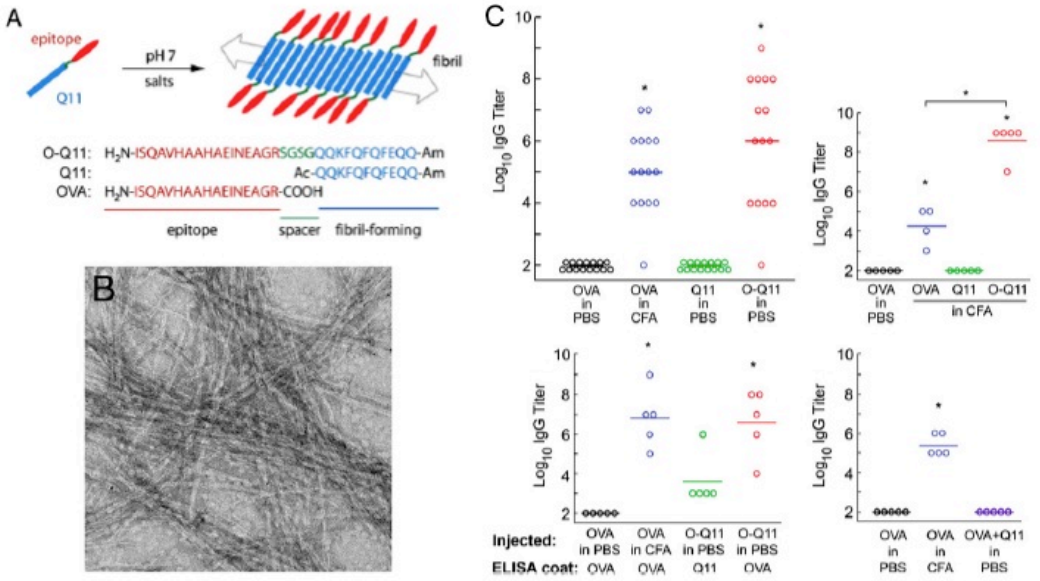

Figure 2-4 (A) Schematic and sequence of epitope-bearing self-assembling peptide O-Q11; (B) O-Q11 self-assembled into long, unbranched fibers; (C) O-Q11 elicit more potent OVA specific humoral response than epitope alone or the mixture of epitope and Q11 (Adapted from reference[10] with permission)

Moreover, even the self-assembling peptide Q11 emulsified in CFA, no detectable antibody was raised in mice. These findings suggest self-assembling peptide based nanoparticles have the capacity of enhancing the antibody response of antigenic peptides,

possibly owning to the repetitive display of B cell epitopes on the surface of nanostructure, which directly stimulated B cells more efficiently. However, for the CTL epitope, which requires to be processed and presented by DCs to prime or stimulate T cells, the efficient cross-presentation of exogenously delivered epitope is more critical for the induction of potent CTL response. The feasibility of self-assembling peptide for the delivery of the CTL epitope has not been well studied or understood.

2.2.3 Ionic-complementary self-assembling peptides

The ionic-complementary peptides are characterized by the periodic repeats of alternating charged hydrophilic and hydrophobic amino acids, the fist member of which was firstly discovered by Zhang from Z-DNA binding proteins[174]. The ordered charge distribution in the sequence leads to the unique electrostatic attractions between oppositely charged residues, which drives the self-assembly of peptides, combining with other interactions, such as hydrophobic interaction, hydrogen bonding. There are three types of charge distribution most widely studied among ionic-complementary peptide: type I, -+; type II, --++; type IV, ----++++[175]. In addition to the charge distribution, other factors such as secondary structure, concentration, pH, and salt effect influence the self-assembly of the peptides. To date, there are many ionic-complementary peptides have been studied, which are derived from either segments of natural proteins, or rationally design, as summarized in the review paper by Zhang S.[175]. Owing to the well-organized nanofiber structure and great water content (over 99%), the ionic-complementary peptides have been widely used for tissue engineering or scaffolds for 3D cell culture[18]. Our group investigated the mechanism whereby they undergo self-assembly, as well as the application in 3D cell culturing and drug delivery.

EAK16-II is a typical ionic-complementary self-assembled peptide, composed of 16 amino acids (AEAEAKAKAEAEAKAK), forms β-sheet rich nanofibers of separated hydrophobic and hydrophilic faces in aqueous solution. The EAK16-II nanofibers were not only resistant to acid and proteases, but also non-immunogenic in mice[174], which features were critical for the application in antigen delivery. Previous data suggested it could efficiently stabilize hydrophobic molecules as pyrene or anticancer drug ellipticine by non-covalent interaction[176,177], demonstrating the potential in drug delivery. Moreover, Zheng and coworkers linked six consecutive histidines at the C-terminus of EAK16-II, which displayed the anti-polyhistidines antibodies (anti-CD4 antibody) on the surface of nanofibers, to engage T cells *in vivo*[178]. Thus, EAK16-II based nanofibers offer the possibility of delivery short peptide or hydrophobic molecules, which could be helpful in the formation of peptide based vaccines.

Chapter 3 *Ex vivo* generated Dendritic cells pulsed with HIV-1 CD8+ T cell epitope-loaded self-assembling nanofibers elicited more potent CD8+ T cell response

Abstract

To focus CD8+ T cell response on the highly conserved epitopes has been considered as an effective strategy to overcome the extensive variability of HIV-1 proteins, which is a major obstacle for the development of HIV-1 vaccine. However, these antigenic peptides induce weak immunogenicity by themselves, thus require proper adjuvants to enhance the efficiency. We conjugated a self-assembling peptide EAK16-II with an HIV-1 CD8+ T cell epitope SL9. The new peptide SL9-EAK16-II self-assembled to short nanofibers in aqueous solution, which were stable in PBS or cell culture medium. The nanostructure efficiently protected the epitope SL9 from degradation in sera or inside DCs. *Ex vivo* generated dendritic cells pulsed with these nanofibers stimulated significantly more SL9-specific CD8+ T cells. The results from confocal microscopy and flow cytometry demonstrated this enhancement in cellular response was mostly due to the sustained antigen level in the cytoplasm of DCs. Our finds suggested EAK16-II offered a potential as delivery vehicle for peptide based vaccine for HIV-1.

3.1 Introduction

To date, no therapeutic or prophylactic Human Immunodeficiency Virus-1 (HIV-1) vaccine is yet available. A major hurdle is the high variability of HIV-1, which impairs

the efficiency of vaccines. One potential approach to overcome it is to induce broad cytotoxic T lymphocytes (CTL) response against multiple conserved epitopes in HIV-1 proteins[8,179]. Several in-vivo studies with direct administration of peptide or peptides mixture have shown enhanced T cell response and reduced viral loading, however, rare overall clinical response from these peptide vaccines is observed so far[180–183]. This might ascribe to: 1) *in vivo*, direct binding of short peptide (8-10 amino acids for CLT epitope sequence) into class I major histocompatibility complex (MHC) could occur on not only professional antigen presenting cells (APCs), but also numerous other cells causing immune tolerance towards the epitopes[184]; 2) rapid degradation by tissue or serum peptidases was another concern in the weak immunogenicity of peptide antigen[185,186]. Thus, proper adjuvants or delivery systems that can protect the antigen from degradation, and facilitate the uptake and processing by dendritic cells (DCs) without any undesirable side effects are required to boost peptide specific immune response.

The self-assembling peptide based delivery system, which has been intensively studied in the applications of regenerative medicine[17], drug delivery[154,187,188], tissue engineering[18,156,158], and vaccines[10,15,173,189–191] can provide various advantages, such as stability, biocompatibility, ease of synthesis and manufacturing, as well as controllability over nanoscale positioning of ligands. Particularly in the vaccine design, more advanced evidences from animal work have proven direct conjugation of the epitope with the self-assembling peptide can elicit potent and long term lasting antibody response, via the ordered and repeating display of B cell epitopes on the surface of nanostructures[10,159,192–194]. However, to prime potent CTL response, exogenously administrated antigen is necessarily processed and cross-presented by APCs to stimulate CD8+ T cells. Whether

the cross-presentation efficiency of peptide-based antigen would be enhanced by the self-assembling peptide was unknown.

Therefore, to answer this question, we conjugated a self-assembling peptide EAK16-II (AEAEAKAKAEAEAKAK) with an HIV-1 specific CD8+ T cells epitope SL9, and determined the cellular response induced by the conjugating peptide SL9-EAK16-II. The peptide EAK16-II is an ionic complementary peptide that in aqueous solution spontaneously assembles into nanofibers or macroscopic membrane, driving by intermolecular hydrogen bonding, hydrophobic interaction from Ala (Alanine), and electrostatic interactions between Glu (Glutamic acid) and Lys (Lysine)[195]. The nanostructure formed by EAK16-II was stable in the presence of proteases, or in the solutions of extreme pH[174]. And SL9, an HLA-A*0201(A2)-restricted CTL epitope derived from HIV-1 P17 protein was tested, since it is highly conserved across circulating HIV-1 strains worldwide, and it produces a dominant SL9-T cell response in 75% chronically HIV-1 infected HLA-A2 positive adults [196–199] . The conjugated peptide SL9-EAK16-II was found to spontaneously assemble into short nanofibers, which were more stable than SL9 with the presence of sera or inside DCs. The *ex-vivo* generated DCs pulsed with these short nanofibers stimulated significantly more SL9-specific CTLs, which might associate with the sustained antigen level in the cytoplasm of DCs. Our results indicated the self-assembling peptide EAK16-II could act as a platform for the design of HIV-1 peptide vaccine.

3.2 Materials and Methods

3.2.1 Materials

All peptides were synthesized with the solid phase peptide synthesis method, and purified by RP-HPLC in the lab. Peptide synthesis reagents were purchased from AApptec. The 5-FAM labeled peptides were purchased from CanPeptide (Montreal, CA). Peptide solutions for nano-structure characterization such as AFM, TEM were prepared in pure Milli-Q water (18.2MΩ; Milli-Q system), with sonication of 15 minutes in water bath, and then allowed to self-assemble at room temperature overnight.

Complete DC medium: serum-free DC medium (CellGenix, Portsmouth, NH) supplemented with 800U/mL GM-CSF, 1,000U/mL IL-4 (R&D system), 100U/mL penicillin, 100μg/mL streptomycin, and 2mM L-glutamine (Life technology); Complete RPMI-1640 medium (R10): RPMI1640 (Life Technologies) supplemented with 10% human AB serum (Sigma), 100 U/ml penicillin, 100 μg/mL streptomycin, and 2mM L-glutamine; DC maturation cytokine cocktail: 5ng/mL (final concentration) TNF- α (R&D System), 5ng/mL IL-1β (R&D System), 1μg/mL prostaglandin E2 (Sigma, Oakville, ON, Canada), and 150ng/mL IL-6 (R&D System); Dyes used in sample preparation for confocal microscope: Lysotracker Deep red, Nucblue Live Ready probes reagent (Life technology)

Subjects Five HLA-A2 HIV-1 infected individuals were recruited under a protocol approved by the ethics committee at St. Michael's hospital, Toronto, an affiliate of the University of Toronto. Written consent was obtained from all 5 participants. Among these 5 subjects, one was a long-term non-progressor (asymptomatic, untreated HIV-1

infection for more than 10 years with CD4+ T cell count=970/mm3 and viral load (VL)=118 RNA copies/mL), one was a treated chronic infection (infected for more than 1 year with more than 1 year of continuous anti-retroviral therapy (ART) before sampling, CD4+ T cell count=460/mm3 and VL=49 RNA copies/mL), and three were untreated chronic infection (infected for more than 1 year without prior ART, mean CD4+ T cell count=473/mm3, range=380-560/mm3 and VL=137,563 RNA copies/mL, range=10,215-373,361 RNA copies/mL). Our collaborator M.D. Mario Ostrowski and M.D. Jun Liu carried out this work.

3.2.2 Methods

Peptide synthesis and purification All peptides were synthesized with Apex396 parallel synthesizer on Rink Amide resin (AApptec, KY) using standard Fmoc-based solid phase peptide synthesis. Briefly described, the deprotection of Fmoc from amino acid was accomplished by the treatment with 20% piperidine in DMF (N, N-dimethylformamide), followed by coupling with activated carboxyl group of next amino acid, using HCTU/DIEA as coupling reagent. After the synthesis, the raw peptide products were cleaved from resin with conventional trifluoroacetic acid (TFA)/ triisopropylsaline (TIS)/H_2O cocktails, and collected by precipitation into the cold methyl t-butyl ether. Then the peptides were purified on Waters 600E HPLC, with acetonitrile (0.1% TFA) and water (0.1% TFA) as eluents. The pure products were confirmed with mass spectrometry (Appendix Fig.1-3), and stored at 4°C. Potential lipopolysaccharide (LPS) contamination in all peptide solutions for *in-vitro* study was checked with Chromogenic LAL Endotoxin Assay Kit (GenScript, Piscataway, NJ) according to manufacturer's

protocol. LPS in all peptide preparations was negligible (less than 0.007 EU LPS/μg peptide).

Surface tension measurement Axisymmetric drop shape analysis-profile (ADSA-P) was used to measure the surface tension of the peptide solutions as previously reported[200]. The peptide solutions were prepared in pure Milli-Q water, at various concentrations ranging from 0.005mg/mL to 0.7mg/mL. The very low concentrations (<0.10mg/mL) were obtained by preparing 0.15mg/mL peptide stock solution in THF, adding the stock solution of a calculated volume into the glass vial, evaporating the solvent, and then adding 1mL of pure Milli-Q water, which was followed by sonication for 10mins in a water bath.

Circular Dichroism (CD) spectra Far-UV circular dichroism spectra of the peptide samples were measured at room temperature using a Jasco J-815 CD spectrometer (Tokyo, Japan). 150μL peptide solution was scanned in a 0.1cm quartz cell from 190 to 250nm. The water spectrum was used as the baseline for data collection. The final spectrum shown here was an average of three independent measurements.

Morphology characterization with Atomic Force Microscopy (AFM) and Transmission Electron Microscopy (TEM) Atomic force microscopy was used to determine the nano-structures of peptide self-assemblies. 100μL peptide solution was dropped on the surface of a freshly cleaved mica sheet for various times ranging from 5mins to 30mins, depending on the concentration of solutions. Then the free peptide was removed by blotting, and washed with 300μL pure water. After air-dry, AFM imaging was carried out at room temperature using the Peak Force tapping mold on a Dimension Icon AFM (Bruker, Santa Barbara, CA). To confirm the structures acquired from AFM,

TEM was also utilized. 10μL peptide solution was applied to a 400 mesh Formvar coated copper grid for 3-5 minutes, followed by negative staining with 10μL 2% uranyl acetate, blotted drying, and analysis on TEM (Philips CM10 TEM, operating at 60KeV).

Particle size measured by dynamic light scattering (DLS) The hydrodynamic diameter of the sample was measured using DLS on a Zetasizer Nano ZS (Malvern Instruments, Malvern, UK) equipped with a 4mW He-Ne laser operating at 633nm. 50μL solution was added in low volume disposable polystyrene cuvette and the scattered light intensities were collected at an angle of 173°. Three independent measurements were performed to generate the intensity based size distribution profile.

Serum stability assay Peptide stabilities were carried out in fetal bovine serum (FBS). FBS was centrifuged at 13000 rpm for 10mins to remove lipids and the supernatant was collected and diluted in DPBS to obtain 10% (volume percentage), 50%, and 100% FBS, which would be incubated at 37°C for at least 10min before the assay. 100μM peptide stock solutions, including SL9 or SL9-EAK16-II were prepared separately as described above. The assay was initiated upon the addition of peptide to the serum for a final concentration at 23 μM. The incubation time points were taken as 15, 30, 60, 90 and 120 min, followed by the precipitation of proteins with trichloroacetic acid (TCA) at a final concentration of 10%. The mixture was then kept at 0°C for 10mins for complete precipitation. The suspension was then centrifuged at 13000 rpm for 10mins, in which the supernatants were taken out and analyzed on RP-HPLC. The analysis was run on Waters 600E HPLC, using a linear gradient of 10%-60 % solvent C (0.1% TFA in acetonitrile) in 25mins. The retention time for each peptide was determined by the peptide solution in DPBS for a final concentration of 23 μM (which equals to the final concentration adopted

for the *in-vitro* studies) as control at 0 min. The peptide remaining in FBS at each time point was calculated with the area of peptide peak in Waters 2487 dual UV detector at 215nm as a percentage of the area of the 0 min DPBS treated peptide peak. Each experiment was performed in triplicate. The raw data from HPLC was shown in Appendix 1.

Peptide degradation in thimet oligopeptidase (TOP) Hydrolysis of the peptide in TOP (Abcam, Toronto, CA) was carried out as previously described[201]. Briefly, 23μM peptide was incubated at 37°C for various time intervals with 46nM TOP in 100μL 50mM Tris/HCl buffer (pH 7.8, 2mM $MgCl_2$, 0.1mM dethiothreitol). The reaction was stopped with 10μL acetic acid, which was further assessed with the amount of intact peptide using RP-HPLC, as described above.

Ex-vivo **Generation of monocyte-derived dendritic cells (MDDCs)** Peripheral blood mononuclear cells (PBMCs) were isolated from the whole blood from the donors, using Ficoll-Hypaque gradient centrifugation media (GE healthcare life science, Mississauga, Canada), which was conducted by our collaborator Jun Liu (M.D.) in University of Toronto. Monocytes were then isolated from PBMCs with Human Monocyte Isolation Kit-II (Miltenyi, San Diego, CA) and cultured in complete DC medium (as described in material subsection) for 5 days to generate immature MDDCs. The purity of the obtained MDDCs was determined with flow cytometry. For the analysis, the MDDCs were stained with fluorophore labeled anti-human HLA-DR and anti-human CD1a mAbs (eBiosciences) as two surface markers for DCs.

Fluorescent peptide tracking in MDDCs SL9 and SL9-EAK16-II were labeled with 5-carboxyfluorescein (5-FAM) at the N-termini. Immature MDDCs were pulsed with 5-

FAM-SL9, mixture of 5-FAM-SL9 and EAK16-II, 5-FAM-SL9-EAK16-II or culture medium R10, then maturated with the cytokine cocktails (as described in material subsection). After 12hrs, the MDDCs were thoroughly washed with PBS to remove the free peptides, which were then re-cultured in fresh medium. At various time intervals, the MDDCs were collected and analyzed with flow cytometry (BD LSRII, BD). The live 5-FAM+ MDDCs were quantified with FlowJo (Treestar, Ashland, OR).

Intracellular location of antigen in MDDCs To investigate the intracellular distribution of peptide, 10^6 immature MDDCs were cultured with 5-FAM-SL9 or 5-FAM-SL9-EAK16-II (the final peptide concentration was kept at 15μM) at 37°C for 4 hours, which were then thoroughly washed with PBS to remove the free peptides. Immediately or 12h after the peptide loading, the cells were stained by 75nM Lysotracker Deep red for 0.5hr, and washed with PBS, followed by re-cultured in fresh medium. Prior to being observed under confocal microscopy, one drop of Nucblue Live Ready probe reagent was added per well and incubated for 10mins to stain DCs' nuclei. All images were acquired using Zeiss LSM700 laser scanning confocal microscope. The co-localization coefficient between 5-FAM and Lysotracker Red channels was calculated by ImageJ software with the Menders Coefficients plugin. 20 cells were counted for each sample.

SL9-specific CTL response Immature MDDCs were seeded in 96-well plate with 10^5 cells in 50μL complete DC medium per well. Then, the MDDCs were pulsed with SL9, EAK16-II, mixture of SL9 and EAK16-II, or SL9-EAK16-II at the concentration of 23μM, with culture medium R10 (described in the material subsection above) as blank control, and further activated with DC maturation cytokine cocktails (described in the material subsection above). After 24h, the supernatants and cells were harvested. The

collected MDDCs were washed thoroughly 3 times with complete RPMI-1640 medium and then co-cultured with autologous PBMCs at 1:10 ratio in medium R10 for 7days. The PBMC were then re-stimulated with autologous Epstein-Barr virus (EBV)-immortalized B cells (prepared by our collaborator) that were pre-treated by SL9 in advance. After 6h incubation, the PBMCs were stained with fluorophore labeled SL9-tetramer, anti-human CD3, anti-human CD8, anti-Interferon-γ (IFN-γ), anti-Tumor necrosis factor-α (TNF-α) and anti-CD107a mAbs (eBiosciences), which was followed with the analysis on flow cytometry (BD LSRII, BD). The frequency of CD8+ T cells binding with SL9-tetramer or expressing IFN-γ, TNF-α and CD107a was quantified with FlowJo (Treestar, Ashland, OR). Isotype control antibodies were used as gating control.

Statistic analysis The one-way analysis of variance (ANOVA) was used for the comparison between multiple groups, with the software Prism (version 6) (Graphpad software, SD, USA). $P < 0.05$ was considered as significant.

3.3 Results

3.3.1 SL9-EAK16-II self-assembled to stable nanofibers in aqueous solution or cell cultural medium

For the work reported here, we utilized the self-assembling peptide EAK16-II to conjugate in tandem with SL9, between which a hydrophilic spacer Ser (Serine)-Gly (Glycine)-Ser-Gly was inserted, leaving the epitope domain positioned at the N-terminus, as shown in Fig.3-1. When dissolved in water at the concentration up to 3.0mM, no visible precipitate was observed. AFM and TEM were used to investigate the morphology of SL9-EAK16-II aggregates before or after addition to cell culture medium.

As shown in Fig (3-2a, 3-2b), SL9-EAK16-II self-assembled to short nanofibers (~1.37nm for height and ~8.04nm for width) of various lengths, but mostly shorter than 150nm, as well as some globules with the diameter ranging from 10 to 20nm; while adding to the medium, the peptide was visualized as short nanofibers predominately, without any further aggregation or dissociation (Fig. 3-2c, 3-2d). From the CD spectra as shown in Fig. 3-3a, the secondary structure analysis of SL9-EAK16-II indicated a transition from a β-sheet rich structure (minimal ellipticity at 208nm) for EAK16-II to α-helical conformation (minimal ellipticity at 206nm and 222nm), while SL9 itself was unstructured random coil. Similar transition was observed when EAK16-II was appended with H6 domain[178]. The conformational structure of the peptide was not critical when eliciting CTL response, but could be important for B cell epitope, especially conformational B cell epitope to induce antibody response[23].

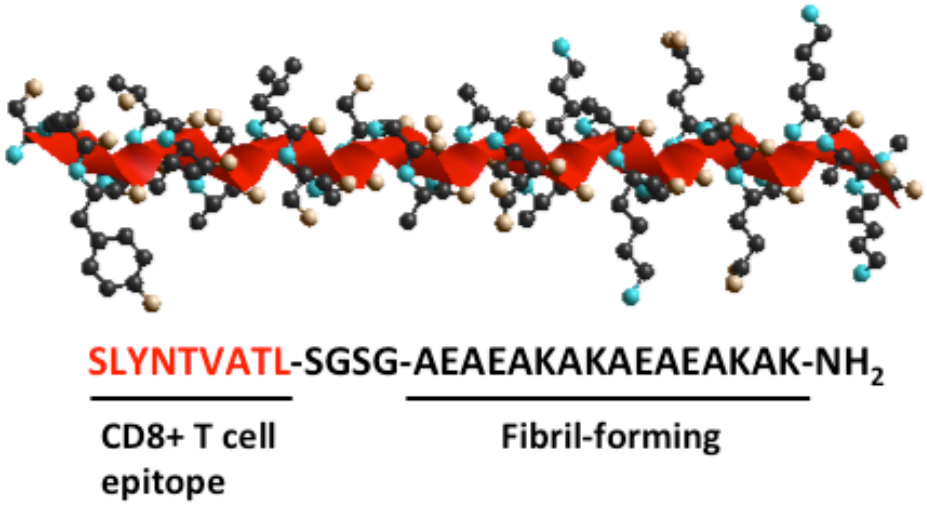

Figure 3-1The molecular structure of SL9-EAK16-II was simulated with Hyper Chem software, displaying carbon atom with black, nitrogen atom with cyan, oxygen atom with white, and the secondary structure shown as red ribbon.

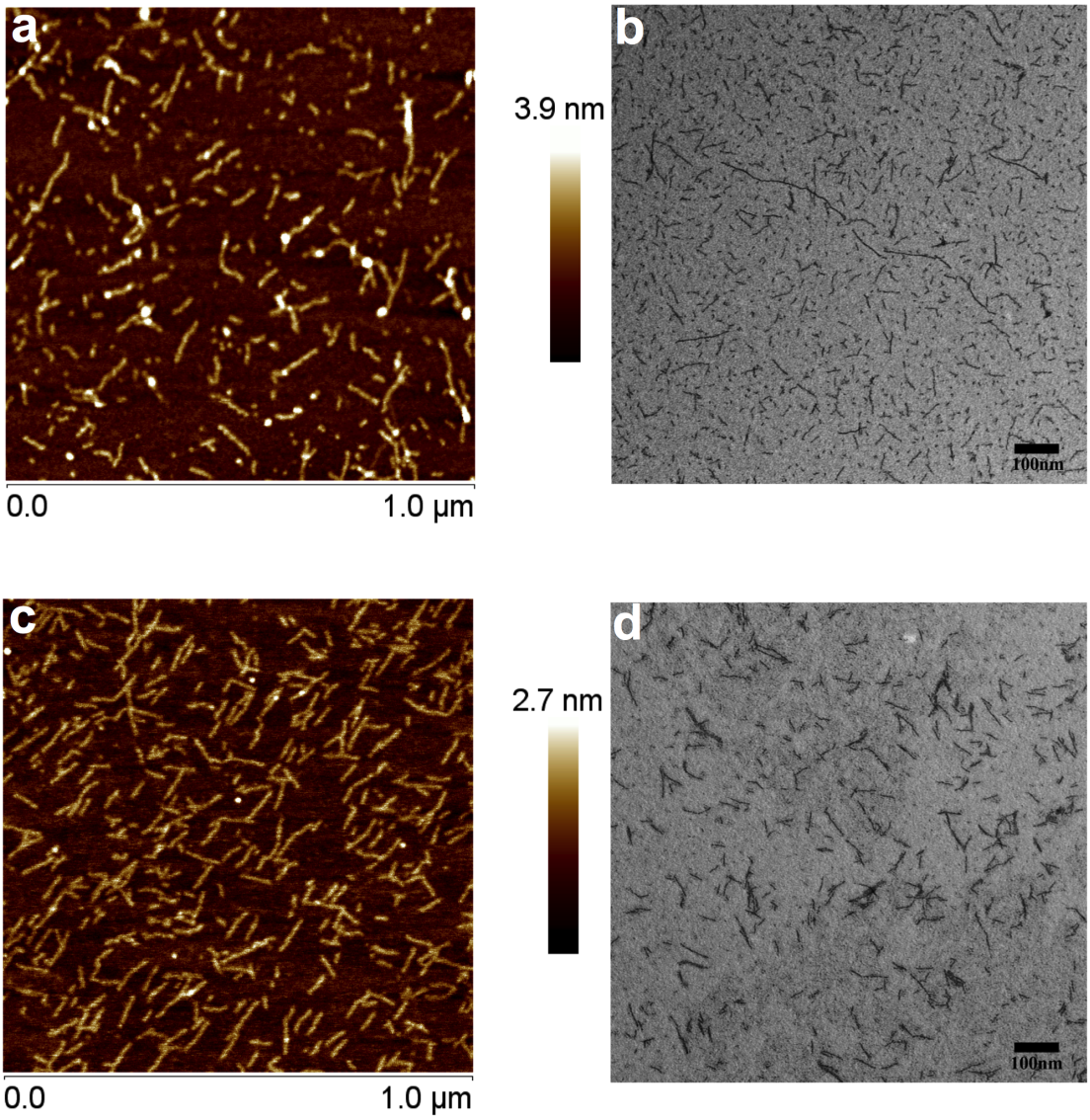

Figure 3-2 AFM (a) and TEM (b) for 100 μ M SL9-EAK16-II in water; the morphology of 23 μ M SL9-EAK16-II self-assemblies in cell culture medium was also characterized with AFM (c) and TEM (d). Before added with peptide solution, the medium was treated by 10000rpm centrifugation of 30mins and filtration with 0.1 μ m syringe filter to remove the big particles including lipid and proteins.

As an important parameter in controlling the stability of peptide aggregates, the critical assembly concentration (CAC) of SL9-EAK16-II was measured by surface tension method. As shown in Fig.3-3b, when the peptide concentration increased, the surface tension dropped dramatically down to a minimum value, and then it slightly increased to a plateau**.** The CAC of SL-9-EAK-16-II was estimated at around 0.02mg/mL (~7μM), which was much lower than the one of EAK-16-II itself (0.10mg/mL or 62μM)[202]. The

low CAC would prevent the nanostructure from dissociation at the injection site by the dilution effect from body fluid.

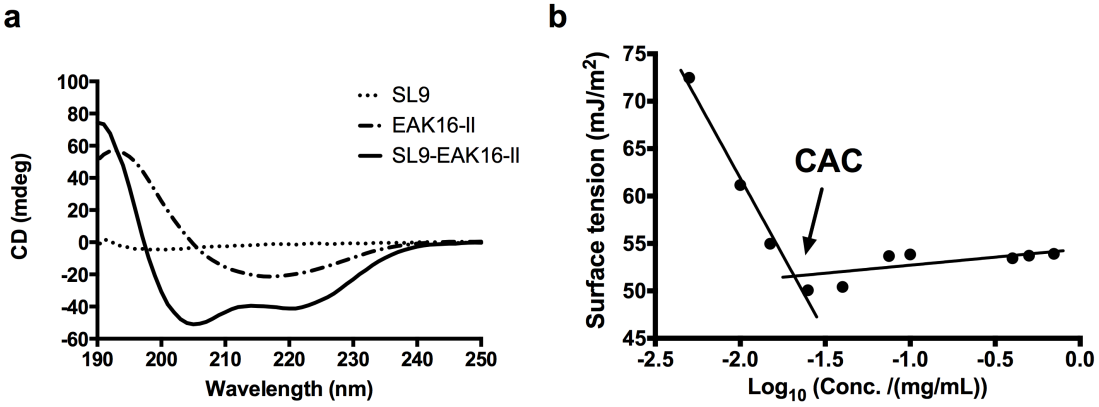

Figure 3-3 CD spectra of the peptides including epitope SL9, EAK16-II, and SL-EAK16-II (a); the equilibrium surface tension of SL9-EAK16-II was plotted versus peptide concentration (b), from which its critical assembling concentration (CAC) was estimated.

In addition to the concentration effect, the ubiquitous existence of salts in physiological environment would also influence the assembly behavior of the ionic complementary self-assembling peptides[202]. Thus, we determined the stability of SL9-EAK16-II nanofibers in PBS for various time intervals, which were monitored with DLS and AFM for hydrodynamic size and morphology respectively. As shown in Fig. 3-4a, the hydrodynamic size of SL9-EAK16-II aggregates in water was around ~44nm, while added to PBS, the size slightly increased to ~68nm; after one day, the hydrodynamic size of the particles increased to ~103nm, however, which did not further change significantly during the following 7-day's storage at 4°C (Fig.3-4b).

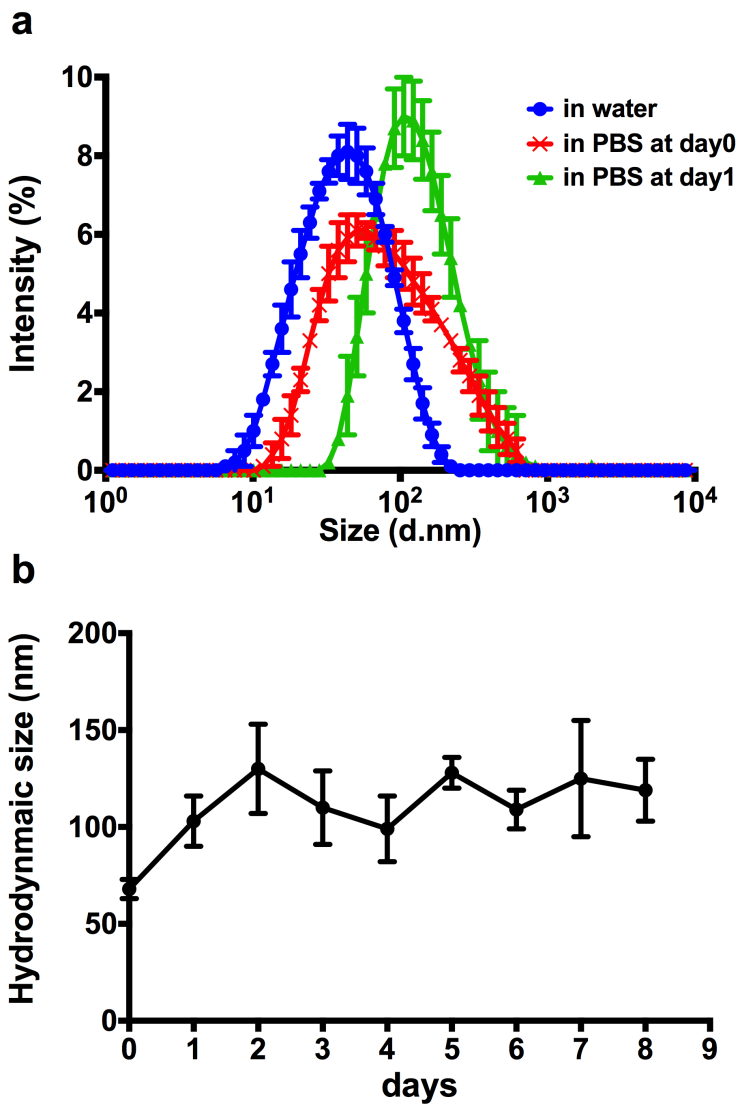

Figure 3-4 Hydrodynamic size distribution of SL9-EAK16-II nanoparticles in water or PBS was measured by DLS (a); the stability of the nanoparticles in PBS stored at 4 was monitored with DLS (b) for up to 7days.

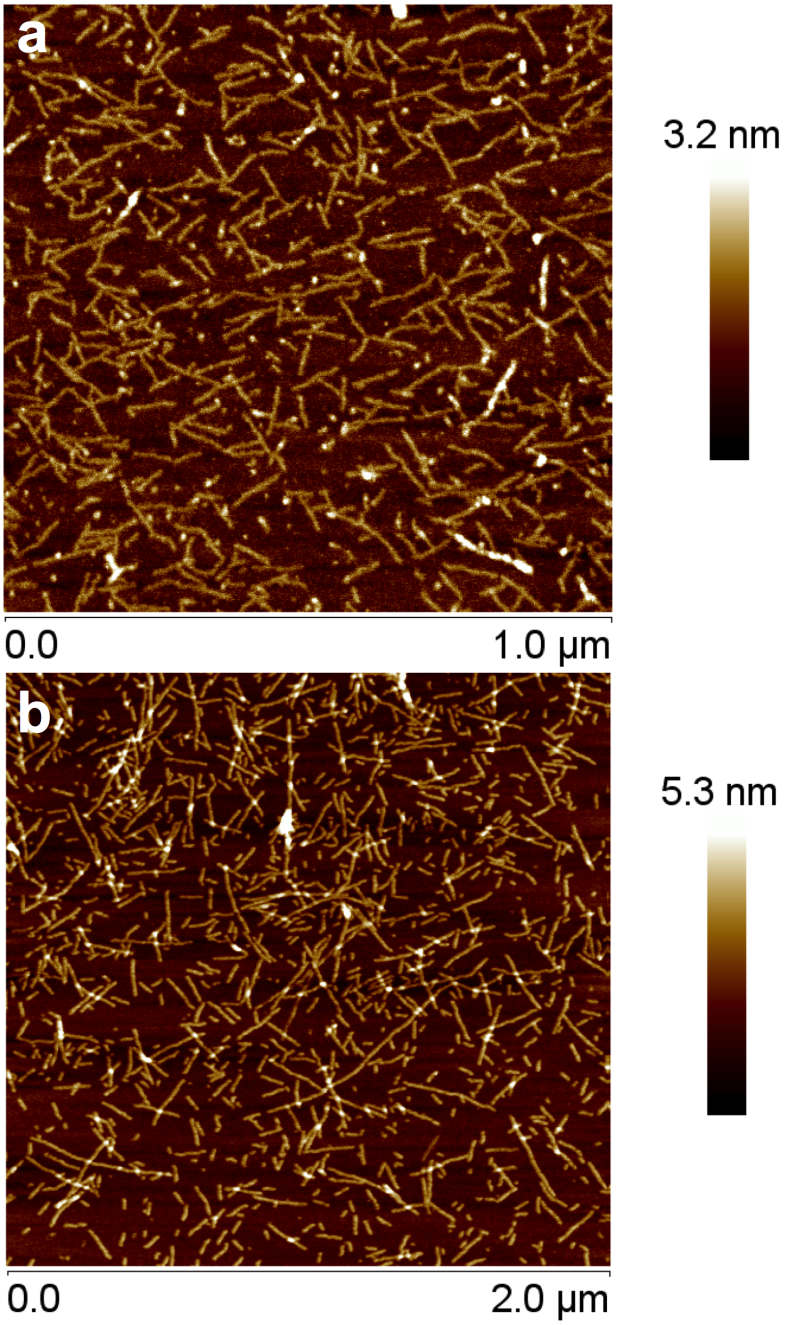

Figure 3-5 AFM images of SL9-EAK16-II self-assemblies in PBS at day 0 (a) or day1.

The short nanofibers in PBS at day0 (Fig.3-5a) or day1 (Fig.3-5b) were similar to the ones observed in pure water, but with less globular particles, suggesting that the addition of salt would facilitate nanofiber forming. The width and height of the nanofibers in different solutions were further quantitatively analyzed using Gwyddion software on

AFM images, as summarized in Table 3-1. With the exception of the peptide in PBS at day1, the heights of the aggregates in water (~1.37nm), culture medium (~1.32nm) or in PBS at day0 (~1.28nm), were consistent with the theoretic diameter of an α-helix (1.2nm, including side chains), which implied that the helical peptide monomers assembled side by side to form monomolecular layered structure. In comparison, the height of short fibers in PBS at day1 was almost doubled to ~2.64nm, possibly resulting from the stack of two molecular layers, which might contribute to the increased hydrodynamic size measured by DLS. Overall, SL9-EAK16-II formed stable nanofibers either in the aqueous solution with or without salt, or in culture medium, which was a desirable characteristic for an ideal peptide-antigen delivery system[44].

Table 3-1 Quantitative analysis of particles on AFM images for SL9-EAK16-II self-assemblies in different solvents

	Water	**Medium**	**PBS (day0)**	**PBS (day1)**
Height (nm)	**1.37 ± 0.15**	**1.32 ± 0.16**	**1.28 ± 0.11**	**2.64 ± 0.20**
Width (nm)	**8.04 ± 1.21**	**7.70 ± 1.23**	**9.15 ± 1.60**	**9.78 ± 1.78**

3.3.2 Self-assembling SL9-EAK16-II showed higher resistance to extracellular proteases or intracellular peptidase

We compared the degradation rate of SL9 and SL9-EAK16-II in the buffers consisting of different content of FBS, by tracking the remaining amount of peptide with RP-HPLC after various incubation times, as summarized in Fig. 3-6(A-C) for 10%, 50% and 100% FBS, respectively. For SL9 alone, it was degraded rapidly by FBS, with half-life decreasing from 30mins to 10mins when FBS content in buffer increased from 10% to 100%; after 2 hours, almost rare SL9 could be detected. In contrast, the degradation of

SL9-EAK16-II in serum proceeded at a significantly slower rate leaving ~70% peptide detectable in 100% FBS after an incubation time of 2 hours.

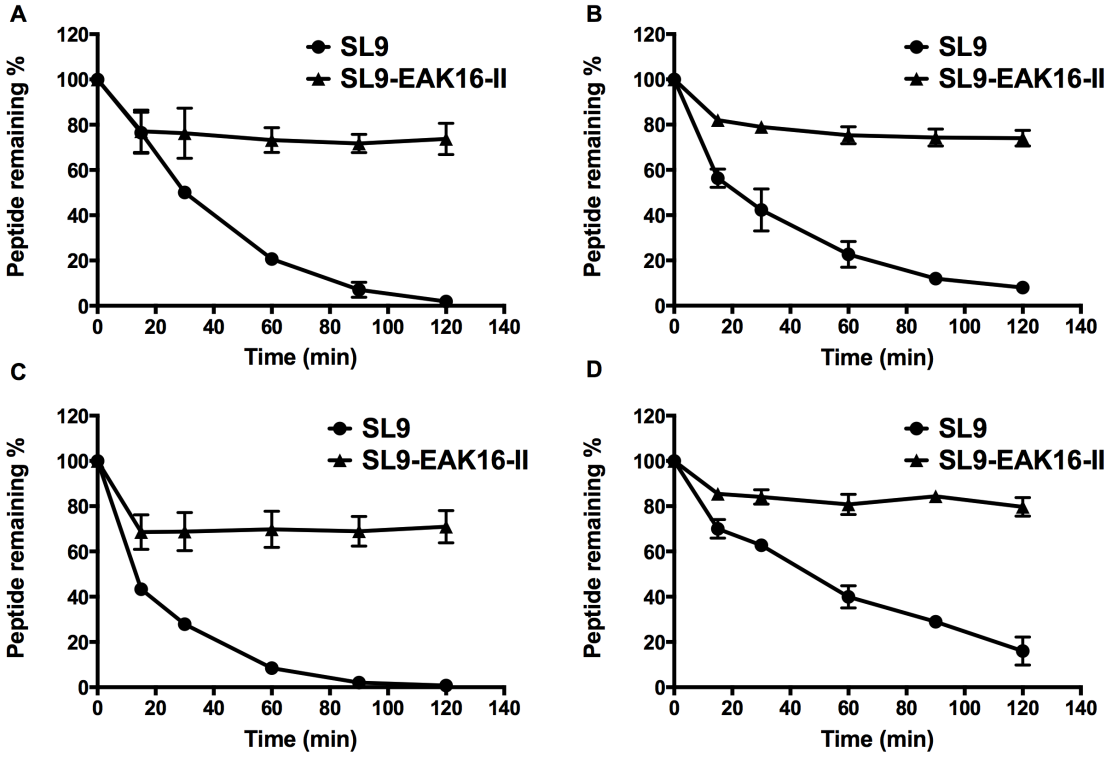

Figure 3-6 Stability comparisons between SL9 and SL9-EAK16-II in 10%FBS (A), 50% FBS (B), 100% FBS (C), and thimet oligopeptidase (TOP) (D). The intial concentration of peptide at fixed at 23μM, while the molar ratio of peptide to TOP was at 500:1.

Afterwards, we further determined the degradation fate of these two peptides with the presence of an intracellular peptidase, thimet oligopeptidase (TOP) that was found as a primary cytosolic oligopeptidase in DCs to destroy antigenic peptide and limit the extent of MHC I antigen presentation *in vivo*[201,203]. As show in Fig. 3-6D, SL9 was hydrolyzed quickly by TOP with ~17% remaining after 2 hours incubation, while the self-assembling SL9-EAK16-II was more persistent in TOP, leaving approximately 80% peptide intact after 2 hours. This significant stability of SL9-EAK16-II in TOP implied the nanostructure could sustain the antigen level in the cytosol, which could prolong the cross-presentation of exogenous antigen by DCs to stimulate T cells.

3.3.3 SL9-EAK16-II induced stronger SL9 specific CTL response than SL9 in vitro.

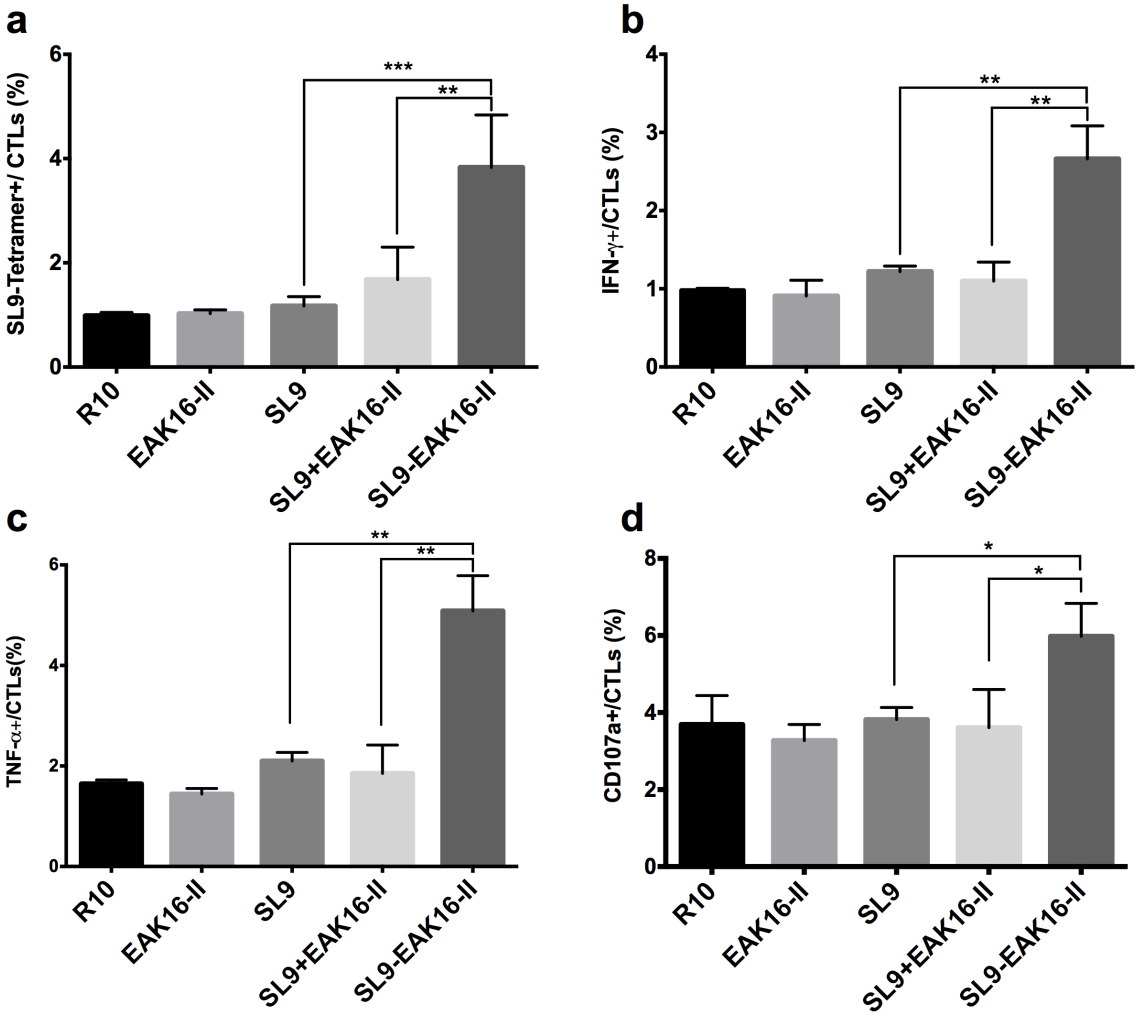

Figure 3-7 *Ex-vivo* generated MDDCs were treated with different antigens, including R10 (blank control), EAK16-II, SL9, mixture of SL9 and EAK16-II, and SL9-EAK16-II for 24h, which then co-cultured with PBMCs from HLA-A2 HIV-1 infected patents for additional 7days. SL9-specific CTL response were revealed by SL9-tetramer and intracellular cytokine staining with flow cytometry. The data was shown as the frequency of CTLs binding SL9-tetramer (a), or expressing IFN-γ (b), TNF-α (c) or CD107a (d). The experiments were carried out with PBMCs from 5 HIV-1 infected patients. *: $p \leq 0.05$, **: $p \leq 0.01$, ***: $p \leq 0.001$.

These physicochemical characterization results confirmed the stable nano-fibrillar structure effectively protected the loaded epitope from degradation. To examine if this enhanced stability would be beneficial to recall the SL9 specific CTL response, we tested the efficiency of the MDDCs pulsed with different antigens to stimulate CD8+ T cells. *Ex-vivo* generated MDDCs were treated with SL9, EAK16-II, the mixture of SL9 and EAK16-II or SL9-EAK16-II, and then co-cultured with autologous PMBCs, which was followed by re-stimulation with SL9-pulsed autologous EBV-immortalized B cells as targeting cells. The antigen specificity of the activated CD8+ T cells was determined by staining the cells with fluorophore labeled SL9-tetramer. The frequency of SL9-tertramer positive CD8+ T cells was quantified with flow cytometry. As shown in Fig. 3-7a, the MDDCs pulsed with SL9-EAK16-II stimulated more SL9-specific CD8+ T cells than the ones treated with other antigens. The functionality of the SL9 specific CTLs was further assessed. The frequency of SL9-specific CTLs that expressed IFN-γ, TNF-α, or CD107a was measured and shown in Fig. 3-7 (b-d). SL9-EAK16-II stimulated significantly more functional CTLs than either SL9 or EAK16-II. Furthermore, the mixture of SL9 with EAK16-II did not bring about any improvement in CTL response compared to SL9 alone, suggesting the peptide bond linking between SL9 and EAK16-II was critical for the enhanced CTL response.

3.3.4 SL9 in nanostructure form was more persistent in MDDCs

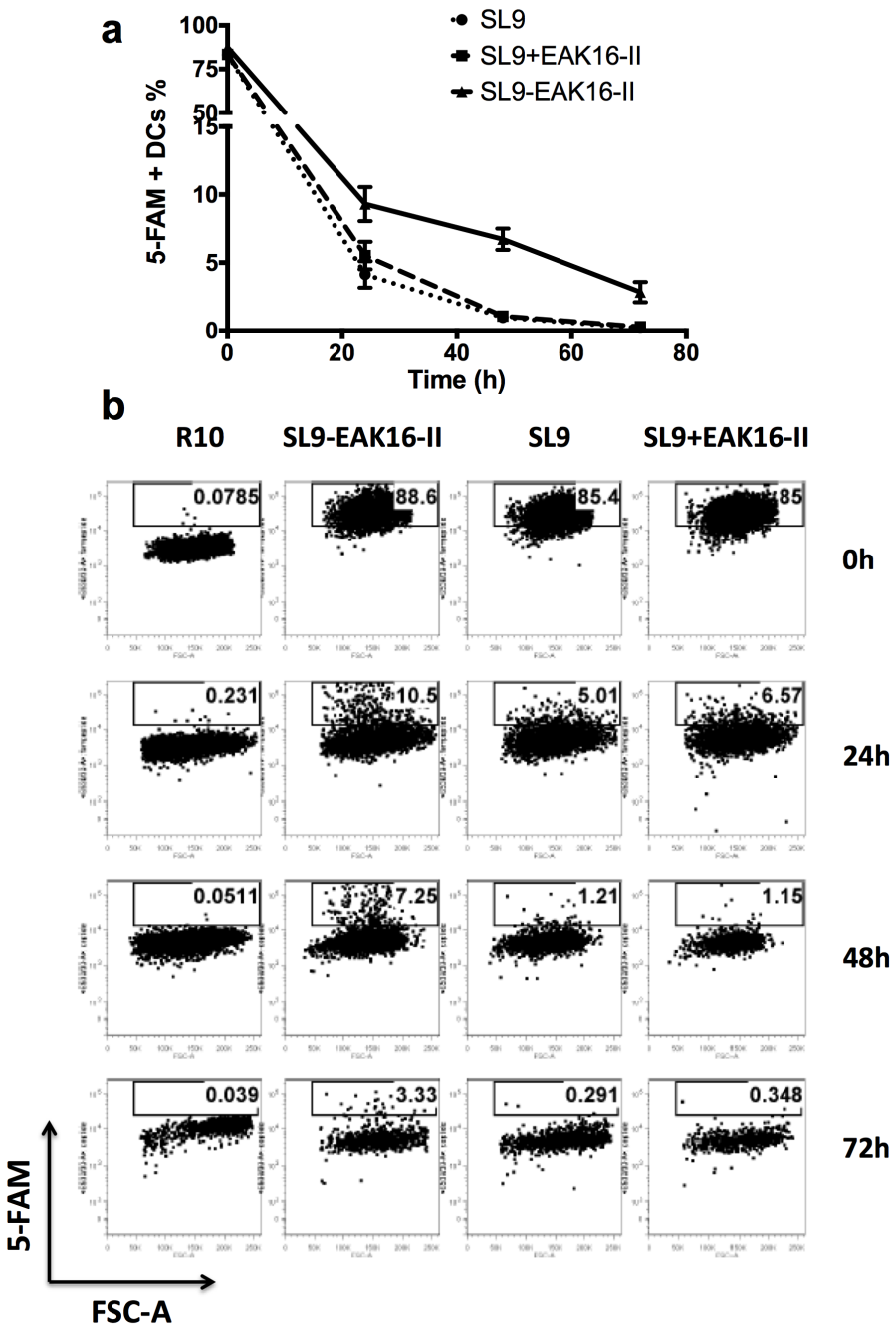

Figure 3-8 MDDCs were pulsed with 5-FAM-SL9-EAK16-II, 5-FAM-SL9, mixture of 5-FAM-SL9 and EAK16-II, or medium R10 as blank control, which were further maturated with cytokines cocktail. After 12h, MDDCs were thoroughly washed to remove the free peptides, and further tracked 5-FAM+ MDDCs after certain intervals with flow cytometry (a). The data point was shown as mean ± SD (n=3). A representative flow cytometry profile from one experiment is provided (b).

To determine whether the enhancement in CTL response facilitated by SL9-EAK16-II nanofibers was associated with prolonged presentation by DCs, the persistence amounts of fluorophore labeled peptides inside DCs were tracked over time. MDDCs were pulsed with 5-FAM labeled SL9, SL9-EAK16-II or the mixture of 5-FAM-SL9 and EAK16-II for 12 hours, which were then thoroughly washed to remove the free peptides. At certain time, the MDDCs were analyzed by flow cytometry for intracellular fluorescence level, which was summarized in Fig.3-8. Immediately after peptide loading, SL9 either alone or conjugating with EAK16-II was taken up efficiently by MDDCs (almost 90% 5-FAM+ DCs), which did not show significant difference in the percentage of 5-FAM+ MDDCs. 24 hours later, the amounts of the peptides remaining inside MDDCs decreased dramatically, however, more SL9-EAK16-II remained in MDDCs. After 80 hours' incubation, SL9-EAK16-II was still detectable in ~3.33% MDDCs.

3.3.5 SL9-EAK16-II more efficiently escaped from endocytic compartments to cytosol

Though short synthetic CTL epitope is possibly cross-presented by DCs via directly extracellular binding with MHC I expressed on the surface of DCs[204], extensive experimental evidences suggest the exogenous antigens are necessarily processed in cytoplasm to be efficiently cross-presented[205]. Therefore, confocal microscopy was then utilized to observe the intracellular distribution of 5-FAM-SL9 or 5-FAM-SL9-EAK16-II inside DCs at different time intervals. Immature MDDCs were loaded with 5-FAM labeled SL9 or SL9-EAK-16-II for 4 h, which were washed thoroughly, then stained with Lysotracker deep red to label acidic organelles (endosome and lysosome) immediately or after additional 12h incubation.

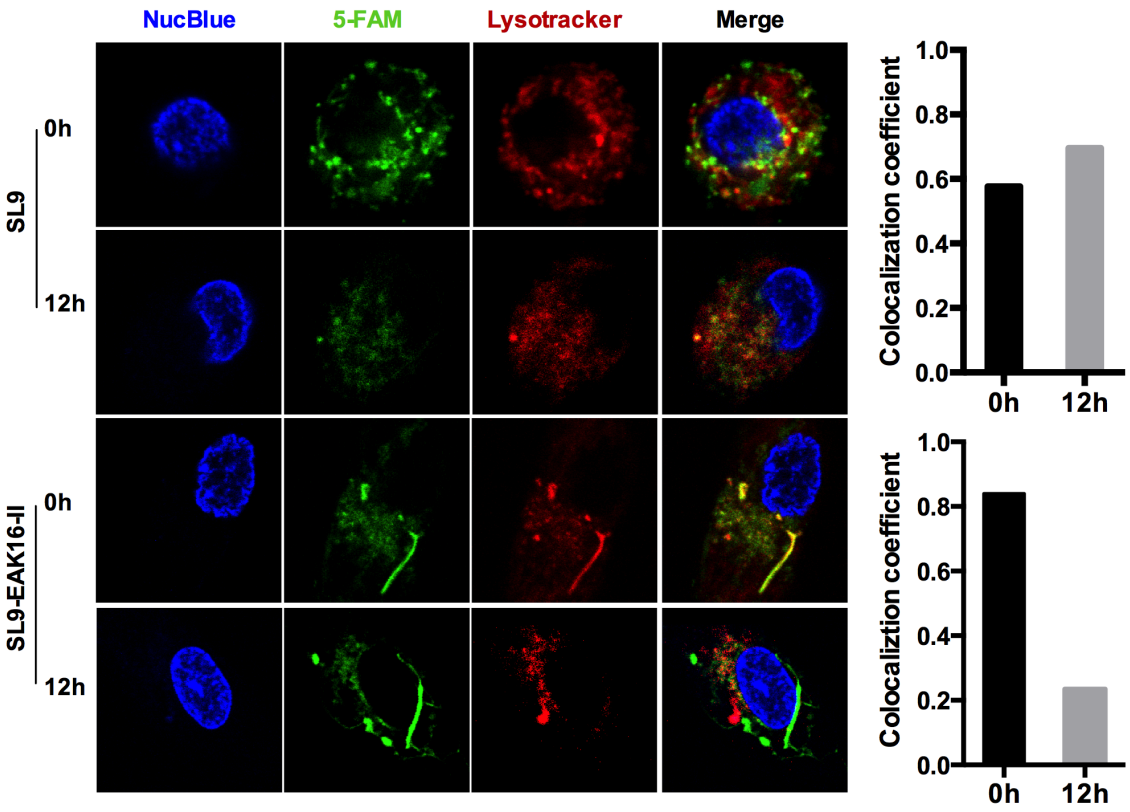

Figure 3-9 MDDCs were pulsed with 5-FAM labeled peptides, and maturated. After 4h, MDDCs were washed with PBS to remove the free peptides, and observed under confocal microscopy immediately (panels labeled as 0h) or re-cultured in fresh medium for another 12h (panels labeled as 12h). Prior to microscopy, acidic organelles were stained by Lysotracker deep red, and nuclei were stained with NucBlue. The co-localization coefficients between green and red channels were calculated with ImageJ software based on 20cells per sample.

As shown in Fig. 3-9, both 5-FAM-SL9 and 5-FAM-SL9-EAK16-II were internalized by MDDCs efficiently, however, the intracellular distributions varied. For the DC pulsed with the epitope, the fluorescent peptide was observed in both acidic compartments (stained with red fluorescence) and cytoplasm, suggesting both endocytosis and direct entry mechanism involved in the uptake. After 12 hours, the fluorescent intensity from the peptide faded, leaving only weak fluorescence observed and located in endo-lysosomes. By contrast, the 5-FAM-SL9-EAK16-II was taken up by MDDCs mainly through endocytosis pathway, indicated by the co-localization coefficient (>0.8) between

the red and green channels; with further incubation, the co-localization coefficient decreased to almost 0.2, suggesting the peptide escaped from the endo-lysosomes to the DC's cytosol. This endosomal escape implied a cytosolic cross-presentation mechanism for the conjugating peptide[134].

3.4 Discussion

In this study, we demonstrated that directly conjugating an HIV-1 CTL epitope SL9 with self-assembling moiety EAK16-II significantly enhanced the immunogenicity of the epitope *in vitro*. Our results suggested this enhancement mostly benefited from the prolonged cross-presentation of the exogenous epitope which was delivered to the cytoplasm of DCs by the self-assembling peptide.

By solid phase peptide synthesis, the epitope SL9 was easily loaded with the fibril forming sequence (EAK16-II). Physicochemical characterizations including morphology and CAC, demonstrated the addition of the epitope into the EAK sequence did not impair the self-assembling behavior, though altered the secondary structure from β-sheet to α-helix. A similar transition was observed when EAK16-II was conjugated with other sequences; however, no mechanism has been proposed to explain it. From the initial computer modeling of the EAK sequence, a helical structure was suggested, in which the side chains of glutamic acids and lysines provided electrostatic interaction to stabilize the conformation[206]. Moreover, after conjugation, the amino acid flanking the N-terminus of the peptide changed from Alanine to Serine. The side chain of Serine but not Alanine could form hydrogen bond with the free NH group of peptide helix (from the first four residues in helix), which might also stabilize helix formation in peptide[207]. More precise explanation could be obtained with molecular simulation.

The nanostructure formed from the conjugating peptide protected the epitope from the proteolytic degradation, thus could be conserved for longer time (up to 72h) inside mature MDDCs. It was reported when PLGA microparticles were loaded with ovalbumin (OVA), they served as intracellular antigen reservoirs, providing sustained MHC class I presentation up to 96h, which was described as a major advantage over soluble antigen[65]. This prolonged antigen presentation has been shown highly correlated with the enhance T cell response *in-vitro* and *in vivo*[208,209]. Moreover, the process time for professional APCs such as DCs to encapsulate the exogenous antigen in peripheral and migrate to lymphoid tissues has been estimated last to 24-48h[210]. Before the antigen loaded DCs contact with T cells in lymphoid tissues, to keep the quantity of epitope-MHC complexes on DCs above certain level plays an important role for the potent stimulation towards T cells. Therefore, the prolonged antigen cross-presentation of the conjugate peptide could contribute to the augmented immunogenicity.

Furthermore, our confocal microscopy results implied the conjugating peptide SL9-EAK16-II underwent a different presentation pathway from the epitope SL9. Depending on the binding affinity, two distinct pathways for exogenous epitope loading to MHC I molecule have been demonstrated, as direct binding on the surfaces of APCs, or internalization and loaded with MHC I molecules in endoplasmic reticulum (ER), with the latter one involved in the cross-presentation of SL9 to CTLs[204,211]. Consistent with these reports, our finds suggested that SL9 would be internalized by DCs through both endocytosis and direct penetration into cytoplasm. Moreover, the fraction of SL9 inside endosomal compartments did not escape to the cytosol. By contrast, SL9-EAK16-II nanofibers were dominantly internalized to endosomal compartment, and subsequently

escaped to the cytoplasm. The endosomal escape of epitope-bearing nanofibers implied a cytosolic pathway for the cross-presentation of SL9-EAK16-II, which was suggested as more efficient[120]. The liposome leakage assay (Appendix Fig.4) illustrated different membrane permeability for the two peptides: At pH7.0, SL9 caused more leakage, however, this was abolished when pH decreased to 5.0, while the permeability of SL9-EAK16-II was slightly decreased with lower pH. The different membrane permeability of SL9 at different pH values might explain the entrapment of SL9 inside endolysosomes after internalization. Moreover, the membrane disrupting activity was rarely discussed for the peptide EAK16-II or any peptide containing the same sequence as EAK16-II. From our results, the moderate membrane permeability of the SL9-EAK16-II promoted the endosomal escape of the antigen, but without causing cytotoxicity. Nevertheless, the mechanism of this membrane penetration remains unclear, which should be studied in future. These results show that EAK16-II can offer not only protection against extra-/intracellular degradation that elongated the persistence of epitope inside DCs, but also enhanced endosomal escape for a more efficient cross-presentation pathway.

However, the conjugating peptide SL9-EAK16-II did not show any maturation activity against MDDCs *in-vitro*, which might cause immune tolerance. Thus, the immunogenicity of SL9-EAK16-II was examined in the form of DC based vaccine, i.e. *ex vivo* generated MDDCs were pulsed with SL9-EAK16-II, further maturated with cytokine cocktails, and then used to simulate T cells. By contrast, several biodegradable materials, such as γ-PGA-Phe, PLGA nano- or micro-particles, liposomes, or cationic polystyrene microparticles, have been reported possessing the ability to maturate DCs[13]. However, the mechanism for the activation towards DCs from these materials remains unknown, and

even reverse results were observed for the same materials[61]. The self-assembling peptide, Q11, when coupled with a model peptide antigen from OVA, significantly enhanced the expression of CD80 and CD86 on DCs *in vivo*[212]. Since the conjugating peptide SL9-EAK16-II exhibits a similar nano-fibrilar structure as OVA-Q11, we expect to observe a similar DC maturation property if SL9-EAK16-II was administrated into mice. Compared to this controversial self-adjuvanting strategy, the combination of TLR agonists with nanoparticle-based delivery system appears to be more promising for the design of peptide-based vaccine. Therefore, to harness SL9-EAK16-II with DC maturation activity, the incorporation of TLR agonist into the EAK-based system would be introduced in the following chapter.

Chapter 4 Self-assembling peptide for co-delivery of HIV-1 CD8+T cell epitope and Toll-like receptor 7/8 agonists R848 to induce maturation of monocyte derived dendritic cell and augment polyfunctional cytotoxic T lymphocyte (CTL) response

Abstract

A peptide based vaccine that incorporates one or several highly conserved CD8+ T cell epitopes to induce potent cytotoxic T lymphocyte (CTL) response is desirable for some infectious diseases, such as HIV-1 (human immunodeficiency virus-1), and cancers. However, the CD8+ T cell epitope is often weakly immunogenic, and thus requires a specific adjuvant or delivery system to enhance the efficiency. Here we investigated the use of self-assembling peptide EAK16-II based platform to achieve the co-delivery of CD8+ T cell epitope and TLR7/8 agonists (R848 or R837) for augmenting DCs maturation and HIV-1 specific CTL response. HIV-1 CTL epitope SL9 was conjugated with EAK16-II to obtain SL9-EAK16-II, which further spontaneously co-assembled with R848 or R837 in aqueous solution, forming co-assembled nanofibers. Fluorescence spectra and calorimetrical titration revealed the interaction between SL9-EAK16-II assemblies and R848 or R837 via hydrogen bonding and hydrophobic interaction, with the binding affinity (dissociation constant K_d) of 0.62 μM or 0.53 μM, respectively. Furthermore, *ex vivo* generated DCs from HIV-1+ patients pulsed with the SL9-EAK16-

II/R848 nanofibers stimulated significantly more polyfunctional SL9 specific CTLs, compared to the DCs pulsed with SL9 alone or the mixture of SL9 and TLR agonist. Our findings suggest self-assembling peptide EAK16-II might be used as a new delivery system for peptide based vaccine.

4.1 Introduction

Synthetic peptides have attracted considerable attention as antigens for subunit vaccine design, since they offer several advantages over live or attenuated pathogenic microorganisms, including lower risk of reverting to virulent form, ease of manufacturing, reduced cost, and more precise control of antigen specific immune response[23,24]. However, owning to the rapid degradation and lack of "danger signal" to maturate dendritic cells (DCs)[184], it is particularly challenging for exogenously administrated peptide to induce potent cytotoxic T lymphocyte (CTL) response, which is considered to be critical for effective vaccination against some infectious diseases, such as Human Immunodeficiency Virus (HIV-1), hepatitis C, and cancers[8,184]. To address this issue, a common approach has been to use micro- or nanoparticles to co-deliver the antigens and the immnostimulatory molecules, such as toll like receptor (TLR) agonist to target the same DC, which have a synergistic effort in enhancing antigen specific CTL reseponse[61,94,133–135,213].

Self-assembling peptide is rapidly becoming a synthetic delivery platform of choice, which has been explored for a variety of biomedical and biotechnology applications, such as regenerative medicine[17], tissue engineering[18,156], and antigen delivery[10,173,193]. In these applications, the self-assembling peptides provide several advantages, including biostability, biocompatibility, synthetic definition, and controllability over the structure

of nanoparticles. EAK16-II (AEAEAKAKAEAEAKAK), an ionic-complementary peptide, self-assembles into β-sheet rich nanofibers with separated hydrophilic and hydrophobic faces, driven by hydrophobic interaction from Alanine (A) and electrostatic interaction between oppositely charged Glutamine (E) and Lysine (K)[174]. The spontaneously organized nanofibers are resistant to acidic environment with the presence of proteases, without inducing immune response when injected into mice[20,174]. These characteristics make it ideal for protecting and delivering antigenic peptide to DCs. Moreover, as a delivery vehicle, EAK16-II can incorporate with cargos by either direct conjugation[178], or co-assembling process via non-covalent interactions[214]. Combing these two strategies, it provides an opportunity to achieve co-delivery of CTL epitope and TLR agonist.

Therefore, in the current study, we conjugated EAK16-II with an HIV-1 specific CTL epitope SL9 to obtain SL9-EAK16-II, which further co-assembled with TLR7/8 agonist, R848 (Resiquimod) or R837 (Imiquimod) to form a tripartite formulation (CTL epitope, immune potentiator and delivery carrier). The co-assembly mechanism was investigated with fluorescence microscopy and calorimetric titration. The SL9 specific CTL response induced by the tripartite formulation was examined as a DC-based vaccine.

4.2 Materials and Methods

4.2.1 Materials

All peptides were synthesized as described in previous chapter. Complete DC medium: serum-free DC medium (CellGenix, Portsmouth, NH) supplemented with 800U/mL GM-CSF, 1,000U/mL IL-4 (R&D system), 100U/mL penicillin, 100μg/mL streptomycin, and

2mM L-glutamine (Life techenology); Complete RPMI-1640 medium R10: RPMI1640 (Life Technologies) supplemented with 10% human AB serum (Sigma), 100 U/ml penicillin, 100 μg/mL streptomycin, and 2mM L-glutamine; DC maturation cytokine cocktail: 5ng/mL (final concentration) TNF-α (R&D System), 5ng/mL IL-1β (R&D System), 1μg/mL prostaglandin E2 (Sigma, Oakville, ON, Canada), and 150ng/mL IL-6 (R&D System); Dye used in samples preparation for confocal microscope: Lysotracker Deep red, Nucblue Live Ready probes reagent (Life technology)

The materials and main procedures for *in-vitro* study in this chapter were similar as described in Chapter 3.

4.2.2 Methods

Peptide/TLR ligand complex preparation The peptide was dissolved in Milli-Q water with 30mins sonication in water bath at room temperature and incubated overnight. Then TLR agonist (R837 or R848) was dissolved in THF at 2mM, which was pipetted into glass vials, followed by solvent evaporation. After the peptide solution was added, the mixture was stirred overnight.

Morphology characterization with Atomic force microscopy (AFM) and Transmission electron microscopy (TEM) 50μL peptide or peptide/TLR agonist complex solution was dropped on the surface of a freshly cleaved mica sheet for 5mins. Then free sample was removed by blotting, and washed with 300μL pure water. After air-dry of several hours, AFM imaging was taken at room temperature using the Peak Force tapping mold on a Dimension Icon AFM (Bruker, Santa Barbara, CA). Additionally, TEM was utilized to confirm the nanostructure visualized from AFM. Briefly, 10μL peptide solution was applied to a 400 mesh Formvar (with carbon reinforced) coated

copper grid for 3-5 minutes, followed by negative staining with 10μL 2% uranyl acetate, blotted drying, and analysis on TEM (Philips CM10 TEM, operating at 60KeV).

ANS fluorescence assay 8-anilinonaphthalene-1-sulfonic acid (ANS) solution was prepared in a phosphate buffer (10mM, pH=6.0) at a concentration of 10μM, which was mixed with equal volume of the freshly prepared SL9-EAK16-II solution (0.10mM) or pure water. 70μL of the relevant solution was transferred to a quartz microcell and tested on the Photon Technology International spectrafluorometer (Type QM4-SE, London, Canada) with a continuous xenon lamp as the light source. The fluorescence spectra of ANS were collected from 420 to 670nm with the excitation at 360nm. The excitation and emission slit widths were set at 0.5mm and 1.25mm, respectively.

Isothermal Titration Calorimetry (ITC) For all ITC experiments performed on Nano-ITC (190μL, TA instruments, New Castle, DE) at 298K, Milli-Q water was filled in reference cell. 400μM SL9-EAK16-II was prepared in Milli-Q water with 30 mins' sonication and followed by overnight incubation, while R837 or R848 was prepared at 20μM by stirring overnight to dissolve completely, which was further adjusted pH to the same value as the one of the peptide solution (pH=6.0) using acetic acid. All solutions were degassed for 30mins, before 51μL of peptide solution was loaded into the syringe, and 300μL R837 or R848 was placed in the sample cell. The syringe was set to a stirring speed at 250rpm, after equilibrium time for baseline acquirement, 31 injections were performed with 200s' interval. The first injection volume was 1.0 μL and the heat signal was ignored in the data analysis so as to compensate the error generated from insertion of needle, leakage of the peptide solution from syringe, and so on; the following injections were set at 1.5μL volume each. Blank titrations of the peptides into water (pH was

adjusted to 6.0 with acetic acid) were performed to measure the heat of dilution of the peptide, which was subtracted from the integration data prior to curve fitting. Origin 8 software was used to fit the heat profiles, assuming one-site binding. For each TLR ligand, the experiments were conducted three times.

Fluorescence spectroscopy A Photon Technology International spectrafluorometer (Type LS-100, London, Canada) with a pulsed xenon lamp as light sauce was utilized to measure the fluorescence spectra of R837 or R848 to study the interaction between peptide and agonist. Samples (70 μL) were transferred to a quartz cell (1cm × 1cm), which were exited at 245nm for R837, 248nm for R848 respectively. The emission data was collected in the range of 300-450nm. Different volumes of SL9-EAK16-II solution were added to the fixed agonist concentration at 15μM to obtain peptide/agonist molar ratio from 0.5:1 to 6:1.

Circular Dichroism (CD) spectrum Far-UV circular dichroism spectra were measured at 298K with Jasco J-815 CD spectrometer (Tokyo, Japan) for the secondary structure of peptide and peptide/agonist complexes. 150μL sample solutions were scanned in a 0.1cm quartz cell from 260nm to 190nm, with solvent spectrum as baseline for data collection. The raw CD ellipticity (in millidegree) was converted to molar ellipticity (deg cm^2 $dmol^{-1}$). The results reported here were the averages of three replicates.

Particle size measured by dynamic light scattering (DLS) The hydrodynamic diameter of sample was assessed by DLS on a Zetasizer Nano ZS (Malvern Instruments, Malvern, UK) equipped with a 4mW He-Ne laser operating at 633nm. 50μL solution was added in low volume disposable polystyrene cuvette and the scattered light intensities were

collected at an angle of 173°. Three independent measurements were performed to generate the intensity based size distribution profile.

***Ex vivo* Generation of monocyte-derived dendritic cells (MDDCs)** The procedure is similar as the one described in Chapter 3. Monocytes were isolated from peripheral blood mononuclear cells (PBMCs) with Human Monocyte Isolation Kit-II (Miltenyi, San Diego, CA) and cultured in complete DC medium for 5 days to generate immature MDDCs.

Visualization of uptake of SL9-EAK16-II/R848 by Confocal microscope The peptide SL9-EAK16-II was labeled with 5-carboxyfluorescein (5-FAM) at N-terminal, which then co-assembled with R848 or R837 as described above. Immature MDDCs were seeded in 4-well Lab-Tek chamber slide with 10^6 cells in 450μL complete DC medium per well and incubated at 37°C for 24h. Then, MDDCs were pulsed with 5-FAM-SL9-EAK16-II/R848 for 0.5h, followed by staining the intracellular acidic organelles with Lysotracker Deep red. After additional 0.5h incubation, cells were washed with PBS and re-cultured in fresh medium. Before the visualization under confocal microscopy, one drop of Nucblue Live Ready probe reagents were added per well and incubated for 10mins to stain DCs nuclei. All images were acquired using Zeiss LSM700 laser scanning confocal microscope.

Maturation of MDDCs Immature MDDCs were collected and seeded in 96-well plate at 37°C with 10^5 cells in 50μL complete DC medium per well, which were treated by SL9, the mixture of SL9 and EAK16-II or SL9-EAK16-II with the absence or presence of the agonists (peptide final concentration at 0.03mM), or DC medium as control. After 24h,

the MDDCs were collected and stained with anti-human CD83 mAbs. The percentage of CD83 expressing cells in MDDCs was determined by flow cytometry.

HIV-1 SL9 epitope-specific CD8+ T cell response Following the procedures described in Chapter 3, the ex-vivo generated MDDCs were pulsed with different antigens for 24 hours, which were then washed thoroughly 3 times with complete RPMI-1640 medium, followed by co-culturing with autologous PBMCs at 1:10 ratio in medium for 7 days. The PBMCs were then stimulated with autologous EBV-immortalized B cells pulsed with SL9 for 6 h, stained with fluorochore labeled mAbs against human CD3, CD8, IFN-γ, TNF-α, and CD107a and acquired by a flow cytometer (BD LSRII, BD). CD8+ T cells expressing IFN-γ, TNF-α, and CD107a were quantified with FlowJo (TreeStar). Isotype control antibodies were used as gating control.

Statistic analysis The two-way analysis of variance (ANOVA) was used for comparison between multiple groups, with the software Prism 6.0 (Graphpad software, SD, USA). $P < 0.05$ was considered as significant.

4.3 Results

4.3.1 SL9-EAK16-II / TLR agonist co-assembled to nanofibers.

As described in Chapter 3, we conjugated SL9 at the N-termini of fibril forming moiety EAK16-II, with a flexible spacer –Ser-Gly-Ser-Gly- in between. The second structure of SL9-EAK16-II was measured as α-helix (data shown in Chapter 3). This altered secondary structure might have an impact on the self-assembly mechanism of epitope-bearing EAK16-II and its capability of delivering TLR agonists, since our previous works suggested EAK16-II stabilized hydrophobic compounds with the hydrophobic face of its

β-sheet microstructure[176,215]. Thus, prior to using the TLR agonist, we studied the hydrophobic character of the conjugated peptide with 8-anilinonaphthalene-1-sulfonic acid (ANS) as probe molecule, of which the fluorescence spectrum shifts towards lower wavelength (blue shift) with enhanced intensity in a less polar environment[216]. Fig.4-1a showed in pure water, the fluorescence spectrum of ANS had a peak located at ~524nm; by contrast, in SL9-EAK16-II solution, the emission maxima was blue-shifted to ~482nm, and the intensity increased significantly, which demonstrated the conjugated peptide aggregated in aqueous solution and the formed nanostructure could provide a hydrophobic interior to stabilize hydrophobic compounds.

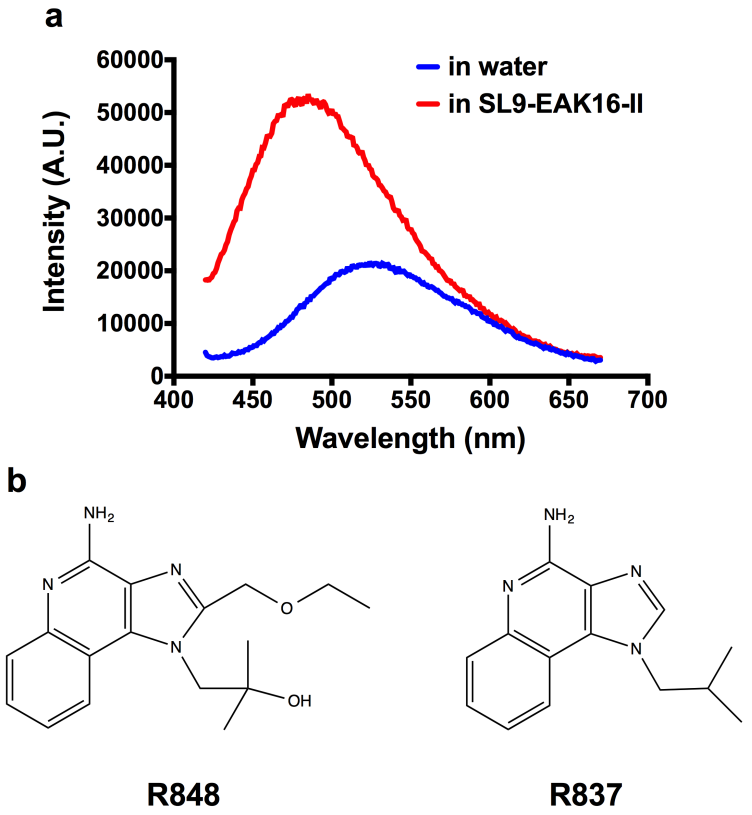

Figure 4-1 The fluorescence spectra of ANS with or without the presence of SL9-EAK16-II (b); Molecular structures of TLR 7/8 agonist R848 (left) and TLR7 agonist R837 (right).

Then, we mixed the conjugated peptide with TLR agonist (R848 or R837 as shown in Fig. 4-1b) to form the complexes/co-assemblies of SL9-EAK16-II/R848 or SL9-EAK16-II/R837, and employed fluorescence microscopy to investigate the interactions between the peptide and the agonist. The fluorescence spectra of R848 or R837 with the different peptide concentrations were determined. As presented in Fig. 4-2(upper), the fluorescence intensity of R848 increased with the addition of SL9-EAK16-II; upon the peptide concentration increasing, the intensities of the emission peaks located at ~327nm, ~343 nm increased, while the emission intensity at ~356nm barely changed. This enhancement in the fluorescence intensity could be due to the less polar environment where R848 resided. To further analyze the data, the intensity ratio of R848 emission bands (I_{327}/I_{343}) was plotted as a function of the molar ratio between peptide and agonist (Fig.4-2 lower). It was obviously observed that the intensity ratio (I_{327}/I_{343}) increased with more peptide adding, which however approached a plateau from the molar ratio of 4:1. The intersection might indicate the molar ratio for the saturation binding between R848 and SL9-EAK16-II, which was estimated as 3.28:1. The same method was applied to investigate the co-assembly between SL9-EAK16-II and R837. Since the two TLR agonists were both imidazoquinoline derivatives, the fluorescence spectra of R837 (Fig. 4-3 upper panel) exhibited a similar pattern as those of R848, however, with the emission bands blue-shifted by 3nm. And the saturation binding between SL9-EAK16-II and R837 was found at the molar ratio of 3.94:1 from Fig. 4-3(lower panel).

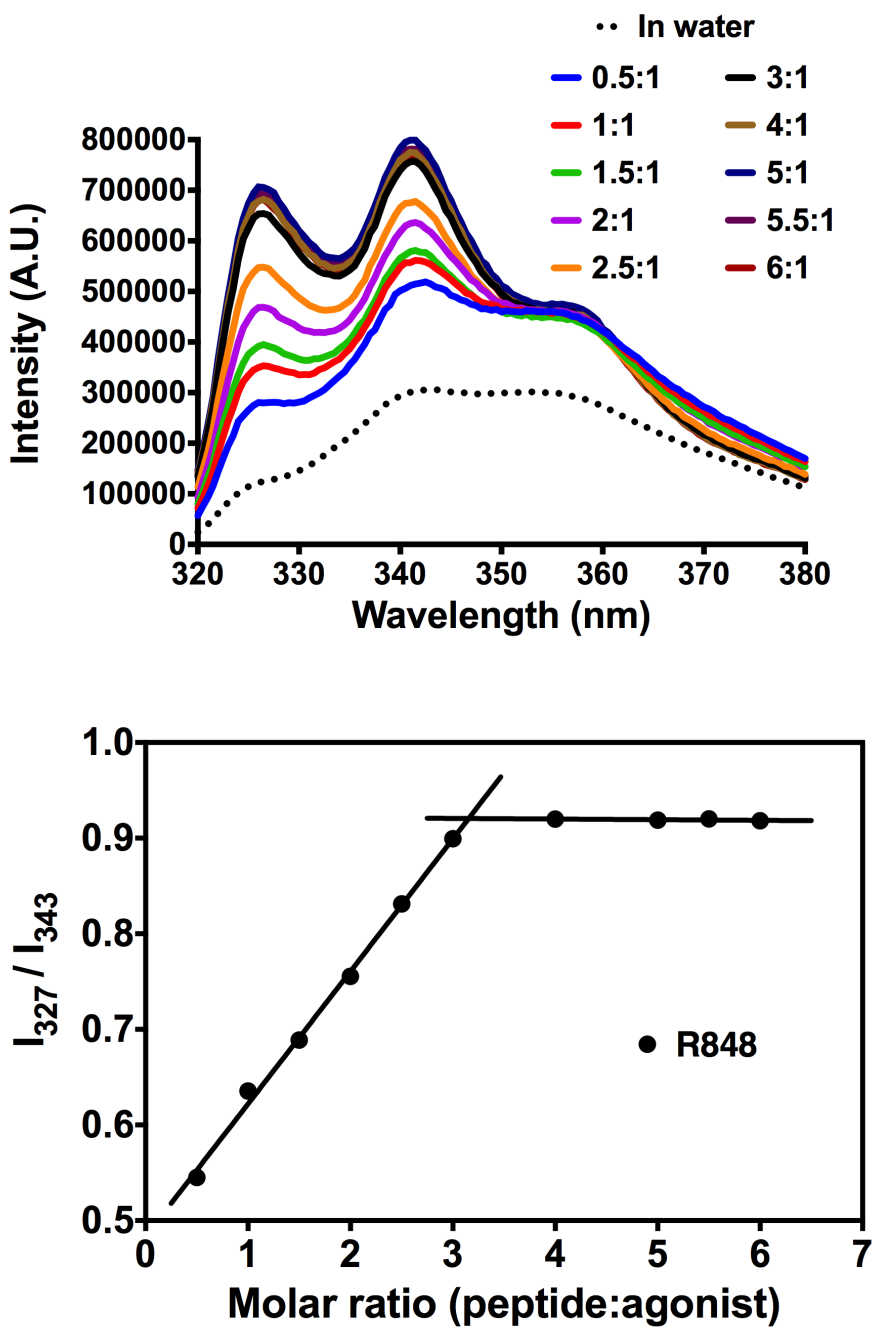

Figure 4-2 The fluorescence spectra (upper) of R848 with different concentrations of SL9-EAK16-II, in which the one for R848 in water was shown with dashed line. The emission intensity ratio I_{327}/I_{343} was plotted versus the molar ratio of peptide over R848 (lower). The concentration of R848 was fixed at 15μM.

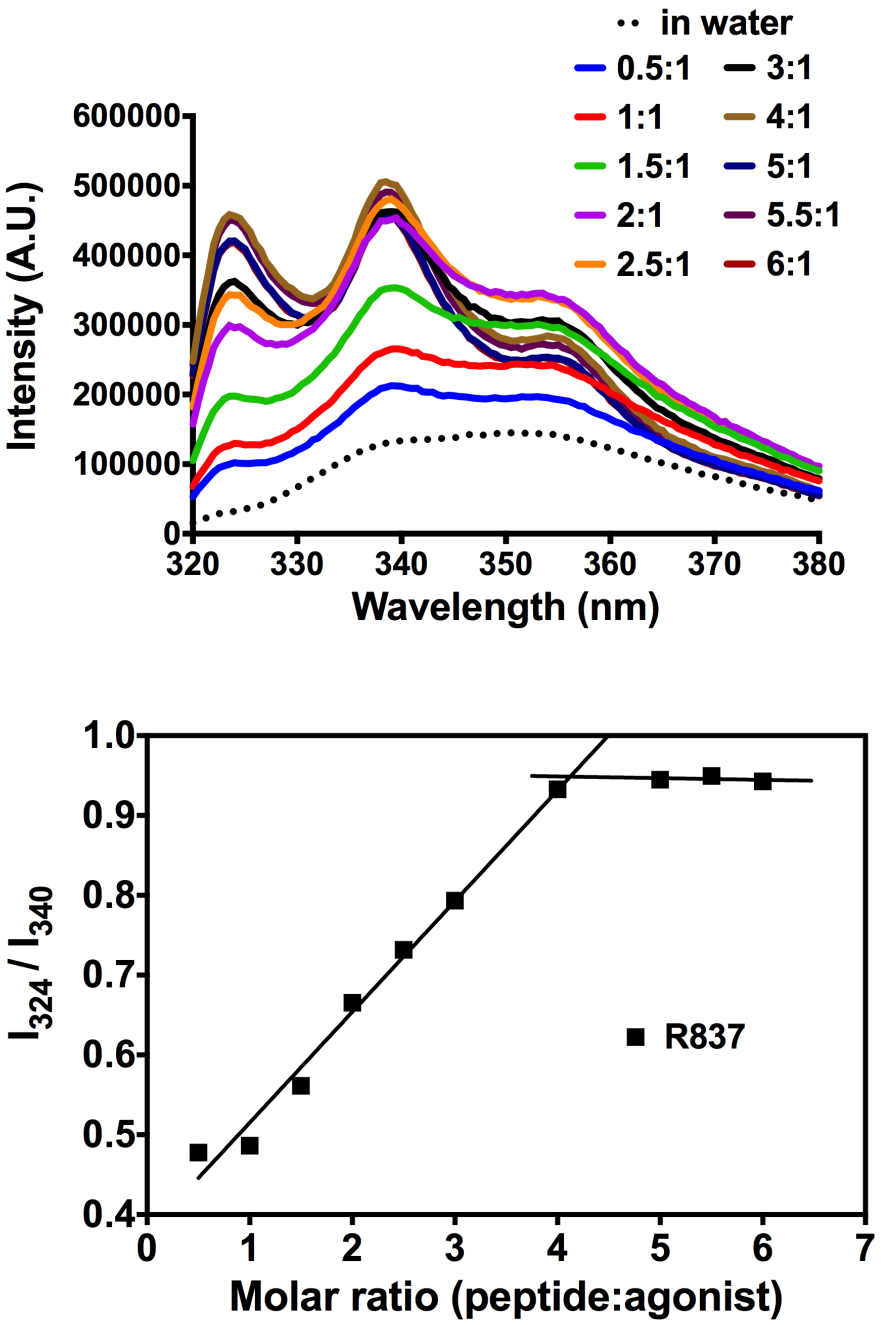

Figure 4-3 The fluorescence spectra (upper) of R837 with different concentration of SL9-EAK16-II, in which the one for R837 in water was shown with dashed line. The emission intensity ratio I_{324}/I_{340} was plotted versus the molar ratio of peptide over R837. The concentration of R837 (lower) was fixed at 15μM.

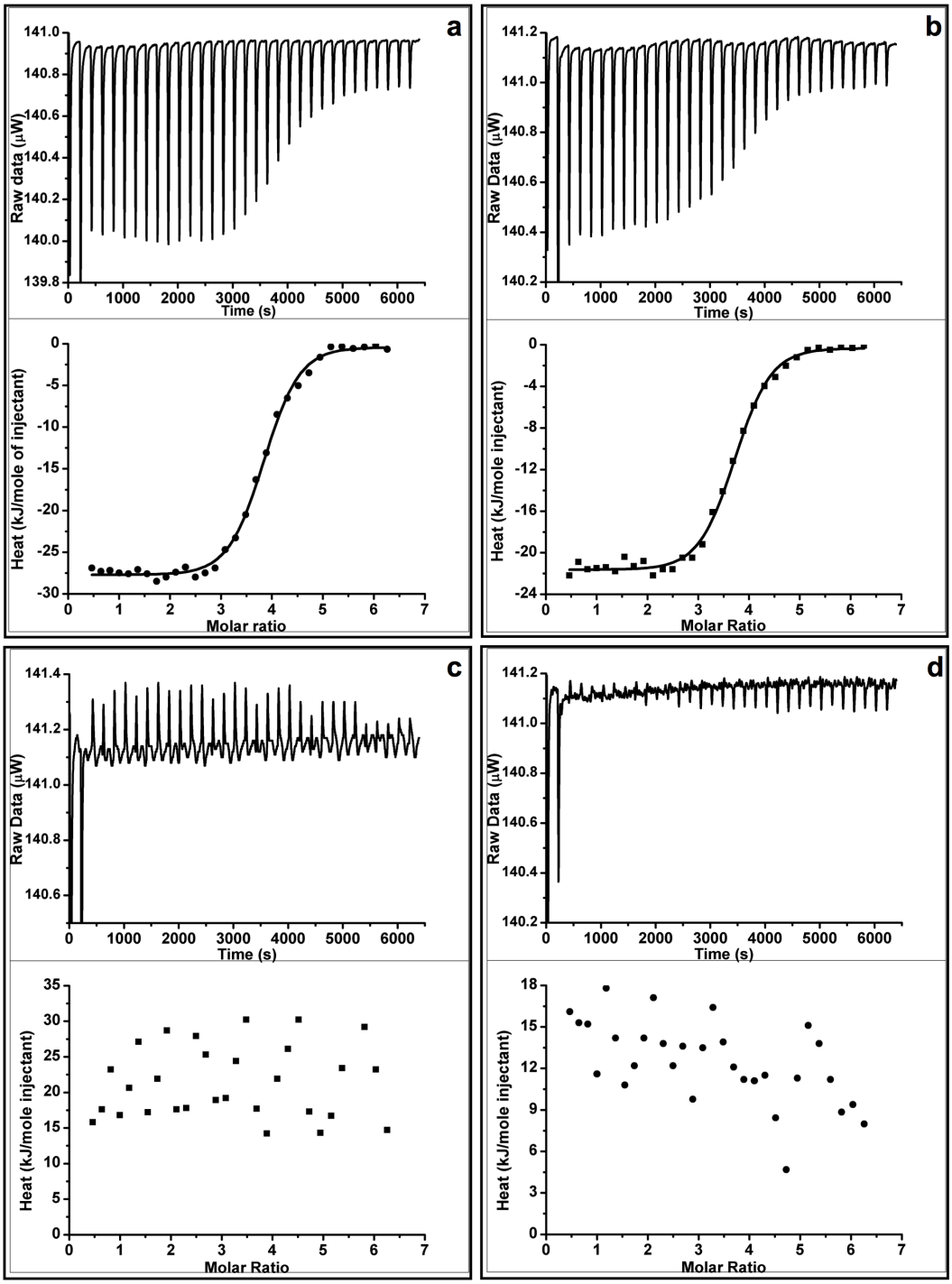

Figure 4-4 Calorimetric titration of peptide solutions into R837 (Left panel) or R848 (right panel) at 298K: SL9-EAK16-II was titrated to R837 (a), or R848 (b); SL9 to R837 (c) or R848 (d) The heat profiles was obtained by the integration of peaks, from which the heat generated in the titration of peptide into water was subtracted.

Table 4-1 Thermal dynamic parameters (mean ± SD, n=3) of SL9-EAK16-II/TLR agonist binding obtained by ITC

	R837	R848
ΔH (kJ mole^{-1})	**-28.43±0.63**	**-21.18±0.32**
ΔS (J mole^{-1} K^{-1})	**24.94±2.18**	**47.8±0.86**
-TΔS (kJ mole^{-1})	**-7.43±0.65**	**-14.24±0.26**
K_d (μM)	**0.53±0.02**	**0.62±0.06**
N	**3.94±0.20**	**3.25±0.23**

To further understand the mechanism of the co-assembly, isothermal titration calorimetry (ITC) was utilized to determine the thermodynamic parameters (including stoichiometry *N*, dissociation constant K_d, ΔH, and ΔS) of the binding between the conjugated peptide and the TLR agonist. As shown in Fig.4-4 (upper panels), the injection of SL9-EAK16-II into R848 or R837 generated exothermic peaks, which were further integrated to obtain the heat released in each titration. The heat profiles were adequately fitted to one-site binding model (Fig.4-4 lower panels). The obtained thermodynamic parameters are listed in Table 4-1. The negative enthalpy change (-21.18 kJ/mole for R848, -28.43 kJ/mole for R837) and the positive entropy change (47.8 J/mole/K for R848, 24.94 J/mole/K for R837) indicated the binding process was favored by both enthalpy and entropy, which suggested except the hydrophobic interaction, hydrogen bonding also participated in the co-assembly process[217]. However, the enthalpic and entropic contributions for the two agonists binding with SL9-EAK16-II were slightly different. From R848 to R837, the enthalpy change (ΔH) decreased by 7.25kJ/mole, while the entropic contribution (-TΔS) increased by 6.81 kJ/mole, almost compensating the favorable change in the binding enthalpy. Thus, the resulting dissociation constants did not exhibit a remarkable difference: 0.62μM for R848 vs 0.53μM for R837 (Table 4-1), indicating that the agonist

binds SL9-EAK16-II with a similar affinity. This phenomenon is usually termed as enthalpy-entropy compensation, especially when the two ligands share a similar molecular structure as here R837 and R848 do[218]. Furthermore, the stoichiometry values calculated from the ITC data were consistent with the saturation-binding ratios estimated from the fluorescence spectra: 3.25 vs 3.28 for SL9-EAK16-II/R848, and 3.94 vs 3.94 for SL9-EAK16-II/R837. Therefore, the molar ratio of peptide to agonist was fixed at 4:1 when preparing the peptide/agonist co-assemblies for the following experiments.

By contrast, the titration profiles for epitope SL9 into the two agonists (Fig. 4-4c, d) demonstrated an endothermic process, and the heat change during titration was positive and chaotic, which implied the bindings between the epitope SL9 and the agonists were negligible. These results suggested the binding between SL9-EAK16-II with the agonists was dominantly due to the EAK16-II moiety, rather than the specific sequence from the CTL epitope.

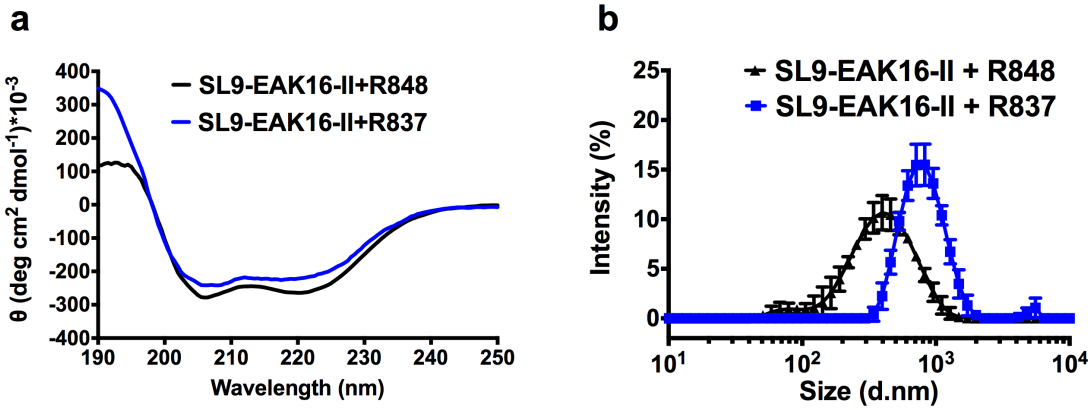

Figure 4-5 Secondary structure of the peptide in the co-assemblies of SL9-EAK16-II /R848 or SL9-EAK16-II /R837 was characterized with CD (a); the hydrodynamic size distributions of the co-assemblies were measure with DLS (b).

The further characterizations for the co-assemblies of peptide/agonist at the molar ratio of 4:1 were conducted. Fig. 4-5a presented the α-helical structure of SL9-EAK16-II in the

co-assemblies, indicating the addition of agonist did not alter the conformational structure of the peptide. Moreover, the particle size distribution of the co-assemblies was characterized with dynamic light scattering (DLS). As shown in Fig. 4-5b, the mean hydrodynamic diameter of the peptide/agonist co-assemblies was ~400nm for SL9-EAK16-II/R848, and ~710nm for SL9-EAK16-II/R837.

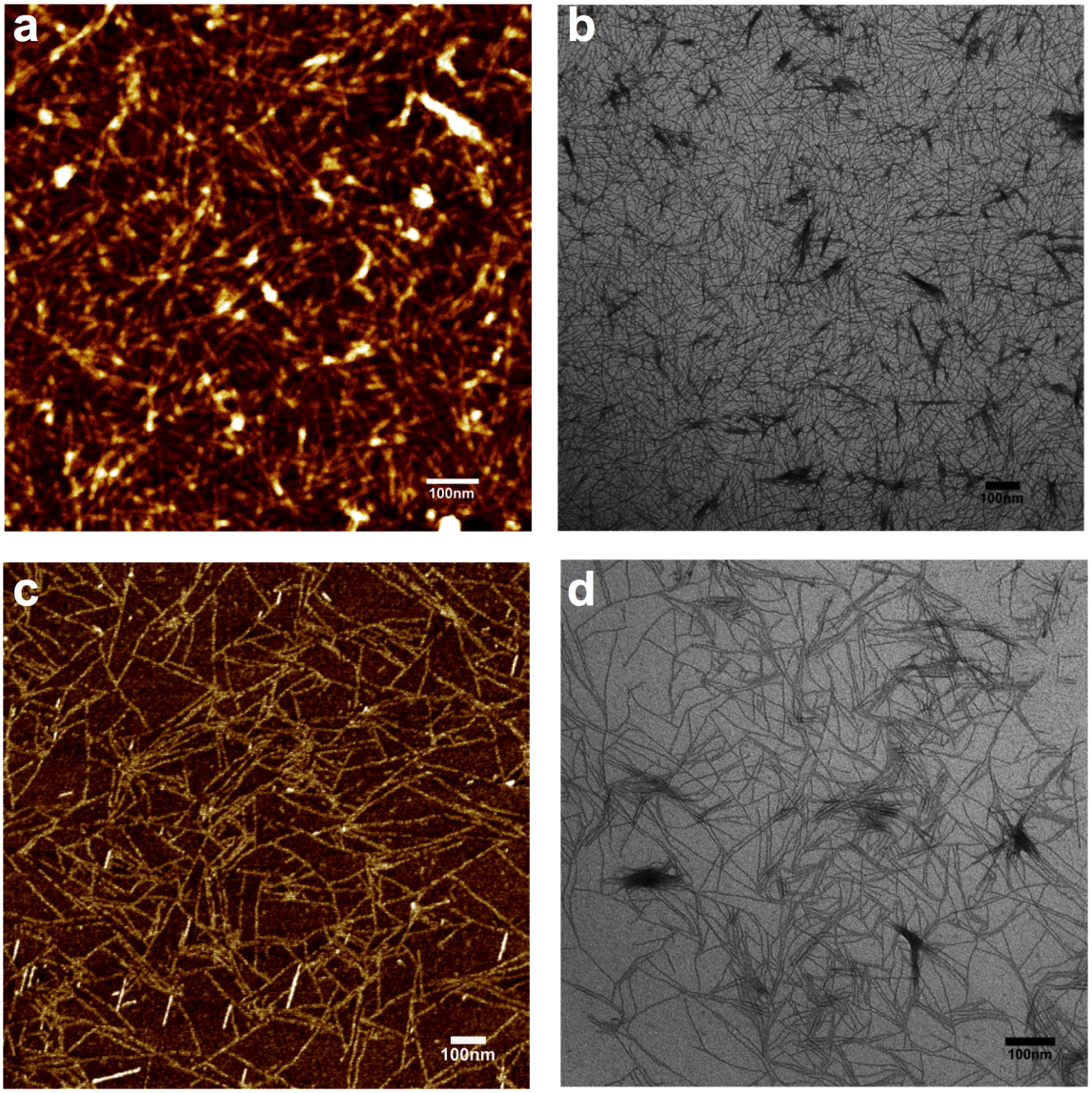

Figure 4-6 AFM and TEM were used to characterize the structures of the co-assemblies: AFM image (a) and TEM image (b) for SL9-EAK16-II/R848; AFM (c) and TEM (d) for SL9-EAK16-II/R837. The scale bars represent 100nm.

The morphology of the co-assemblies was visualized by AFM and TEM, appearing as interweaved nanofibers, for SL9-EAK16-II/R848 (Fig. 4-6a and 4-6b), or SL9-EAK16-II/R837 (Fig. 4-6c and 4-6d). We further analyzed the AFM images with software Gwyddion, obtaining the average width of the fibers, 9.2 ± 0.7nm, and 8.4 ± 0.9nm for SL9-EAK16-II/R848 or R837 respectively. This structural resemblance together with the similar binding affinity evidently suggested when the conjugated peptide SL9-EAK16-II co-assembled with R848 or R837, it followed the same mechanism. In our proposed model as depicted in Fig. 4-7, the helical peptide molecules aggregated side by side, primarily driven by the electrostatic interaction between the side chains of glutamic acid and lysine, as well as the hydrophobic interactions provided by alanine and the non-polar amino acids in the epitope sequence; the agonist was buried and stabilized within the hydrophobic faces of the peptide helices, via hydrophobic interaction and hydrogen bonding, as suggested by the evidences from the study of fluorescence spectra and calorimetric titration.

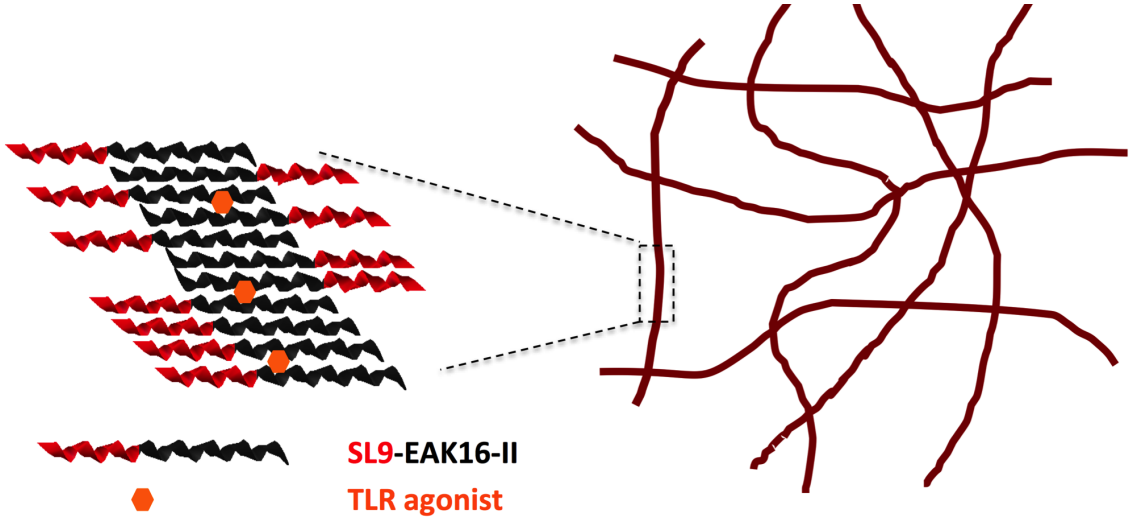

Figure 4-7 The schematic illustration of the co-assembly between SL9-EAK16-II and the TLR agonist.

Collectively, the above results demonstrated EAK16-II could be used as a carrier to achieve the co-delivery of the antigenic peptide SL9 and the hydrophobic TLR agonists (R837 or R848) by direct conjugating or non-covalent interactions respectively. And the co-existence of the two cargoes in the fibril structure would facilitate the uptake of the antigen and immune potentaitor into the same phagosome of antigen presenting cells (APCs), which was critical for the efficient antigen presentation to T cells[31,138,219].

4.3.2 SL9-EAK16-II/R848 aggregates were internalized by MDDCs through endosomal pathway and activated MDDCs efficiently.

Since DCs are the most effective APCs, and in particular the main APCs for cross-presenting exogenous antigens to T cells[31], we evaluated the uptake and intracellular localization of SL9-EAK16-II/R848 nanofibers in MDDCs with confocal microscopy. The immature MDDCs were treated with 5-FAM-SL9-EAK16-II/R848 for 0.5h, which were further stained acidic organelles with Lysotracker deep red, and nuclei with Nucblue. As presented in Fig. 4-8a, fluorescence labeled nanofibers (green) were internalized MDDCs quickly and co-localized with lysotracker (red), suggesting the nanofibers were taken up to endosomal compartments, where TLR7/8 was mainly expressed[33]. Similar result was observed for SL9-EAK16-II/R837 (data not shown).

Afterwards, we determined the efficiency of the peptide/agonist co-assemblies to maturate MDDCs. The immature MDDCs were pulsed with different antigenic formulations for 24 hours, and then the expression level of maturation marker CD83 on DCs were assessed with flow cytometry.

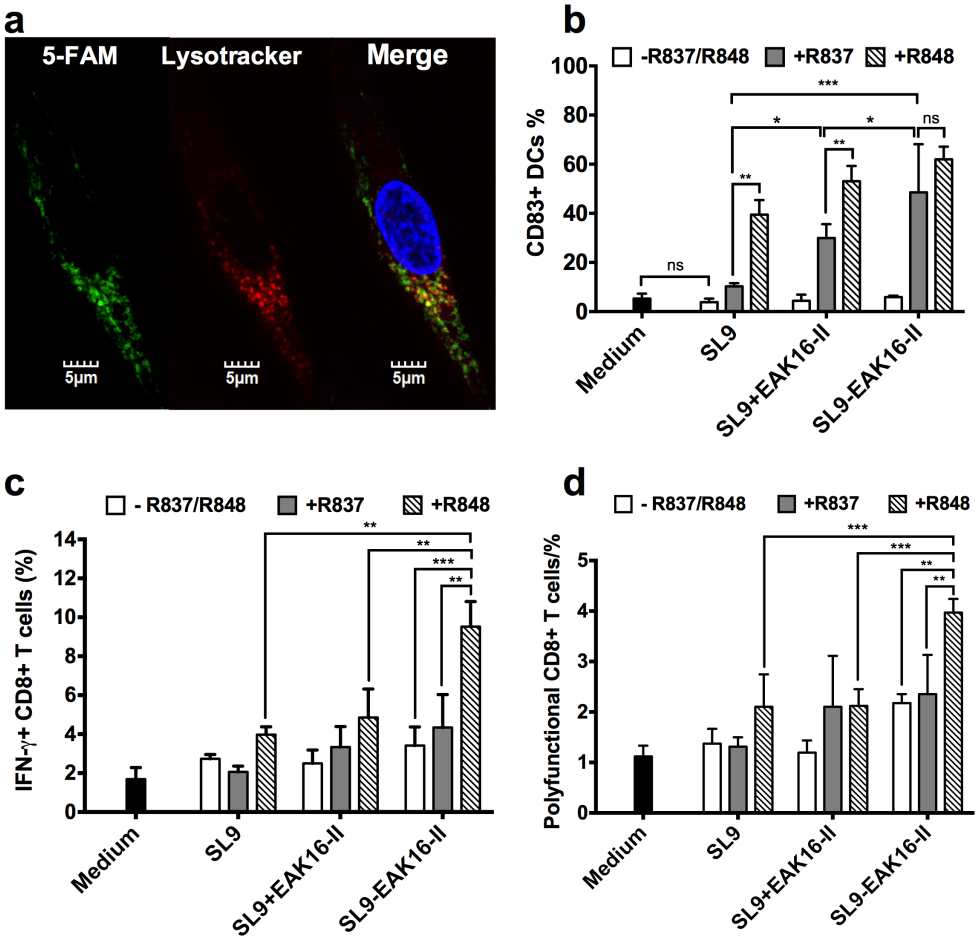

Figure 4-8 Confocal microscope was applied to study the intracellular localization of 5-fam-SL9-EAK16-II/R848 in MDDCs (a); Maturation marker CD83 on DCs was stained and analyzed with flow cytometry. The data was shown as the percentage of CD83 expressing cells in total MDDCs (mean ± SEM, n=3), with the MDDCs treated by medium as control (b); PBMCs from HLA-A2 HIV-1 infected individuals were co-cultured with MDDCs that were already pulsed with different antigen formulations (medium as control), and then re-stimulated with SL9-pulsed autologous B cells. The secretion of IFN-γ, TNF-α, and CD107a were assessed by intracellular cytokine staining and polychomatic flow cytometry. The frequency of CD8+ T cells secreting IFN-γ (c) or the combination of IFN-γ, TNF-α, and CD107a (d) was presented (mean ± SEM, n=3). **: $p \leq 0.01$, ***: $p \leq 0.001$, ns: $p > 0.05$.

Fig.4-8b shows the frequencies of CD83-highly expressing DCs stimulated by SL9, the mixture of SL9 and EAK16-II, or SL9-EAK16-II with the absence or presence of the TLR agonists. The peptides themself did not induce MDDCs maturation. By contrast, a notable up-regulation of cell surface marker CD83 was detected when MDDCs were treated with the peptide in the presence of R837 or R848. Since R848 was a more soluble

and potent analog of R837, which was reported to produce 50-to 100-fold cytokine response compared to R837[220], when mixed with SL9 or the mixture of SL9 and EKA16-II, R848 maturated more MDDCs than R837. However, the co-assemblies of SL9-EAK16-II/R837 could induce up-regulation of CD83 to a similar extent as observed for SL9-EAK16-II/R848. Moreover, these two formulations maturated more MDDCs compared to SL9, or the mixture of SL9 and EAK16-II with the presence of R837 or R848. Taken together, these results demonstrated that the co-assembled nanofibers (SL9-EAK16-II/R837 or R848) could be effectively taken up to endosomal compartments of MDDCs, and augmented the MDDCs maturation.

4.3.3 DCs pulsed with SL9-EAK16-II/R848 nanofibers elicited significantly stronger SL9 specific CD8+ T cell response.

Having demonstrated that the TLR agonist delivered within the nanofibers induced potent DCs maturation, we further determined if the SL9 sequence that was conjugated with the self-assembling peptide could be efficiently processed and presented to CD8+ T cells, using an MDDC-T cell co-culture system. The ex-vivo generated MDDCs were loaded with different antigenic formulations for 24h, followed by co-culturing with autologous peripheral blood monocytes (PMBCs) for 7days. PBMCs were then re-stimulated for 6h with autologous B cell line that was pulsed with SL9 peptide in advance. The CD8+ T cells co-expressing IFN-γ+, TNF-α+, and CD107a+ in response to the SL9 re-stimulation were then measured with flow cytometry. As shown in Fig. 4-8c, the MDDCs pulsed with SL9-EAK16-II/R848 nanofibers stimulated significantly higher percentage of IFN-γ expressing CD8+T cells, when compared to those treated with SL9, or the mixture of SL9 and EAK16-II in the absence or presence of the TLR agonists. Recent data suggested the

simultaneous expression of multiple cytokines could provide a better picture of CTLs functional quality[221,222]. Fig. 4-8d presented the frequency of these so-called polyfunctional (IFN-γ+, TNF-α+, and CD107a+) SL9 specific CTLs. SL9-EAK16-II/R848 nanofibers consistently stimulated more polyfunctional CTLs than the other formulations. Moreover, by comparing the CD8+ T cell response stimulated by the MDDCs that were treated with the SL9-EAK16-II/R848 nanofibers to the one elicited by the MDDCs loaded with the mixture of SL9, EKA16-II and R848, it was implied that not only enhanced DCs maturation, but also the conjugating between the epitope and self-assembling peptide played an essential role in the improvement of the CD8+ T cell response by SL9-EAK16-II/R848.

It was notable that SL9-EAK16-II/R837 did not perform as efficiently as SL9-EAK16-II/R848, while they exhibited a similar nanostructure (nanofibers) as well as a comparable efficiency in the maturation of MDDCs. This might be related to the fact that MDDCs from HIV-1 infected patients were severely impaired in their ability to stimulate T cells, though after stimulation, the expression of maturation markers on them was as up-regulated as on the ones from normal humans[223,224]. TLR7/8 agonist R848 but not TLR7 agonist R837 was reported with the capability to restore this dysfunction, since R848 could activate TLR7 and TLR8 synergistically on DCs to induce the production of IL-12, which played an important roll in T cell stimulation[225]. Consistent with these previous reports, our results suggested R848 could be preferentially used as an effective immune potentiator in the design for HIV-1 nanovaccine, such as SL9-EAK16-II/R848, in therapeutic vaccination.

4.4 Discussion

Peptide based vaccine that uses antigenic epitopes as the immunogen offers considerable advantages over the traditional ones generated from killed or attenuated microorganisms. However, the intrinsic immunogenicity of epitope is normally weak, which is mainly ascribed to the ease of proteolytic degradation and the lack of "danger signal. Thus, an efficient adjuvant should provide not only protection against degradation, but also activating innate immunity. Our previous results have demonstrated the self-assembling peptide EAK16-II can effectively shield the epitope from rapid degradation. However, the conjugating peptide itself failed to activate DCs, which provide a crucial link between the innate immunity and the acquired immune protection[31]. The activation of pattern-recognition receptors (PRRs) on DCs can cause DCs up-regulating MHC and co-stimulatory molecules, providing "signal 2" for the interactions between DCs and T cells[127]. In the absence of this co-stimulatory signal, immune tolerance rather immunity is induced[226]. Therefore, the incorporation of immune potentiators that can mimic the "danger signal"—pathogen-associated molecular pattern (PAMP) of microbial pathogens, is necessary for our self-assembling peptide based system to induce potent cellular response.

TLRs, which have been well characterized as an important type of PRRs, can activate DCs and produce predominantly Th1 cells evoking cell-mediated immune response[31]. A number of TLR agonists have been developed to active cognate receptors, as adjuvants for vaccine design[33]. Up to date, only TLR 4 agonist monophosphoryl lipid A (MPLA) and TLR 7 agonist R837 are licensed for human use, with the later one only approved for topical administration. The combination of TLR agonists with antigen can be achieved

with various strategies, including directly mixing, linking with chemical bond, and co-delivery within nanoparticles (NPs). However, compared with using protein as antigen, there are much less works for the co-delivery of peptide antigen and TLR agonist with NPs published. Torben and colleagues reported when T cell epitopes from Friend Virus (FV) were co-encapsulated with TLR 9 ligand CpG inside calcium phosphate NPs, the NP-based peptide vaccine induced potent T cell response and provided efficient protective immunity during acute and chronic virus infection[227]. Besides, both liposomes and PLGA microparticles were also applied for the co-delivery of antigenic peptides and the agonist CpG, to enhance the antigen specific T cell response *in vivo*[228,229]. Either conjugation or surface absorption was adopted for the loading of CpG. For our EAK16-II based delivery system, it has been studied as an efficient vehicle to deliver/stabilize hydrophobic molecules, such as anticancer drugs[230]. Therefore, two hydrophobic imidazoquinoline derivatives, R837 and R848, which activate TLR7/8, were incorporated into our CD8+ T cell epitope loaded peptide SL9-EAK16-II.

The self/co-assembly between amphiphilic SL9-EAK16-II and the hydrophobic agonist was investigated with fluorescence spectroscopy and ITC. As a much used "hydrophobic probe", 1,8-ANS was considered to bind with hydrophobic surfaces and its fluorescence blued-shirted with enhanced intensity[216]. The ANS assay with SL9-EAK16-II suggests the self-assembled nanostructure from the conjugating peptide can provide a hydrophobic interior for the residence of hydrophobic molecules. The intrinsic fluorescence intensity of the agonist (R837 or R848) also increased with the addition of SL9-EAK16-II, suggesting a more hydrophobic environment where the agonist resides. These implied the hydrophobic interaction played an important role in the co-assembly process. Moreover,

the maximum emission wavelength of the agonist was observed with blue shift when the agonist was mixed with SL9-EAK16-II. This might be due to that the π-conjugate of the quinolone ring extended by the substitute of amino group was weakened or impaired by the addition of the peptide molecules, resulting in the energy difference between the first singlet-spin excited state (S_1) and singlet-ground state increasing (S_0)[231]. The results from ITC further confirm the interactions involved in the self-/co-assembly. From our results, the SL9-EAK16-II/R837 (or R848) co-assembly was favored by both enthalpy and entropy. The entropy-driven binding is primarily correlated with hydrophobic interaction[217], which was supported with the fluorescence assay. Additionally, the computer modeling combined with crystal structure analysis of TLR7/8, reveals that when R837 or R848 binds with its corresponding TLR, both the hydrophobic cores provided by the TLR's Leucine-rich region and the hydrogen bonds formed between the agonist and the side chain of Aspartic acid (Asp), are important for the recognition and activation[232,233]. The Glutamic acids (E) in the sequence of SL9-EAK16-II could provide similar hydrogen bonding sites as Asp did. This hydrogen bonding can be highly associated with the negative enthalpy change. Thus, not only hydrophobic interaction, but also hydrogen bonding participates in the co-assembly process between SL9-EAK16-II and the agonist.

Moreover, the SL9-EKA16-II/agonist co-assemblies maturated significantly more MDDCs, which subsequently stimulated more SL9 specific CTLs *in-vitro*, than the simple mixture of SL9 and agonist. Collectively speaking, with direct conjugating and co-assembly by non-covalent interaction, EAK16-II based platform successfully co-deliver an antigenic peptide and a hydrophobic TLR agonist to DCs, which offers a

simple, yet efficient strategy to formulate a peptide based vaccine. However, as here the immunogenicity of this nanovaccine was only measured *in-vitro*, further assessment *in vivo* would be crucial for the application of the self-assembling peptide for vaccine design.

Chapter 5 Enhanced HIV-1 specific primary CD8+ T cell response elicited by the co-delivery of CD4+, CD8+ epitopes along with R848 with self-assembling peptide

Abstract

Peptide based subunit vaccine can induce potent cellular response when the antigens are administrated in the presence of efficient adjuvants or delivery system. Our previous findings demonstrated EAK16-II based self-assembling peptide could effectively protect antigen epitope from degradation, and succeeded to incorporate both epitope and TLR agonist within the same nanostructure to stimulate more polyfunctional CD8+ T cells *in vitro*. Nevertheless, to prime long-termed and potent CD8+ T cell response *in vivo* is highly CD4+ T cell dependent. In the current chapter, not only CD8+ T cell epitope (SL9) and TLR agonist (R848), but also a CD4+ T cell epitope was formulated into the EAK16-II based delivery platform to obtain multifunctional nanoparticle based vaccine. Physicochemical characterizations revealed the morphology (nanofibers) and hydrodynamic size (~220nm) of the multifunctional nanoparticle, as well as the co-assembling process involved in the formulation. Mice subcutaneously vaccinated with the multifunctional nanofibers generated significantly more SL9 specific CD8 + T cells, compared with either the mixture of two epitopes and R848 or R848 alone. Furthermore, The CD8+ T cell response generated upon nanofibers vaccination displayed central memory phenotype. The findings in this chapter further demonstrated the potential of the self-assembling peptide EAK16-II as the delivery platform for peptide based vaccines.

5.1 Introduction

As the vaccine developments orientate towards the less immunogenic "minimalist" components, such as DNA, protein, or peptides, the artificial formulations mimicking the killed or attenuated pathogenic microorganisms have been studied intensively. An optimal subunit vaccine should be considered with three components: (1) antigen, which provides the pathogen specific epitopes to regulate the targeting of the immune response (humral and/or cellular immunity), (2) immune potentiator that directly activates innate immune cells providing pro-inflammatory context for antigen recognition, (3) delivery system enhancing the targeted delivery of the antigen and the immune potentiator to innate immune cells, such as dendritic cells (DCs)[9], which play a key role in bridging innate and adaptive immunity.

Nanoparticles with the size smaller than 1000 nm have attracted increasing interest in formulating these subunit vaccines, owning to its flexibility in the selection of matrix materials, controllability over components, size, shape and surface properties[44,93,227]. Our previous results suggested EAK16-II based self-assembled nanofibers, which incorporated an antigenic epitope and a TLR agonist within one particle efficiently enhanced the epitope specific cytotoxic T cell (CTL) response as the form of DC based vaccine *in-vitro*. However, the *ex vivo* generation of DCs made the vaccine preparation complicated, and limited the stability and convenience of the vaccine. Thus, to determine whether the self-assembling peptide based nanofibers could be subcutaneously administrated *in vivo*, to elicit potent CTL response, would be critical for the application for the self-assembling peptide as a platform for the vaccine design. Though the existence

of TLR agonist can provide pro-inflammatory cytokines required for the full activation of antigen presenting cells, and bypass the need from CD4+ T cells to prime potent CTL response as proposed in some animal works[234–236], recent studies have suggested the necessity of CD4+ T cell help in the generation of long-lived, functional memory CD8+ T cells that respond rapidly towards secondary exposure to pathogens[127,237–239].

Thus, in current study, to harness the self-assembling peptide formed nanofibers (the SL9-EAK16-II/R848 co-assemblies) with the capacity to stimulate CD4+ T cell response, we incorporated an additional T helper (Th) epitope by conjugating with EAK16-II, which further co-assembled with SL9-EAK16-II prior to the addition of R848. The obtained multifunctional nanoparticle based vaccine was tested in HLA-A2 transgenic mice by the prime-boost strategy for the determination of T cell immunity. The results suggested EAK16-II based self-assembling platform successfully integrated the CTL, Th epitopes, and the TLR agonist (R848) within the nanofibers. The mice vaccinated with these nanofibers produced significantly more memory SL9 specific CD8+ T cells, compared with the ones with the mixture of epitopes and R848, or R848 alone.

5.2 Materials and methods

5.2.1 Materials

All peptides in animal study were purchased from CanPeptide (Montreal, Canada), which were further treated with VariPure IPE column (Agilent, Canada) to remove remaining trifluoroacetic acid (TFA), followed with lyophilization in lab prior to use. HLA-A2 transgenic mice were bred in the Division of Comparative Medicine at University of

Toronto. The experiment was conducted on female mice of 6-8 weeks old. All animal works were approved by University of Toronto, University Animal Care Committee.

5.2.2 Methods

Circular Dichroism (CD) spectra Far-UV circular dichroism spectra of peptide samples were measured at room temperature using a Jasco J-815 CD spectrometer (Tokyo, Japan). 150μL peptide solution was scanned in a 0.1cm quartz cell from 190 to 250nm. Solvent spectrum was used as the baseline for data collection.

Morphology characterization with Atomic Force Microscopy (AFM) and Transmission Electron Microscopy (TEM) Atomic force microscopy was used to determine the nano-structures of peptide self-assemblies. 100μL sample solution was dropped on the surface of a freshly cleaved mica sheet for various times ranging from 5mins to 30mins, depending on the concentration of solution. Then free peptide was removed by blotting, and washed with 300μL pure water. After an air-dry of a couple of hours, AFM imaging was taken at room temperature using the Peak Force tapping mold on a Dimension Icon AFM (Bruker, Santa Barbara, CA). To confirm the structures acquired from AFM, TEM was also utilized. 10μL peptide solution was applied to a 400 mesh Formvar coated copper grid for 3-5 minutes, followed by negative staining with 10μL 2% uranyl acetate, blotted drying, and analysis on TEM (Philips CM10 TEM, operating at 60KeV).

Particle size measured by dynamic light scattering (DLS) The hydrodynamic diameter of sample was measured using DLS on a Zetasizer Nano ZS (Malvern Instruments, Malvern, UK) equipped with a 4mW He-Ne laser operating at 633nm. 50μL solution was added in low volume disposable polystyrene cuvette and the scattered light intensities

were collected at an angle of 173°. Three independent measurements were performed to generate the intensity based size distribution profile.

Surface tension measurement Axisymmetric drop shape analysis-profile (ADSA-P) was used to measure the surface tension of peptide solutions prepared in pure Milli-Q water at various concentrations. The experimental setup for the measurement of dynamic surface tension was described previously[240]. The data was acquired every 30s, for the duration of 5400s. The equilibrium surface tension was estimated by averaging 5 data points at the end of each dynamic surface tension profile and plotted versus concentration of peptide.

Fluorescence spectroscopy A Photon Technology International spectrafluorometer (Type LS-100, London, Canada) with a pulsed xenon lamp as light sauce was utilized to measure the fluorescence spectra of R848 to study the interaction between peptide and agonist. Samples (70 μL) were transferred to a quartz cell (1cm × 1cm), which were exited at 248nm. The emission data was collected in the range of 300-450nm. Different volumes of SL9-EAK16-II/TL13-EAK16-II solution were added to the fixed agonist concentration at 15 μM to obtain peptide/agonist molar ratio from 0.5:1 to 6:1.

Isothermal Titration Calorimetry (ITC) For all ITC experiments performed on Nano-ITC (190μL, TA instruments, New Castle, DE) at 298K, Milli-Q water was carried out as described in previous chapter. Generally, the mixture of epitope-loaded self-assemling peptides or the mixture of epitopes with the total peptide concentration at 400μM was titrated into 20μM R848 solution. Blank titrations of peptides into pH 6.0water were performed to measure the heat of dilution of each peptide, which was subtracted from the integration data prior to curve fitting. Origin 8 software was used to fit the heat profiles,

assuming one-site binding. For each peptide solution, experiments were conducted three times.

Cellular immune response CD4+ or CD8+ T cell epitope loaded self-assembling peptide was dissolved in sterile water at 0.4mM, which was then mixed at equal volume, and incubated at 4°C overnight. The mixture was further stirred in the presence of 0.1mM R848 overnight. HLA-A2 transgenic mice were vaccinated subcutaneously at tail base twice with a 2-week interval between immunizations. For each injection, mice received 500μL of samples or phosphate buffer saline (PBS) (for naïve control group). Two weeks after the second vaccination, spleens were taken from mice and splenocytes were prepared, which were then stained with PE-labelled SL9-dextramer (Immudex, Copenharge, Danmark) and anti-mouse CD3/CD8/CD62L/CD44 mAb (Biolegend, San Diego, CA). Flow cytometry was run on a LSRII flow cytometer (BD Bioscience, San Jose, CA) and data were analyzed with FlowJo software (FlowJo, Ashland, OR).

Statistical analysis Statistical analysis was performed by one-way ANOVA with Tukey's test for comparison between groups. Group mean difference were considered statistically significant according to a p value < 0.05.

5.3 Results

5.3.1 Preparation and characterizations of multifunctional nanofibers based vaccine

The conjugating of IA^b-restricted HBVc128 Th epitope (TPPAYRPPNAPIL, here referred to TL13) with EAK16-II was carried out as similarly as we did for the CD8+ T cell epitope SL9. The CD4+ T cell epitope-loaded conjugating peptide (named as TL13-

EAK16-II) is shown in Fig 5-1a. Firstly, we investigated the secondary structures of the peptides with circular dichroism. SL9 was unstructured and the secondary structure of SL9-EAK16-II was dominated by α-helix, which were consistent with our previous results. For TL13 and its conjugating peptide TL13-EAK16-II, the mixed conformation of random coil and β-sheet was observed for the Th epitope, while TL13-EAK16-II adopted an α-helical structure, similarly with SL9-EAK16-II, as shown in Fig. 5-1b.

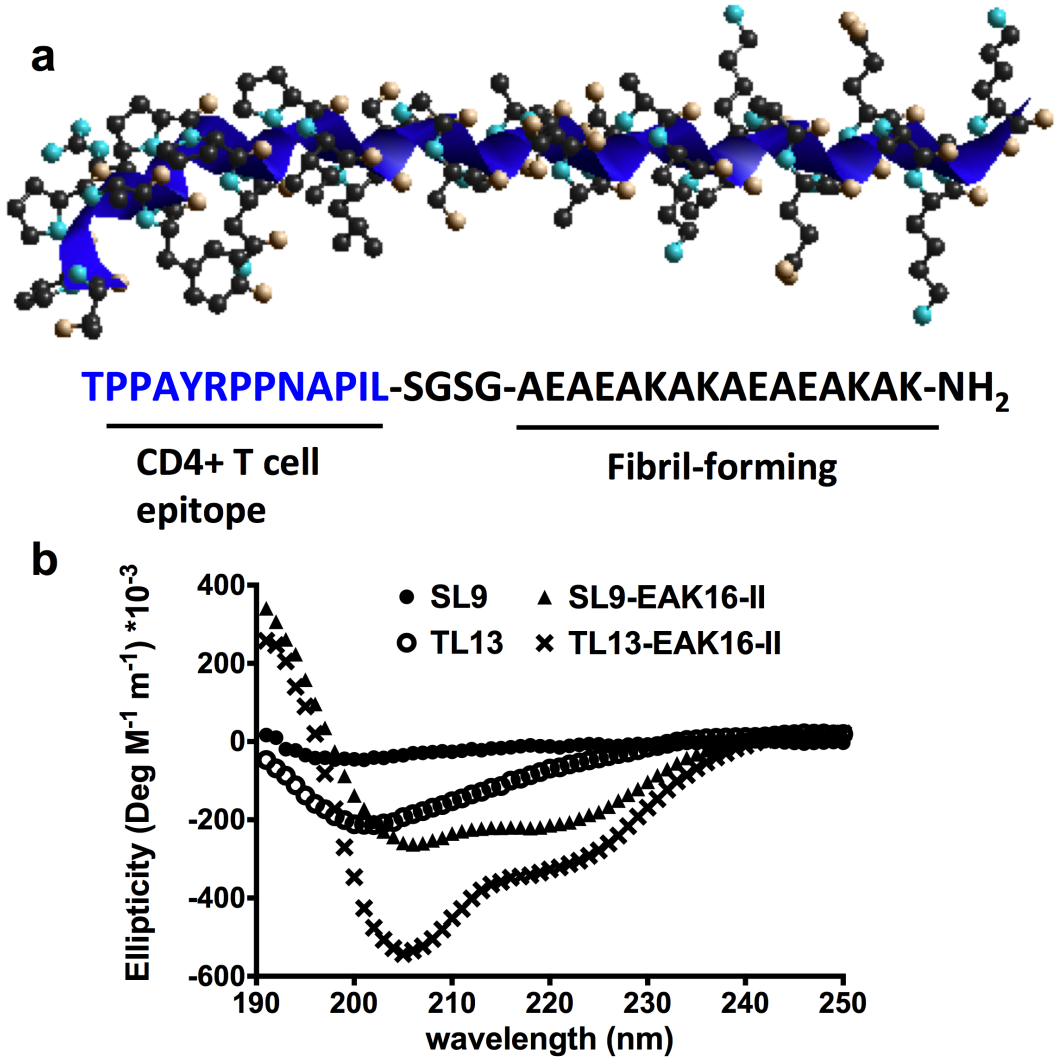

Figure 5-1 Schematic and sequences of TL13-EAK15-II, the molecular structures were stimulated with HyperChem, displaying carbon with black, nitrogen with cyan, oxygen with white, and secondary structure shown as blue ribbon (a); the conformational structures of the peptides were characterized by CD spectra.

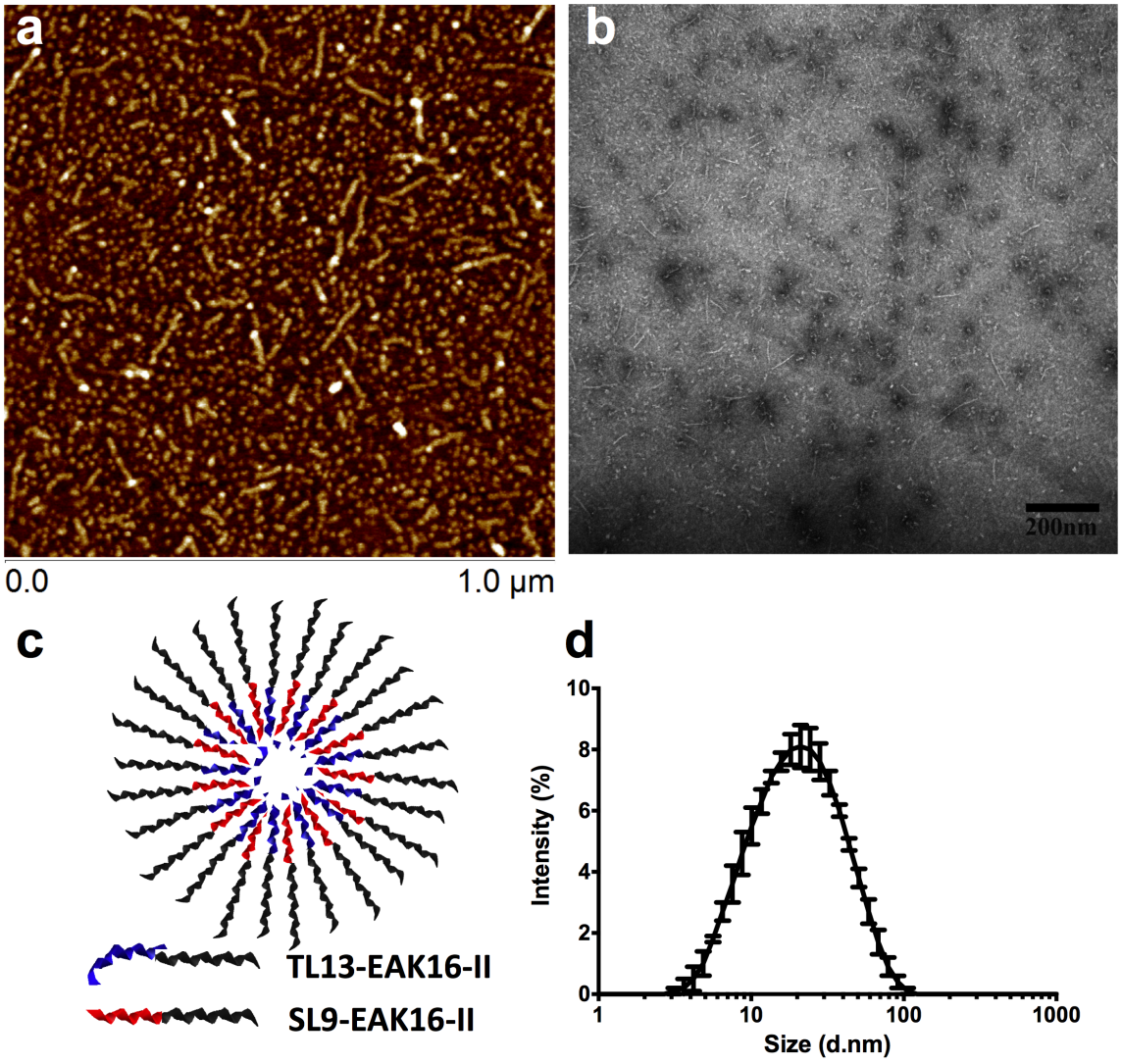

Figure 5-2 The morphology of SL9-EAK16-II/TL13-EAK16-II co-assemblies was characterized with AFM (a) and TEM (b); schematic of the co-assembly between the two peptides (c); the intensity based hydrodynamic size of the co-assemblies was obtained from DLS (d).

To formulate the self-assembling peptide based nano-vaccine, two epitope-loaded peptides were mixed at the molar ratio of 1:1 in advance, and incubated at room temperature over night, which was followed by the addition of R848 at the molar ratio of 4:1 (peptide over agonist), and then stirring overnight. SL-EAK16-II/TL13-EAK16-II co-assemblies were visualized dominantly as globular particles with the diameter of ~17nm, and small fraction of short fibrilar structures with the average length of ~74nm, from

AFM image (Fig.5-2a), which was further confirmed with TEM (Fig. 5-2b). The possible assembly mechanism was proposed as in Fig. 5-2c, relatively more hydrophobic epitope part of the peptides would aggregate in the core of the globular structure, with the EAK16-II moiety in the sequence forming the shell of the structure, driven by hydrophobic interactions, and hydrogen bonding. The hydrodynamic size of the peptides co-assembles was measured by DLS (Fig. 5-2d), with a main population at ~21nm, which was comparable with the size of the globular particles analyzed from the AFM image (Fig. 5-2a)

By contrast, with the addition of R848, the morphology of the co-assemblies of SL9-EAK16-II/TK13-EAK16-II/R848 altered to cross-linked nanofibers characterized with AFM (Fig. 5-3a) and TEM (Fig.5-3b), and the main size of the co-assemblies shifted to ~220nm, as shown in Fig. 5-3d. Our previous results suggested when SL9-EAK16-II/R848 co-assembled into nanofibers, the hydrophobic molecule R848 was encapsulated within the interior environment of the peptide-formed aggregates. A similar co-assembly mechanism was proposed for SL9-EAK16-II/TL13-EAK16-II/R848 (Fig.5-3c), since SL9-EAK16-II and TL13-EAK16-II exhibited the same helical structure. Furthermore, previous reports suggest that the particle size of antigen smaller than 200nm can directly enter the lymphatic system, and efficiently internalized by plasmacytoid DCs to IFN-α that can efficiently facilitate the direct priming of CTLs[241–243].

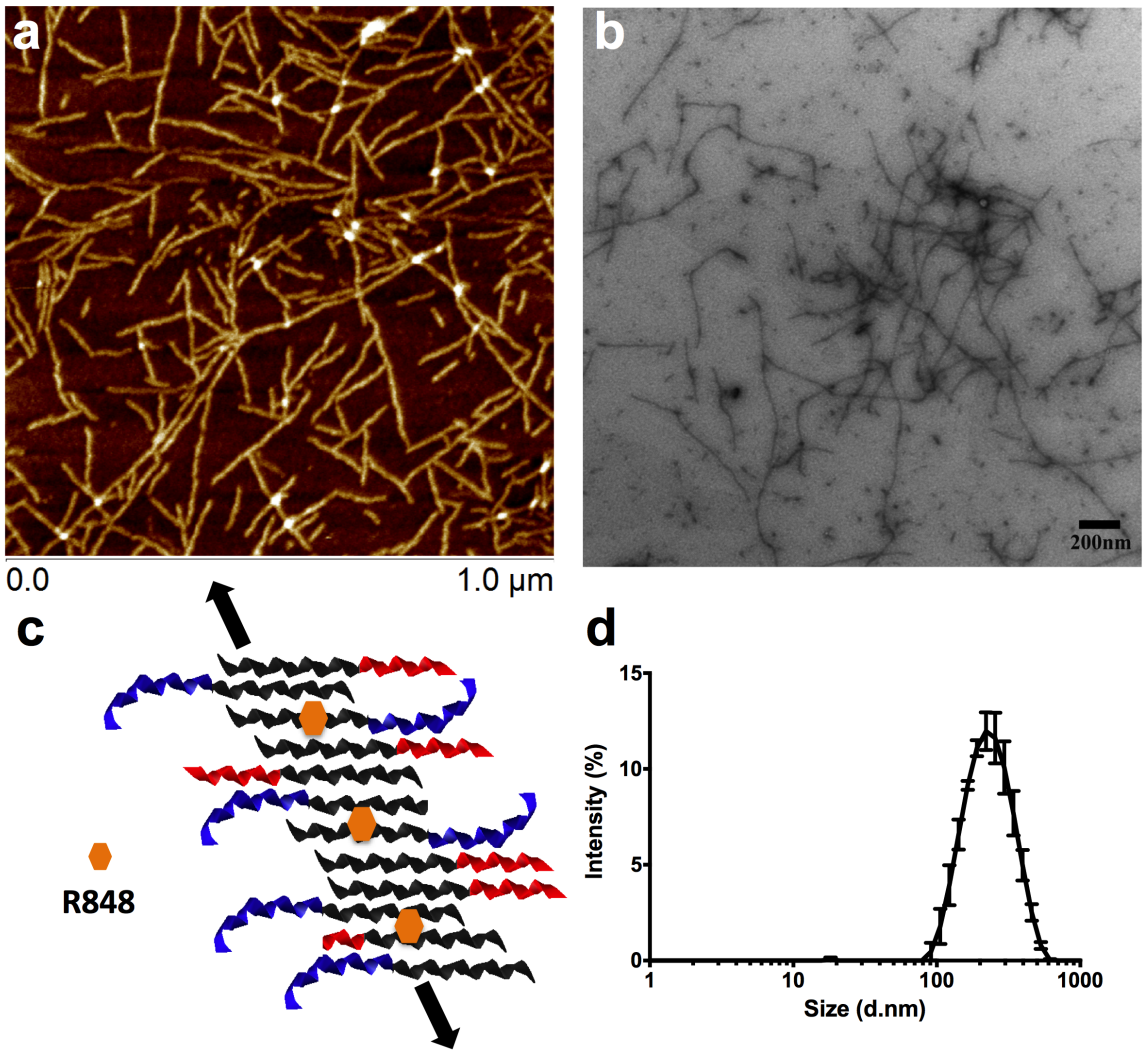

Figure 5-3 The conjugating peptides mixture was further added with R848 at the molar ratio of 4:1 (peptide to agonist), the morphology of the tripartite system was characterized with AFM (a) and TEM (b); schematic of the mechanism for the forming of nanofibers, the arrows represent the growing orientations of the fibers(c); size distribution of the tripartite nanofibers (d).

To investigate the interaction between the two epitope-loaded peptides, surface tension method was applied, which was widely used to study the interactions involved in the mixing of binary surfactants system[244]. The dynamic surface tensions at different concentrations were acquired for SL9-EAK16-II (Fig.5-4a), TL13-EAK16-II (Fig.5-4b) and the mixture of them at the molar ratio of 1:1 (Fig.5-4c), from which the equilibrium surface tension for each concentration was obtained for the relative peptide, as summarized in Fig.5-5.

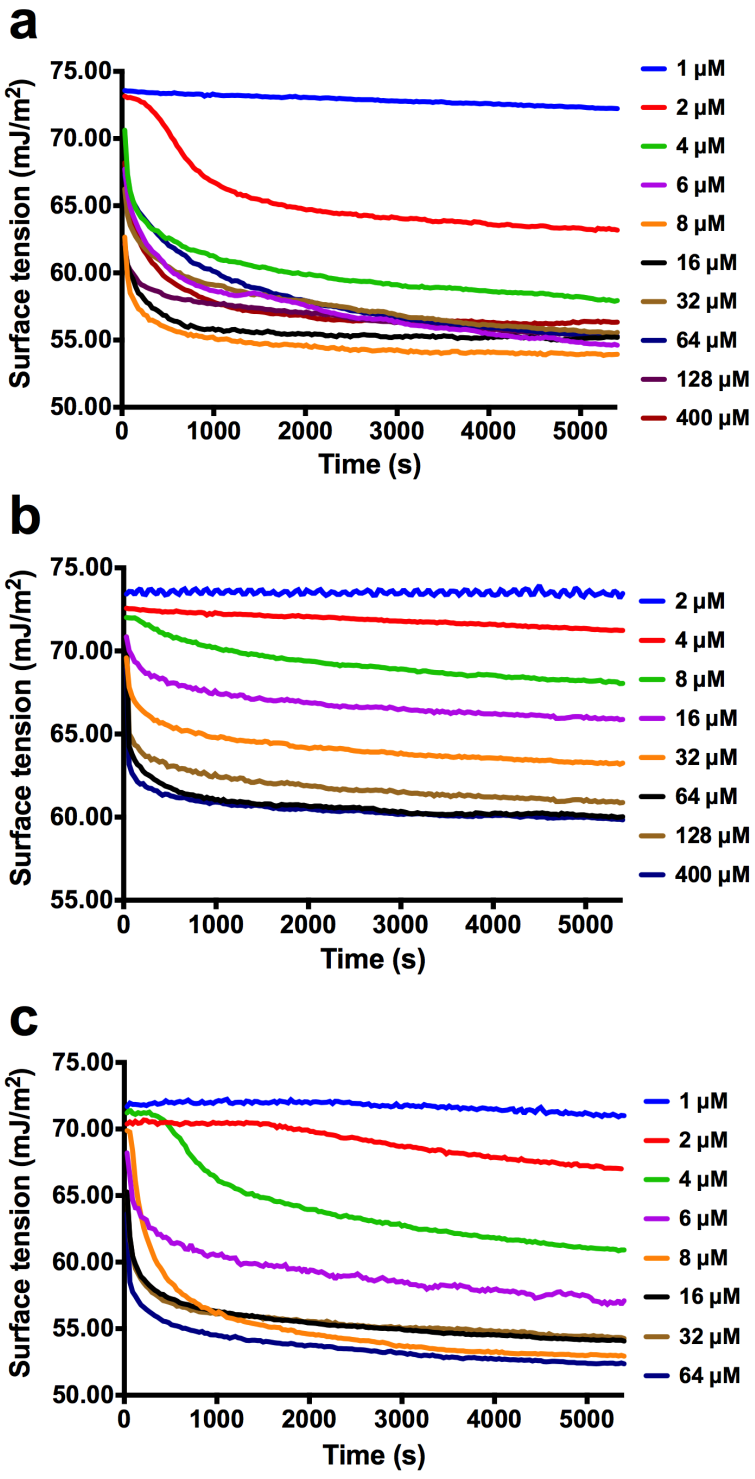

Figure 5-4 Dynamic surface tension of SL9-EAK16-II (a), TL13-EAK16-II (b), and 1:1 mixture of the two peptides (c) at different concentrations.

For these peptide solutions, they exhibited a similar trend, as at the low concentrations, the equilibrium surface tension decreased with the peptide concentration increasing, while the concentration increased to certain value, the surface tension approached a plateau, from which the critical aggregation concentration (CAC) could be estimated. The CAC for SL9-EAK16-II was ~7μM, which was consistent with our previous data, while for TL13-EAK16-II it was ~64μM.

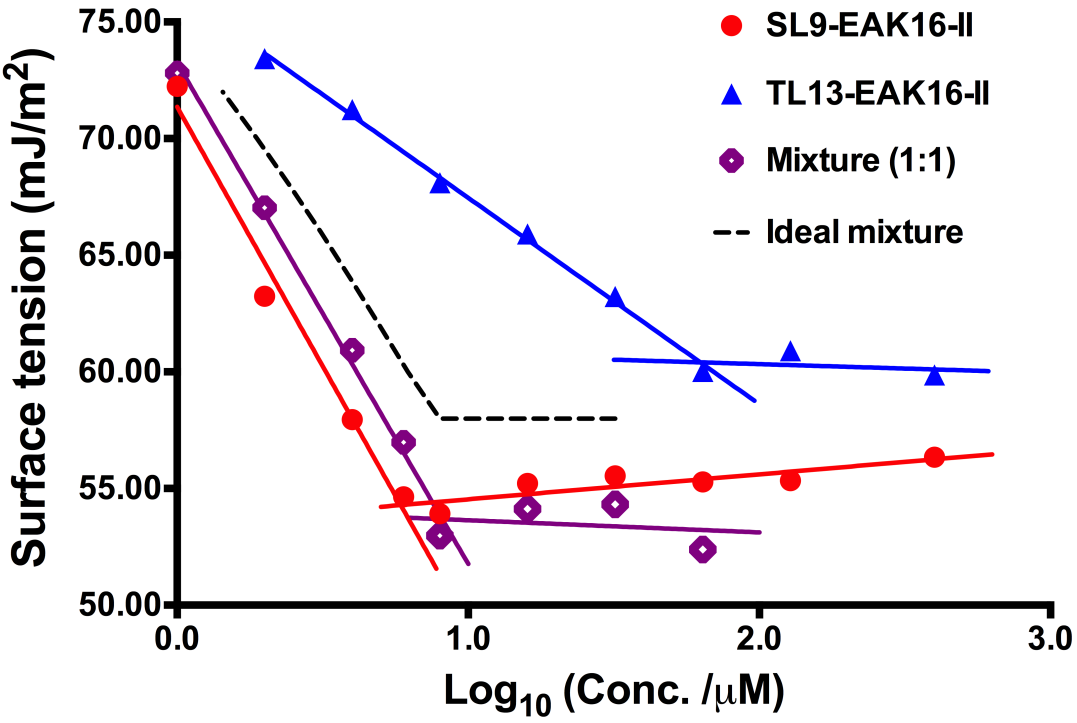

Figure 5-5 The equilibrium surface tension profiles for SL9-EAK16-II, TL13-EAK16-II and the mixture at the molar ratio of 1:1 were obtained and plotted as the function of peptide concentration; the dashed line was predicted by real solution theory for the ideal mixture of the two peptides.

By contrast, when the two peptides mixed, the CAC was estimated at ~9μM. The mixing of a binary system can be described with the regular solution theory as Eq.1.

$$\frac{1}{C_{mix}^{\pi}} = \frac{\alpha_1}{f_1 * C_1^{\pi}} + \frac{\alpha_2}{f_2 * C_2^{\pi}} \qquad (1)$$

Where C_1^{π}, C_2^{π}, or C_{mix}^{π} is the concentration of species 1, 2 or the mixture that individually produces the surface tension of certain value π, α_1 or α_2 is the fraction of each component in the bulk solution, and f_1 or f_2 is the activity coefficient. When the mixing is ideal, namely there is no interaction between the two species, the activity coefficient equals to 1. Thus, the surface tension profile for an ideal mixing could be predicted from Eq.1. For a given value (π), the concentration of SL9-EAK16-II or TL13-EAK16-II that produced such a surface tension could be read from the experimental equilibrium surface tension curve (blue or red straight line in Fig. 5-5). Then the concentration of the ideal mixture acquired to produce the same surface tension was calculated from Eq.1. From a series of π values and the corresponding concentrations, the predicted equilibrium surface tension profile for the ideal mixture was obtained, as shown with dashed line in Fig.5-5. Obviously, the mixture of the two peptides in real case did not follow the pattern of the ideal mixture, which suggested there could be interactions between them. The interaction parameter can be estimated from Eq.2.

$$\beta = \frac{1}{x_2^2} * \ln\left(\frac{\alpha_1 * C_{mix}^{\pi}}{x_1 * C_1^{\pi}}\right) = \frac{1}{x_1^2} * \ln\left(\frac{\alpha_2 * C_{mix}^{\pi}}{x_2 * C_2^{\pi}}\right) \quad (2)$$

Where β is the interaction parameter, x_1, or x_2 is the fraction of each component in the micelle, with other variables representing the same meanings as in Eq.1. At the CAC of the mixture of SL9-EAK16-II and TL13-EAK16-II (mixed at 1:1 molar ratio), the iterative solution of Eq.2 was -2.38 for interaction parameter, and 0.76 for the fraction of SL9-EAK16-II in the micelles formed by the two peptides. By contrast, in the case of ideal mixing, the interaction parameter equaled to 0, and the predicted composition of micelle was 0.93 for SL9-EAK16-II. From the comparison with the ideal mixing predicted from the regular solution theory, the interaction between the two peptides were

illustrated, which suggested the presence of the two peptide within the same nanostructure. And this co-existence of the two epitopes within the nanofibers would facilitate the co-recognition, since it was suggested that CD4+ and CD8+ T cell must recognized the antigens from the same antigen presenting cells for the generation of functional memory CD8+ T cells[245].

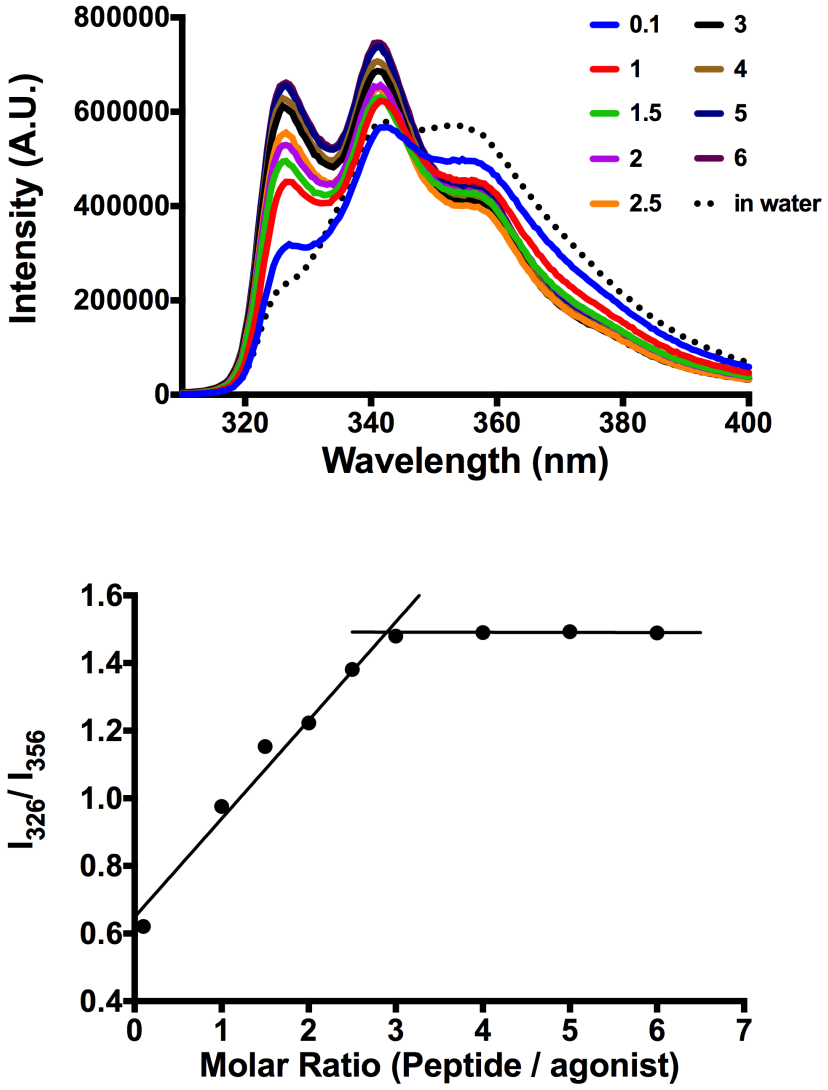

Figure 5-6 The interaction between peptides mixture and R848 was studied with fluorescence spectra.The fluorescence spectra of R848 in the mixture solution of SL9-EAK16-II and TL13-EAK16-II at different peptide concentrations (Top), and the intensity ratio I_{326}/I_{356} was determined and plotted versus molar ratio (bottom).

Then we utilized fluorescence spectra to investigate the co-assembly process between the peptides and the TLR agonist R848, as shown in Fig. 5-6. Consistent with previous results, when R848 was mixed with the peptide solutions, λ_{max} blue shifted to ~341nm, and the intensity of emission peak at 326nm also increased with the peptide concentration increasing, while the intensity at 356nm decreased, indicating the interactions such as hydrogen bonding and hydrophobic interaction participated in the co-assembly between R848 and the peptides. The molar ratio for saturation binding was approximately at 3:1 (peptide to R848), as illustrated in Fig.5-6 (bottom).

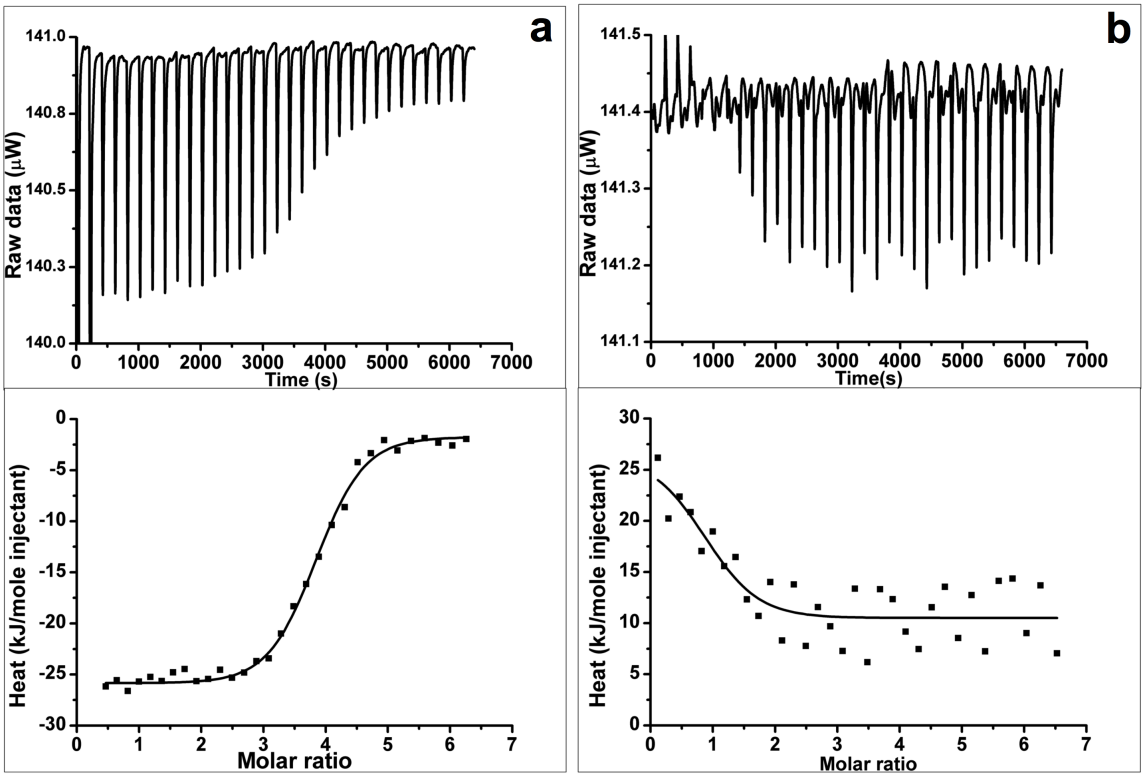

Figure 5-7 Isothermal titration profiles for peptides solutions injected into R848. The mixture of conjugating peptides into R848 (a); the mixture of epitopes into R848 (b)

The calorimetric titration profiles for the mixture of epitope conjugating peptides or the mixture of epitopes into R848 were shown in Fig. 5-7. And the thermodynamic parameters for the two bindings were summarized in Table 5-1. Similar to the injection of

SL9-EAK16-II into R848 as discussed in Chapter 4, the binding between SL9-EAK16-II/TL13-EAK16-II and R848 was exothermic process, which was favored by both enthalpy and entropy.

Table 5-1 Thermodynamic parameters (mean ± SD, n=3) obtained with ITC

	SL9-EAK16-II + TL13-EAK16-II	**SL9 + TL13**
ΔH (kJ mole^{-1})	**-23.73±0.93**	**40.87±4.19**
ΔS (J mole^{-1} K^{-1})	**38.06±4.02**	**203.94±3.76**
TΔS (kJ mole^{-1})	**11.34±1.20**	**60.77±1.12**
K_d (μM)	**0.72±0.04**	**343.27±5.09**
N	**3.66±0.40**	**0.71±0.34**

By contrast, an endothermic binding driven by entropy between the mixture of epitopes and R848 was observed, which was different from the result for SL9/R848 as shown in Chapter 4. This might be resulted from the different self-assembling behaviors of TL13 and SL9. As shown in the CD spectra, TL3 exhibited both random coil and β-sheet, while SL9 was unstructured random coil. From the AFM images (data not shown), the β-sheet structural TL13 could assemble to nanofibers by itself, which possibility co-assembled with R848 in the mixture. However, the obtained binding affinity (K_d =343.27 μ M) between the epitopes and R848 was relatively weak. The concentration of R848 in the mixture of SL9/TL13/R848 that was used for *in vivo* study was 100μM, lower than the dissociation constant K_d. This implied when the mixture was injected into mice, the weak binding between the epitopes and R848 could be neglected.

5.3.2 Multifunctional nanofibers primed significantly more potent CTL response that displayed central memory phenotype.

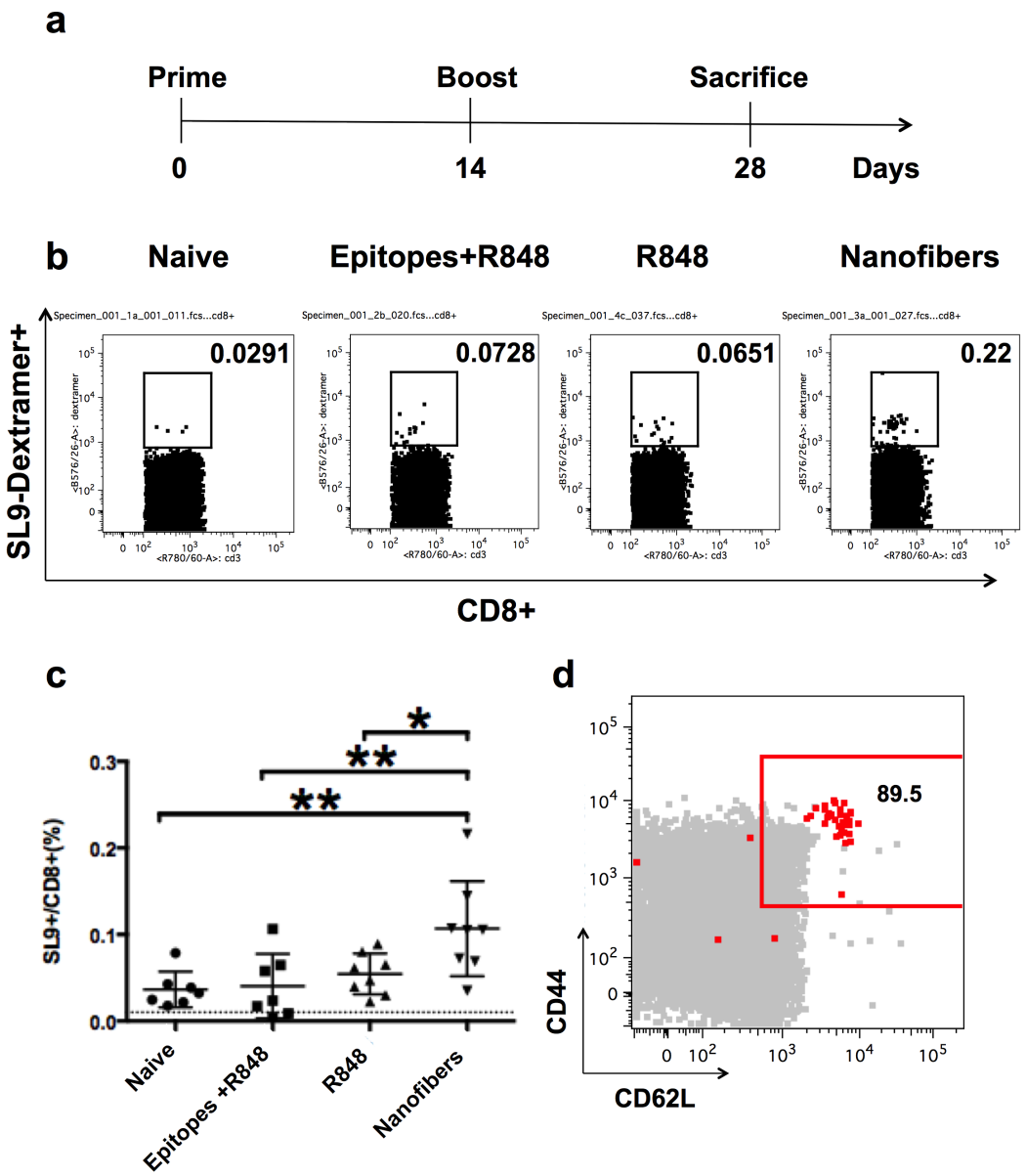

Figure 5-8 HLA-A2 transgenic mice were subcutaneously vaccinated with SL9/TL13/R848, R848 alone, SL9-EAK16-II/TL13-EAK16-II/R848, and PBS as naive control group, following the schedule illustrated in (a); at day 28, the mice were sacrificed, and the lymphocytes were then collected from spleens. Dextramer flow cytometry was applied to measure the number of SL9 specific CD8+ T cells. A representative flow cytometry profile from one mice were shown, in which the numbers presented the percentage of SL9-specific CD8+ T cells in the total CD8+ T cells (b). The frequencies of SL9 specific CD8+ T cells from mice vaccinated with different antigen formulations (c). 8 mice per group, * $P<0.05$, ** $P<0.01$. The central memory antigen specific CD8+ T cells were stained with CD62L+CD44+ from flow cytometry (d), in which the number presented the percentage of memory CTLs in the total CD8+ T cells.

Then we evaluated the cellular immunity of the different antigen formulations *in vivo*. HLA-A2 transgenic mice were injected subcutaneously with SL9-EAK16-II/TL13-EAK16-II/R848, SL9/TL13/R848, or R848, with PBS as naïve control, following the vaccination schedule as shown in Fig. 5-8a. At day 28, the splenocytes were collected from mice, and stained with fluorophore labeled SL9-dextramer, anti-mouse CD3, CD8, CD62L and CD44 mAbs, for the analysis with flow cytometry. The frequencies of SL9-Dextramer positive CD8+ T cells were showed in Fig. 5-8b and 5-8c. It was observed that more SL9 specific CD8+ T cells were generated in the mice vaccinated with the nanofibers, compared to in the ones with the mixture of epitopes and R848 ($p<0.01$), or R848 alone ($p<0.05$). An ideal prophylactic vaccine for inducing cellular response should generate memory CD8+ T cells, which respond rapidly to the secondary infection[246]. Therefore, we further analyzed the phenotypes of the SL9 specific CTLs according to the expression of the surface markers $CD62L^{high}$ and $CD44^{high}$, which were the characteristic of memory CD8+ T cells[247,248]. As shown in Fig.5-8d with the red frame that represented the CD62L/CD44 double positive CTLs, 89.5% of SL9 specific CD8+ T cells displayed a central memory phenotype. These results demonstrated not only an enhanced magnitude, but also a higher quality of T cell response was induced by the nanofibers-based vaccine. By priming the memory CD8+ T cells against HIV-1 antigen SL9, in theory the memory CTLs could respond immediately after the virus infection.

5.4 Discussion

In this chapter, we incorporated a CD4 epitope-bearing EAK16-II into SL9-EAK16-II/R848 nanofibers to formulate a nanovaccine. The surface tension studies revealed the interaction between SL9-EAK16-II and TL13-EAK16-II, and the further co-assembly

between the conjugating peptides and R848 was studied by fluorescence spectra and calorimetric titration. These results demonstrated the integration of the CD4, CD8 epitopes and the TLR 7/8 agonist R848 into the same nanostructure with the presence of the self-assembling peptide EAK16-II. The nanovaccine stimulated significantly more SL9 specific central memory CTLs in HLA-A2 transgenic mice, compared with either the mixture of epitopes and TLR agonist, or the TLR agonist alone.

When the CD4+ or CD8+ T cell epitope was conjugated with EAK16-II, a α-helical secondary structure was obtained. Though the conformational structure is not required by T cell epitopes biding with MHC molecules for the presentation to T cells, it is crucial to generate B cell epitopes with conformations that resemble the native protein for the induction of potent humoral response[24]. However, it was very challenge for synthetic epitopes to fold into helical structure by themselves, or even delivered by other NPs based platforms, such as liposomes, or polymeric NPs. Our EAK16-II peptide offers a promising strategy to promote the conformational structure of epitope, especially for non-linear B cell epitope. Moreover, though our understanding of how CD4+ T cells and CD8+ T cells interact has been improved remarkably, the role of CD4+ T cell help for the primary CTL response remains an open question[127]. Olivier and colleagues[229] reported that liposome-encapsulated CD8+ T cell epitopes did not require the help from CD4+ T cells or immune potentiators to prime CTLs in HLA-A2.1 mouse model. However, more recent studies have shown that the generated memory CTLs with the absence of T cell help are defective in the induction recall response following secondary challenge[236,238,239]. Thus, it is very important to investigate the importance of CD4+ T cell epitope in our self-assembling peptide based nanovaccine in future.

Our most recent *in-vivo* study suggested that when the antigen either mixture of epitopes and R848 or the nanovaccine was injected, most of the fluorophore labeled antigen was taken up by DCs, which are considered as the most crucial APCs for the induction of T cell response. Moreover, the fluorophore labeled nanovaccine persisted a longer duration inside DCs than the mixture of epitopes and R848, which was consistent with our *in-vitro* study discussed in Chapter3. As we did not incorporate any DC targeting ligand, why the nanovaccine was primarily found in DCs remains unclear for us. The physical attributes of NPs, such as size, shape, surface charge, and hydrophobicity can strongly influence the adjuvant properties[242,249]. A number of research findings have been reported and attempted to establish a correlation between the particle properties and the produced immune response, whereby, these reports are conflicting and debated[131,132,241,242,250–255]. For the purpose of targeting lymphoid DCs, NPs of 20-200nm, are preferable to larger particles, since the smaller particles can directly reach the lymph nodes[242]. The hydrodynamic size of our nanovaccine was measured as ~220nm, which is slightly larger than the top limit of the criterion. Thus, our nanovaccine could be captured and carried into initial lymph node by peripheral DCs in the injection site.

Molecular definition is becoming more favored for the vaccine design. To induce precise immune response with simple mechanism, NPs have been intensively studied for the delivery of antigenic peptide, among which Liposomes and polymeric NPs are the most used materials. We did not conduct a head-to-head comparison against these materials in our animal work, so there is no quantitative readout to compare the efficiency of our self-assembling peptide with them. Over liposome or polymeric NPs, the self-assembling peptide can offer a number of unique characteristics. First, the loading of antigen to self-

assembling domain is easily achieved by peptide synthesis, with higher antigen loading capacity. In contrast, liposomes and polymeric NPs normally deliver antigen with encapsulation, with which the loading capacity is much lower, and the integrity of the antigen might be impaired, since organic reagents, extrusion, or ultra-sonication were applied. Also, the self-assembling peptide can be applied to control the secondary structure of conformational B cell epitope. Moreover, highly repetitive display of antigenic peptides on nanoscale particles can be directly obtained from the self-assembling of peptide molecules. However, there are also some drawbacks for the self-assembling peptide based system when applied for antigen delivery. Compared with liposome or polymeric NPs, which can provide a gradual release of antigen up to 8-10 weeks, the self-assembling peptides are easily degraded, which would be the biggest obstacle for the application in vaccine delivery. Moreover, due to the nature of self-assembling peptide, when it is used with the presence of potent immune potentiator, possible immune response against its sequence might be primed, which is necessary to confirm in future.

Generally, self-assembling peptide provides a simple, chemically defined strategy for enhancing cellular response to peptide epitopes.

Chapter 6 Original Contributions and Recommendations

6.1 Original contributions to research

This thesis presented the application of the self-assembling peptide EAK16-II as a delivery platform in the formulation of HIV-1 peptide-based vaccine. With direct conjugation and non-covalent encapsulation, the HIV-1 highly conserved T cell epitopes and the TLR agonists were integrated within the nanostructure, which was evaluated for immunogenicity either in the form of DC-based vaccine *in vitro*, or a prophylactic vaccine *in vivo*. Three progressive parts were involved: (1) the synthesis and characterizations of HIV-1 CD8+ T cell epitope-bearing peptide, which was demonstrated to form nanofibers with improved extra/intra-cellular stability and enhanced cross-presentation efficiency by DCs; (2) the co-delivery of the antigenic epitope and the TLR agonists within the same nanoparticle that further augmented the DC maturation and consequently enhanced CTL response *in vitro*; (3) the formulation of a peptide-based vaccine by integrating the epitopes and the TLR agonist with the presence of the self-assembling peptide to induce potent HIV-1 specific CTL response *in vivo*. The original contributions to research are summarized as following.

Self-assembling peptide enhanced the cross-presentation efficiency of the epitope. The HIV-1 CD8+ T cell epitope SL9 was conjugated with the self-assembling peptide EAK16-II. Though a transition of the secondary structure from β-sheet for EAK16-II to α-helical structure for the epitope-bearing peptide occurred, SL9-EAK16-II still spontaneously aggregated to short nanofibers in PBS with the average hydrodynamic size

of ~103nm. The stability studies in serum or oligopeptidase demonstrated the conjugating peptide was more persistent than epitope alone, proving our hypothesis that nanostructure would prevent the epitope from degradation by proteases or peptidases. *Ex vivo* generated DCs pulsed with the nanofibers stimulated more poly-functional CTLs when co-cultured with PMBCs from HIV-1 infected individuals. Our data suggested this enhancement was beneficial from not only the sustained antigen level within DCs, but also the more efficient endosomal escape. However, the epitope-loaded nanofibers could not maturate DCs by itself, namely requiring the addition of immune potentiator to avoid causing tolerance.

The co-delivery of epitope and TLR agonist with the self-assembling peptide promoted the antigenicity of the epitope. The TLR agonist (R837 or R848) that could target and activate innate immunity to provide pro-inflammatory environment, was incorporated into the epitope-loaded nanofibers, by non-covalent interaction. It was suggested from calorimetric titration and fluorescence spectra that the co-assembly between the self-assembling peptide and the TLR 7/8 agonist was mainly driven by hydrogen bonding as well as hydrophobic interaction, and the ideal molar ratio for peptide to carry TLR agonist was 4:1. AFM and TME confirmed the morphology of the co-assembly as interweaved nanofibers, with increased hydrodynamic size, which were quickly internalized to endosomal compartments by DCs. The increased expression of surface maker CD83 on DCs implied the addition of the TLR agonist enhanced the stimulation of these nanofibers towards DCs. Consequently, relative to the DCs loaded with the epitope or the mixture of epitope and TLR agonist, the ones pulsed with the nanofibers simulated more SL9-specific poly-functional CTLs *in vitro*. Notably, R848

was suggested as a preferential TLR7/8 agonist when designing the therapeutic HIV-1 vaccine.

Integrated formulation of a peptide-based HIV-1 vaccine with the self-assembling peptide as the delivery platform: To generate long lasting memory antigen specific CTLs, the help from CD4+ T cell is necessary. Thus, we conjugated a CD4 epitope with EAK16-II, which co-assembled with the previously described CD8 epitope-bearing EAK16-II. The morphology of the co-assemblies was characterized as globular nanoparticles. The integrated formulation of the peptide-based vaccine was obtained by further assembling between the two epitope-bearing peptides with the TLR7/8 agonist R848. Physicochemical characterizations revealed the formulation as cross-linked nanofibers with an average hydrodynamic size of ~220nm. Then we examined the immunogenicity of these nanofibers in the transgenic mice by subcutaneous vaccination. Remarkably, the mice treated by the nanofibers based formation produced more SL9 specific memory CD8+ T cells, than either the mixture of epitopes and R848, or R848 alone. This strongly supported the potential of self-assembling peptide as matrix to formulate efficient HIV-1 peptide vaccine with low cost and ease of manufacturing.

6.2 Recommendations

This project is still in progress, for which currently great efforts are focusing on the *in-vivo* tracking of peptide, as well as measuring functionality of the *in-vivo* generated antigen specific CTLs. Additionally, since some important control groups, including the antigen without R848, the antigen without CD4+ T cell epitope, and epitopes adjuvanted with IFA or CFA as positive control, were missing in the previous *in vivo* study, more animal work will be carried out in future. Furthermore, the enhancement of T cell

response provided by the current formulation of nanovaccine is not sufficiently potent to provide protection against infection, thereby, some recommendations are proposed for the formulation optimization, as discussed in the following.

Firstly, the more CTL epitopes replacing SL9 should be tested in the transgenic mice to determine the enhancement by utilizing the self-assembling peptide is applicable to a broad range of epitopes, rather than any specific epitope. Moreover, since even in the "highly conserved" epitopes, residual variability still exists, the coverage of these immunogenic epitopes is not optimally sufficient. Inspired from the "mosaic" approach in engineering immunogen, a better CTL epitope can be artificially constructed to comprise more conserved epitopes in one sequence[8]. This strategy can contribute to generate a more efficient vaccine with a wider coverage. Alternatively, to avoid the potential risk of using such artificial epitope, we also can include more CTL epitopes in the vaccine formulation, rather than only one as we did in Chapter 5. Therefore, the self-assembling peptide might display the multiple CTL epitopes in the same nanoparticles, via co-assembly process. Compared with the means with dendrimer, which was more complicated in synthesis and more difficult in purification[256], this strategy exhibits obvious advantages in producing and manufacturing.

Furthermore, as suggested by our results and previous reports, the cross-presentation efficiency is critical for the immunogenicity of an antigen, especially for the exogenously administrated peptides. Two possible strategies can be considered in the future work. The first one is to further enhance the endosomal escape efficiency of the system by incorporating cell-penetrating peptides such as TAT, or a moiety with "proton sponge" effect. The other is that we can utilize various linking spacers between the epitope and the

self-assembling peptide, such as proteasome preferentially cleaving sequence[257], or replacing peptide bond with disulfide bond, which was suggested as an better choice for CTL response[130,258].

Last but not least, because of the central role of the dendritic cells in primary immune response, targeted delivery of the antigens to DCs is critically important for the design of an efficient vaccine. Despite the passively targeting strategies using nanosized or particulate vaccine carries, the most efficient approach is the actively targeting via the receptor-ligand interaction, such as mannose receptor, Fc receptor, and DC-SIGN (DC-Specific Intracellular adhesion molecule-3 Gabbing Non-integrin) receptor[259]. Therefore, we can incorporate one of these targeting ligands with the self-assembling peptide, to enhance targeting efficiency towards DCs.

Appendix

Method:

Liposome leakage assay Calcein-loaded liposome was prepared by POPC/POPG (3:1) as described. In a quartz cuvette, 5μL POPC/POPG liposome was mixed with 595μL HEPES buffer (10mM, pH7.0), in which 10μL peptide solution was added. The kinetic fluorescence was monitored every 12s for 38mins before Triton X100 (10μL, 5%) was added to fully rupture the liposome and the fluorescence was read again.

Results:

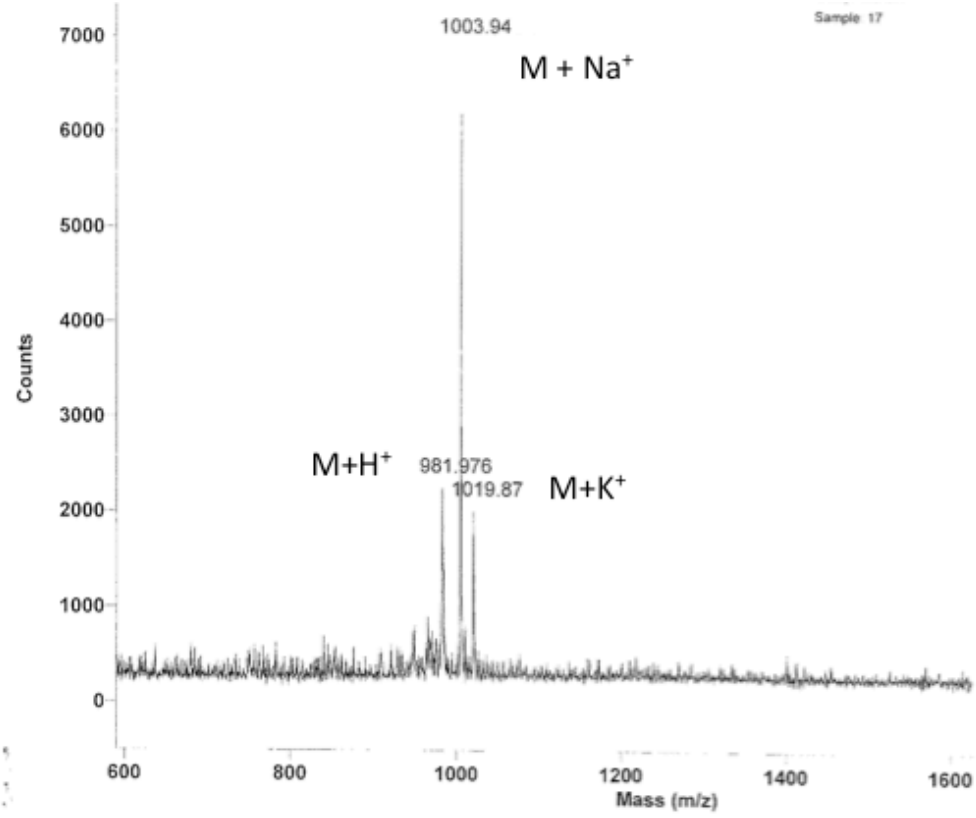

Figure 6-1 MS spectrum of SL9. The theoretical MW=980.13

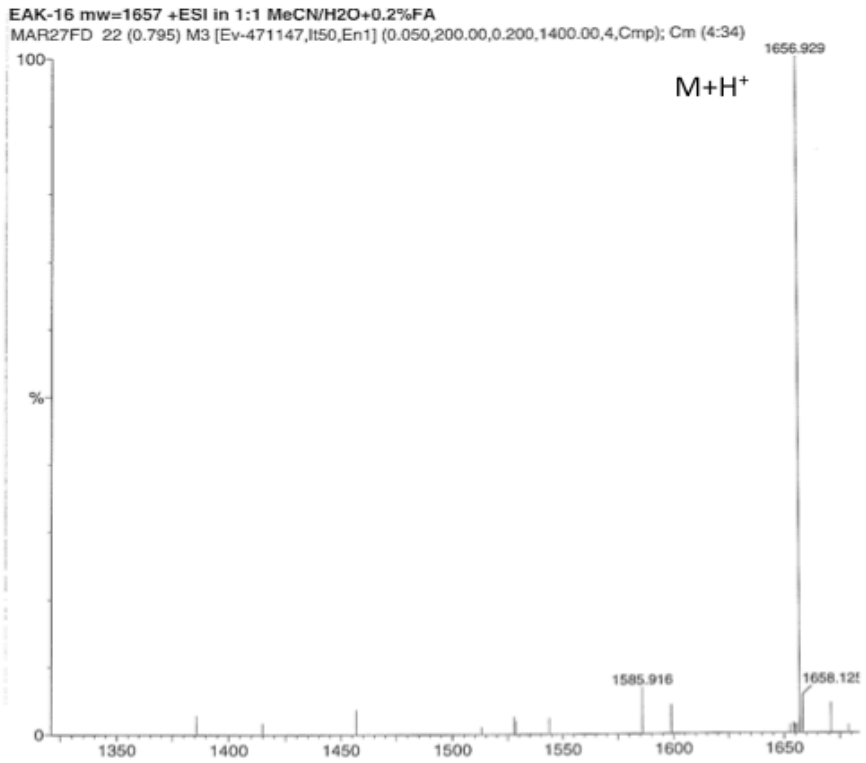

Figure 6-2 MS spectrum of EAK16-II. The theoretical MW=1655.85

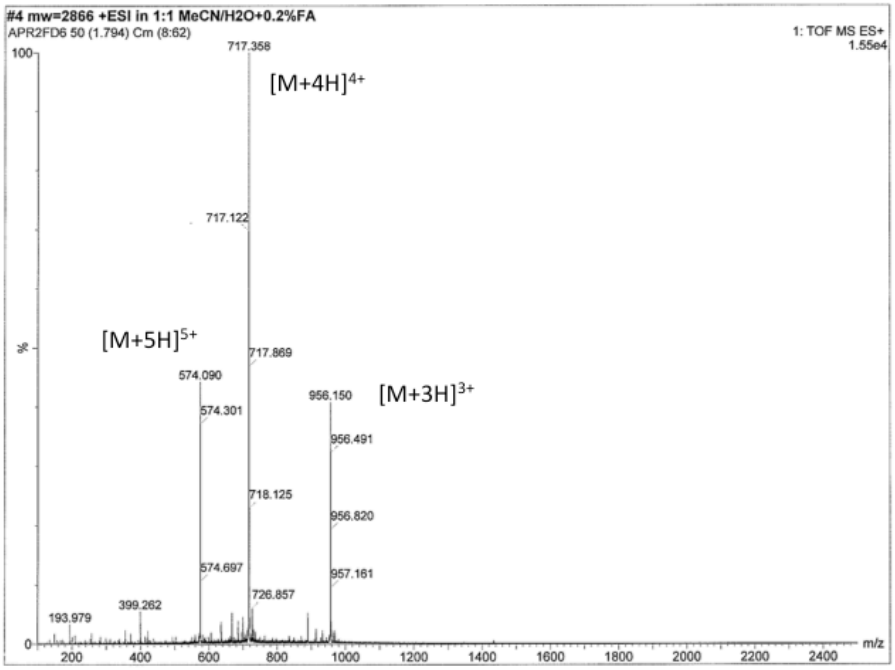

Figure 6-3 MS spectrum of SL9-EAK16-II. The theoretical MW=2866.18

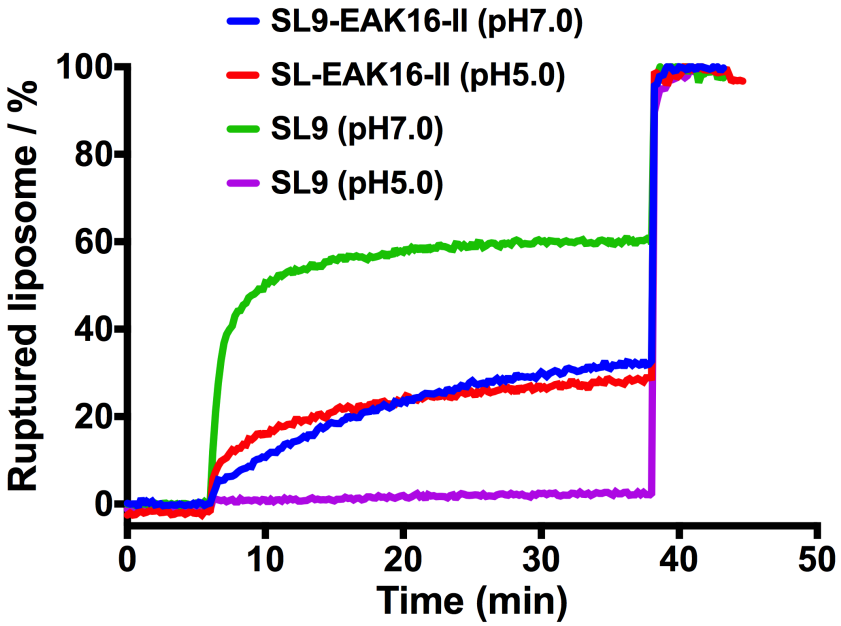

Figure 6-4 Kinetics of fluorescence increase indicated liposome rupture after mixing peptide solution with calcein-loaded POPC/POPG liposome.

JOHN WILEY AND SONS LICENSE TERMS AND CONDITIONS

Oct 29, 2015

This Agreement between YONG DING ("You") and John Wiley and Sons ("John Wiley and Sons") consists of your license details and the terms and conditions provided by John Wiley and Sons and Copyright Clearance Center.

License Number	3730350536023
License date	Oct 15, 2015
Licensed Content Publisher	John Wiley and Sons
Licensed Content Publication	Chemical Biology & Drug Design
Licensed Content Title	Peptide Nanoparticles as Novel Immunogens: Design and Analysis of a Prototypic Severe Acute Respiratory Syndrome Vaccine
Licensed Content Author	Tais A. P. F. Pimentel,Zhe Yan, Scott A. Jeffers,Kathryn V. Holmes,Robert S. Hodges,Peter Burkhard
Licensed Content Date	Dec 18, 2008
Pages	9
Type of use	Dissertation/Thesis
Requestor type	University/Academic
Format	Print and electronic
Portion	Figure/table
Number of figures/tables	1
Original Wiley figure/table number(s)	Figure2
Will you be translating?	No
Title of your thesis / dissertation	self-assembling peptide for HIV-1 vaccine design
Expected completion date	Nov 2015
Expected size (number of pages)	135
Requestor Location	YONG DING 309-545 belmont avenue west kitchener, ON n2m 5g7 Canada Attn: YONG DING
Billing Type	Invoice
Billing Address	YONG DING 309-545 belmont avenue west kitchener, ON n2m 5g7 Canada

Frank(Yong Ding) <dy1027@gmail.com> Thu, Oct 15, 2015 at 3:42 PM
To: PNASPermissions@nas.edu

Dear Sir or Madam,

Can I request for the permission of the use of figures in one paper from PNAS in my thesis? The required informations are listed as following:

My information:
name: YONG DING
Affiliation: University of Waterloo
Title: graduate student
Mailing address: 4612 QNC, University of waterloo, 200 University west, waterloo, ON N2L 3G1, Canada
Phone #: +1 226-9296577

Paper information:
Title: A self-assembling peptide acting as an immune adjuvant
Vol 107, No.2, Page 622-627,
PNAS author name: Joel H. Collier
Figure 1 on page 623 and Figure 3 on page 624 are to be reprinted.

My thesis information:
Title: self-assembling peptide for HIV-1 vaccine design;
Author: YONG DING

Thank you very much.

YONG DING (Frank)
PhD Candidate
Department of Chemical Engineering
University of Waterloo
200 University Avenue West
Waterloo, ON, Canada N2L 3G1
Tel:(519)888-4567 x 36864

PNAS Permissions <PNASPermissions@nas.edu> Fri, Oct 16, 2015 at 9:06 AM
To: "Frank(Yong Ding)" <dy1027@gmail.com>

Permission is granted for your use of the figures as described in your message. Please cite the PNAS article in full when re-using the material. Because this material published after 2008, a copyright note is not needed. There is no charge for this material, either. Let us know if you have any questions.

Best regards,

Kay McLaughlin for

Diane Sullenberger

Executive Editor

Reference:

1. Barouch, D. H. & Deeks, S. G. Immunologic strategies for HIV-1 remission and eradication. *Science.* **345,** (2014).

2. Alchin, D. R. HIV vaccine development: an exploratory review of the trials and tribulations. *Immunol. Res.* 35–37 (2014).

3. Pitisuttithum, P. *et al.* Randomized, double-blind, placebo-controlled efficacy trial of a bivalent recombinant glycoprotein 120 HIV-1 vaccine among injection drug users in Bangkok, Thailand. *J. Infect. Dis.* **194,** 1661–1671 (2006).

4. Priddy, F. H. *et al.* Safety and immunogenicity of a replication-incompetent adenovirus type 5 HIV-1 clade B gag/pol/nef vaccine in healthy adults. *Clin. Infect. Dis.* **46,** 1769–1781 (2008).

5. Barouch, D. H. Challenges in the development of an HIV-1 vaccine. *Nature* **455,** 613–619 (2008).

6. Wang, H.-B., Mo, Q.-H. & Yang, Z. HIV Vaccine Research: The Challenge and the Way Forward. *J. Immunol. Res.* **2015,** 1–5 (2015).

7. Hansen, S. G. *et al.* Immune clearance of highly pathogenic SIV infection. *Nature* **502,** 100–4 (2013).

8. McMichael, A. J. & Koff, W. C. Vaccines that stimulate T cell immunity to HIV-1: the next step. *Nat. Immunol.* **15,** 319–22 (2014).

9. O'Hagan, D. T. & Valiante, N. M. Recent advances in the discovery and delivery of vaccine adjuvants. *Nat. Rev. Drug Discov.* **2,** 727–35 (2003).

10. Rudra, J. S., Tian, Y. F., Jung, J. P. & Collier, J. H. A self-assembling peptide acting as an immune adjuvant. *Proc. Natl. Acad. Sci. U. S. A.* **107,** 622–7 (2010).

11. Alving, C. R. Liposomes as carriers of antigens and adjuvants. *J. Immunol. Methods* **140,** 1–13 (1991).

12. Chen, W. & Huang, L. Induction of cytotoxic T-lymphocytes and antitumor activity by a liposomal lipopeptide vaccine. *Mol. Pharm.* **5,** 464–471 (2008).

13. Akagi, T., Baba, M. & Akashi, M. Biodegradable Nanoparticles as Vaccine Adjuvants and Delivery Systems : Regulation of Immune Responses by Nanoparticle-Based Vaccine. *Adv. Comput. Simul. Approaches Soft Matter Sci. I* **247,** 31–64 (2012).

14. Akagi, T., Wang, X., Uto, T., Baba, M. & Akashi, M. Protein direct delivery to dendritic cells using nanoparticles based on amphiphilic poly(amino acid) derivatives. *Biomaterials* **28,** 3427–36 (2007).

15. Ghasparian, A. *et al.* Engineered synthetic virus-like particles and their use in vaccine delivery. *ChemBioChem* **12,** 100–109 (2011).

16. Tissot, A. C. *et al.* Versatile virus-like particle carrier for epitope based vaccines. *PLoS One* **5,** e9809 (2010).

17. Matson, J. B. & Stupp, S. I. Self-assembling peptide scaffolds for regenerative medicine. *Chem. Commun.* **48,** 26 (2012).

18. Jin, R. & Dijkstra, P. J. Hydrogels for Tissue Engineering Applications. *Biomed. Appl. Hydrogels Handb.* **101,** 203–225 (2010).

19. Pimentel, T. A. P. F. *et al.* Peptide Nanoparticles as Novel Immunogens: Design and Ananlysis of a Prototypic Severe Acute Respiratory Syndrome Vaccine. *Chem. Biol.* **73,** 53–61 (2009).

20. Zhang, S., Lockshin, C., Cook, R. & Rich, a. Unusually stable beta-sheet formation in an ionic self-complementary oligopeptide. *Biopolymers* **34,** 663–672 (1994).

21. Peek, L. J., Middaugh, C. R. & Berkland, C. Nanotechnology in vaccine delivery. *Adv. Drug Deliv. Rev.* **60,** 915–28 (2008).

22. L.A., B. Noval viral vaccines for livestock.pdf. *Velerinary Immunol. Immunopathol.* **54,** 355–363 (1996).

23. Purcell, A. W., McCluskey, J. & Rossjohn, J. More than one reason to rethink the use of peptides in vaccine design. *Nat. Rev. Drug Discov.* **6,** 404–414 (2007).

24. Li, W., Joshi, M., Singhania, S., Ramsey, K. & Murthy, A. Peptide Vaccine: Progress and Challenges. *Vaccines* **2,** 515–536 (2014).

25. Marrack, P., McKee, A. S. & Munks, M. W. Towards an understanding of the adjuvant action of aluminium. *Nat. Rev. Immunol.* **9,** 287–93 (2009).

26. Wendorf, J. *et al.* A Practical Approach to the use of Nanoparticles for Vaccine Delivery. *J. pharm Sci* **95,** 2738–2750 (2006).

27. Daftarian, P. *et al.* Eradication of established HPV 16-expressing tumors by a single administration of a vaccine composed of a liposome-encapsulated CTL-T helper fusion peptide in a water-in-oil emulsion. *Vaccine* **24,** 5235–44 (2006).

28. Ishii, K. J. & Akira, S. Toll or toll-free adjuvant path toward the optimal vaccine development. *J. Clin. Immunol.* **27,** 363–71 (2007).

29. Sanders, M. T., Brown, L. E., Deliyannis, G. & Pearse, M. J. ISCOM-based vaccines: the second decade. *Immunol. Cell Biol.* **83,** 119–28 (2005).

30. Engel, A. L., Holt, G. E. & Lu, H. The pharmacokinectics of toll-like receptor agonists and the impact on the immune system. *Expert Rev Clin Pharmacol* **4,** 275–289 (2011).

31. Black, M., Trent, A., Tirrell, M. & Olive, C. Advances in the design and delivery of peptide subunit vaccines with a focus on toll-like receptor agonists. *Expert Rev. Vaccines* **9,** 157–173 (2010).

32. Gomariz, R. P. *et al.* Peptides targeting Toll-like receptor signalling pathways for novel immune therapeutics. *Curr. Pharm. Des.* **16,** 1063–1080 (2010).

33. Steinhagen, F., Kinjo, T., Bode, C. & Klinman, D. M. TLR-based immune adjuvants. *Vaccine* **29,** 3341–3355 (2011).

34. Gorden, K. B. *et al.* Synthetic TLR agonists reveal functional differences between human TLR7 and TLR8. *J. Immunol.* **174,** 1259–1268 (2005).

35. Otero, M. *et al.* Resiquimod is a modest adjuvant for HIV-1 gag-based genetic immunization in a mouse model. *Vaccine* **22,** 1782–1790 (2004).

36. Wille-Reece, U. *et al.* HIV Gag protein conjugated to a Toll-like receptor 7/8 agonist improves the magnitude and quality of Th1 and CD8+ T cell responses in nonhuman primates. *Proc. Natl. Acad. Sci. U. S. A.* **102,** 15190–15194 (2005).

37. Wille-Reece, U., Wu, C.-Y., Flynn, B. J., Kedl, R. M. & Seder, R. a. Immunization with HIV-1 Gag protein conjugated to a TLR7/8 agonist results in the generation of HIV-1 Gag-specific Th1 and CD8+ T cell responses. *J. Immunol.* **174,** 7676–7683 (2005).

38. Harrison, C. J., Miller, R. L. & Bernstein, D. I. Reduction of recurrent HSV disease using imiquimod alone or combined with a glycoprotein vaccine. *Vaccine* **19,** 1820–1826 (2001).

39. Sachan, S. *et al.* Adjuvant potential of resiquimod with inactivated Newcastle disease vaccine and its mechanism of action in chicken. *Vaccine* 1–7 (2015). doi:10.1016/j.vaccine.2015.07.016

40. Othoro, C. *et al.* Enhanced immunogenicity of plasmodium falciparum peptide vaccines using a topical adjuvant containing a potent synthetic toll-like receptor 7 agonist, imiquimod. *Infect. Immun.* **77,** 739–748 (2009).

41. Mark, K. E. *et al.* Topical resiquimod 0.01% gel decreases herpes simplex virus type 2 genital shedding: a randomized, controlled trial. *J. Infect. Dis.* **195,** 1324–1331 (2007).

42. Sabado, R. L. *et al.* Resiquimod as an Immunologic Adjuvant for NY-ESO-1 Protein Vaccination in Patients with High-Risk Melanoma. *Cancer Immunol. Res.* **3,** 278–287 (2015).

43. Adams, S. *et al.* Immunization of malignant melanoma patients with full-length NY-ESO-1 protein using TLR7 agonist imiquimod as vaccine adjuvant. *J. Immunol.* **181,** 776–784 (2008).

44. Zhao, L. *et al.* Nanoparticle vaccines. *Vaccine* **32,** 327–337 (2014).

45. C.R.Parish. Immune response to chemical modified flagellin. *Cell. Immunol.* **6,** 66–79 (1973).

46. Sakaue, G. *et al.* HIV mucosal vaccine: nasal immunization with gp160-encapsulated hemagglutinating virus of Japan-liposome induces antigen-specific CTLs and neutralizing antibody responses. *J. Immunol.* **170,** 495–502 (2003).

47. Singh, S. K. & Bisen, P. S. Adjuvanticity of stealth liposomes on the immunogenicity of synthetic gp41 epitope of HIV-1. *Vaccine* **24,** 4161–6 (2006).

48. Babu, J. S., Nair, S., Kanda, P. & Rouse, B. T. Priming for virus-specific CD8+ but not CD4+ cytotoxic T lymphocytes with synthetic lipopeptide is influenced by acylation units and liposome encapsulation. *Vaccine* **13,** 1669–76 (1995).

49. White, W. I. *et al.* Antibody and cytotoxic T-lymphocyte responses to a single liposome-associated peptide antigen. *Vaccine* **13,** 1111–22 (1995).

50. Saupe, A., McBurney, W., Rades, T. & Hook, S. Immunostimulatory colloidal delivery systems for cancer vaccines. *Expert Opin. Drug Deliv.* **3,** 345–54 (2006).

51. Latif, N. & Bachhawat, B. K. Liposomes in immunology. *J.Biosci.* **6,** 491–502 (1984).

52. Nakanishi, T. *et al.* Positively charged liposome functions as an efficient immunoadjuvant in inducing cell-mediated immune response to soluble proteins. *J. Control. Release* **61,** 233–40 (1999).

53. Guan, H. H. *et al.* Liposomal formulations of synthetic MUC1 peptides: effects of encapsulation versus surface display of peptides on immune responses. *Bioconjug. Chem.* **9,** 451–8 (1998).

54. Takagi, A. *et al.* Highly efficient antiviral CD8+ T-cell induction by peptides coupled to the surfaces of liposomes. *Clin. Vaccine Immunol.* **16,** 1383–92 (2009).

55. Panyam, J. & Labhasetwar, V. Biodegradable nanoparticles for drug and gene delivery to cells and tissue. *Adv. Drug Deliv. Rev.* **55,** 329–347 (2003).

56. Lutsiak, M. E. C., Kwon, G. S. & Samuel, J. Biodegradable nanoparticle delivery of a Th2-biased peptide for induction of Th1 immune responses. *J. Pharm. Pharmacol.* **58,** 739–47 (2006).

57. Singh, M. *et al.* Immunogenicity and protection in small-animal models with controlled-release tetanus toxoid microparticles as a single-dose vaccine. *Infect. Immun.* **65,** 1716–21 (1997).

58. Kasturi, S. P. *et al.* Programming the magnitude and persistence of antibody responses with innate immunity. *Nature* **470,** 543–7 (2011).

59. Tamber, H., Johansen, P., Merkle, H. P. & Gander, B. Formulation aspects of biodegradable polymeric microspheres for antigen delivery. *Adv. Drug Deliv. Rev.* **57,** 357–76 (2005).

60. Mundargi, R. C., Babu, V. R., Rangaswamy, V., Patel, P. & Aminabhavi, T. M. Nano/micro technologies for delivering macromolecular therapeutics using poly(D,L-lactide-co-glycolide) and its derivatives. *J. Control. Release* **125,** 193–209 (2008).

61. Chong, C. S. W. *et al.* Enhancement of T helper type 1 immune responses against hepatitis B virus core antigen by PLGA nanoparticle vaccine delivery. *J. Control. Release* **102,** 85–99 (2005).

62. Partidos, C. D., Vohra, P., Jones, D., Farrar, G. & Steward, M. W. CTL responses induced by a single immunization with peptide encapsulated in biodegradable microparticles. *J. Immunol. Methods* **206,** 143–151 (1997).

63. Partidos, C. D., Vohra, P., Jones, D. H., Farrar, G. & Steward, M. W. Induction of cytotoxic T-cell responses following oral immunization with synthetic peptides encapsulated in PLG microparticles. *J. Control. Release* **62,** 325–332 (1999).

64. Partidos, C. D., Vohra, P. & Steward, M. W. Induction of measles virus-specific cytotoxic T-cell responses after intranasal immunization with synthetic peptides. *Immunology* **87,** 179–185 (1996).

65. Shen, H. *et al.* Enhanced and prolonged cross-presentation following endosomal escape of exogenous antigens encapsulated in biodegradable nanoparticles. *Immunology* **117,** 78–88 (2006).

66. Zhou, S., Liao, X., Li, X., Deng, X. & Li, H. P oly- D , L -lactide – co-poly (ethylene glycol) microspheres as potential vaccine delivery systems. *J. Control. Release* **86,** 195–205 (2003).

67. Deng, X. M., Xiong, C. D., Cheng, L. M., Xu, R. P. & Chemistry, O. Synthesis and Characterization of Block Copolymers from D,L-Lactide and Poly (Ethylene Glycol) with Stannous Chloride*. *J. Polym. Sci. Part C Polym. Lett.* **28,** 411–416 (1990).

68. Deng, X., Zhou, S., Li, X., Zhao, J. & Yuan, M. In vitro degradation and release profiles for poly-dl-lactide-poly(ethylene glycol) microspheres containing human serum albumin. *J. Control. Release* **71,** 165–73 (2001).

69. Holowka, E. P., Pochan, D. J. & Deming, T. J. Charged polypeptide vesicles with controllable diameter. *J. Am. Chem. Soc.* **127,** 12423–8 (2005).

70. Akiyoshi, K., Ueminami, A., Kurumada, S. & Nomura, Y. Self-Association of Cholesteryl-Bearing Poly (L -lysine) in Water and Control of Its Secondary Structure by Host-Guest Interaction with Cyclodextrin. *Macromolecules* **33,** 6752–6756 (2000).

71. Matsusaki, M., Hiwatari, K., Higashi, M., Kaneko, T. & Akashi, M. Stably-dispersed and Surface-functional Bionanoparticles Prepared by Self-assembling Amphipathic Polymers of Hydrophilic Poly(γ-glutamic acid) Bearing Hydrophobic Amino Acids. *Chem. Lett.* **33,** 398–399 (2004).

72. Matsusaki, M. & Fuchida, T. self-assembling bionannoparticles of poly lysine bearing cholesterol as a biomesogen. *Biomacromolecules* **6,** 2374–2379 (2005).

73. Arimura, H., Ohya, Y. & Ouchi, T. Formation of core-shell type biodegradable polymeric micelles from amphiphilic poly(aspartic acid)-block-polylactide diblock copolymer. *Biomacromolecules* **6,** 720–5 (2005).

74. Holowka, E. P., Sun, V. Z., Kamei, D. T. & Deming, T. J. Polyarginine segments in block copolypeptides drive both vesicular assembly and intracellular delivery. *Nat. Mater.* **6,** 52–7 (2007).

75. Jeong, J. H., Kang, H. S., Yang, S. R. & Kim, J.-D. Polymer micelle-like aggregates of novel amphiphilic biodegradable poly(asparagine) grafted with poly(caprolactone). *Polymer (Guildf).* **44,** 583–591 (2003).

76. Kataoka, K., Matsumoto, T., Yokoyama, M. & Okano, T. aspartate) copolymer micelles : their pharmaceutical characteristics and biological significance. *J. Control. Release* **64,** 143–153 (2000).

77. Lin, J., Zhang, S., Chen, T., Lin, S. & Jin, H. Micelle formation and drug release behavior of polypeptide graft copolymer and its mixture with polypeptide block copolymer. *Int. J. Pharm.* **336,** 49–57 (2007).

78. Lee, E. S., Shin, H. J., Na, K. & Bae, Y. H. Poly(L-histidine)-PEG block copolymer micelles and pH-induced destabilization. *J. Control. Release* **90,** 363–74 (2003).

79. Schneerson, R. *et al.* Poly(gamma-D-glutamic acid) protein conjugates induce IgG antibodies in mice to the capsule of Bacillus anthracis: a potential addition to the anthrax vaccine. *Proc. Natl. Acad. Sci. U. S. A.* **100,** 8945–50 (2003).

80. Wang, T. T., Fellows, P. F., Leighton, T. J. & Lucas, A. H. Induction of opsonic antibodies to the gamma-D-glutamic acid capsule of Bacillus anthracis by immunization with a synthetic peptide-carrier protein conjugate. *FEMS Immunol. Med. Microbiol.* **40,** 231–7 (2004).

81. Joyce, J. *et al.* Immunogenicity and protective efficacy of Bacillus anthracis poly-gamma-D-glutamic acid capsule covalently coupled to a protein carrier using a novel triazine-based conjugation strategy. *J. Biol. Chem.* **281,** 4831–43 (2006).

82. Uto, T. *et al.* Targeting of antigen to dendritic cells with poly(gamma-glutamic acid) nanoparticles induces antigen-specific humoral and cellular immunity. *J. Immunol.* **178,** 2979–86 (2007).

83. Akagi, T., Shima, F. & Akashi, M. Intracellular degradation and distribution of protein-encapsulated amphiphilic poly(amino acid) nanoparticles. *Biomaterials* **32,** 4959–67 (2011).

84. Wang, X., Uto, T., Akagi, T., Akashi, M. & Baba, M. Induction of potent CD8+ T-cell responses by novel biodegradable nanoparticles carrying human immunodeficiency virus type 1 gp120. *J. Virol.* **81,** 10009–16 (2007).

85. Okamoto, S. *et al.* Poly(gamma-glutamic acid) nano-particles combined with mucosal influenza virus hemagglutinin vaccine protects against influenza virus infection in mice. *Vaccine* **27,** 5896–905 (2009).

86. Okamoto, S. *et al.* Single dose of inactivated Japanese encephalitis vaccine with poly(gamma-glutamic acid) nanoparticles provides effective protection from Japanese encephalitis virus. *Vaccine* **26,** 589–94 (2008).

87. Yoshikawa, T. *et al.* Nanoparticles built by self-assembly of amphiphilic gamma-PGA can deliver antigens to antigen-presenting cells with high efficiency: a new tumor-vaccine carrier for eliciting effector T cells. *Vaccine* **26,** 1303–13 (2008).

88. Yamaguchi, S. *et al.* EphA2-derived peptide vaccine with amphiphilic poly(gamma-glutamic acid) nanoparticles elicits an anti-tumor effect against mouse liver tumor. *Cancer Immunol. Immunother.* **59,** 759–67 (2010).

89. Stone, J. W. *et al.* Gold nanorod vaccine for respiratory syncytial virus. *Nanotechnology* **24,** 295102 (2013).

90. Chen, Y.-S., Hung, Y.-C., Lin, W.-H. & Huang, G. S. Assessment of gold nanoparticles as a size-dependent vaccine carrier for enhancing the antibody response against synthetic foot-and-mouth disease virus peptide. *Nanotechnology* **21,** 195101 (2010).

91. Xu, L. *et al.* Surface-engineered gold nanorods: Promising DNA vaccine adjuvant for HIV-1 treatment. *Nano Lett.* **12,** 2003–2012 (2012).

92. Niikura, K. *et al.* Gold nanoparticles as a vaccine platform: Influence of size and shape on immunological responses in vitro and in vivo. *ACS Nano* **7,** 3926–3938 (2013).

93. Almeida, J. P. M., Lin, A. Y., Figueroa, E. R., Foster, A. E. & Drezek, R. A. In vivo Gold Nanoparticle Delivery of Peptide Vaccine Induces Anti-Tumor Immune Response in Prophylactic and Therapeutic Tumor Models. *Small* n/a–n/a (2014). doi:10.1002/smll.201402179

94. Lee, I. H. *et al.* Imageable antigen-presenting gold nanoparticle vaccines for effective cancer immunotherapy in vivo. *Angew. Chemie - Int. Ed.* **51,** 8800–8805 (2012).

95. Hudson, S., Cooney, J. & Magner, E. Proteins in Mesoporous Silicates. *Angew. Chemie Int. Ed.* **47,** 8582–8594 (2008).

96. Cheng, K., El-Boubbou, K. & Landry, C. C. Binding of HIV-1 gp120 glycoprotein to silica nanoparticles modified with CD4 glycoprotein and CD4 peptide fragments. *ACS Appl. Mater. Interfaces* **4,** 235–243 (2012).

97. Guo, H.-C. *et al.* Immunization of mice by Hollow Mesoporous Silica Nanoparticles as carriers of Porcine Circovirus Type 2 ORF2 Protein. *Virol. J.* **9,** 108 (2012).

98. Carvalho, L. V *et al.* Immunological parameters related to the adjuvant effect of the ordered mesoporous silica SBA-15. *Vaccine* **28,** 7829–7836 (2010).

99. Mahony, D. *et al.* Mesoporous silica nanoparticles act as a self-adjuvant for ovalbumin model antigen in mice. *Small* **9,** 3138–3146 (2013).

100. Mody, K. T. *et al.* Mesoporous silica nanoparticles as antigen carriers and adjuvants for vaccine delivery. *Nanoscale* **5,** 5167–79 (2013).

101. Akahata, W. *et al.* A virus-like particle vaccine for epidemic Chikungunya virus protects nonhuman primates against infection. *Nat. Med.* **16,** 334–338 (2010).

102. Ruedl, C. *et al.* Virus-Like Particles as Carriers for T-Cell Epitopes : Limited Inhibition of T-Cell Priming by Carrier-Specific Antibodies Virus-Like Particles as Carriers for T-Cell Epitopes : Limited Inhibition of T-Cell Priming by Carrier-Specific Antibodies. *J. Virol.* **79,** 717–724 (2005).

103. Sedlik, C., Saron, M., Sarraseca, J., Casal, I. & Leclerc, C. Recombinant parvovirus-like particles as an antigen carrier: a novel nonreplicative exogenous antigen to elicit protective antiviral cytotoxic T cells. *Proc. Natl. Acad. Sci. U. S. A.* **94,** 7503–7508 (1997).

104. Fausch, S. C., Da Silva, D. M. & Kast, W. M. Heterologous papillomavirus virus-like particles and human papillomavirus virus-like particle immune complexes activate human Langerhans cells. *Vaccine* **23,** 1720–1729 (2005).

105. Fausch, S. C., Da Silva, D. M. & Kast, W. M. Differential uptake and cross-presentation of human papillomavirus virus-like particles by dendritic cells and Langerhans cells. *Cancer Res.* **63,** 3478–3482 (2003).

106. Roy, P. & Noad, R. Virus-like particles as a vaccine delivery system: Myths and facts. *Hum. Vaccin.* **4,** 5–12 (2008).

107. Rock, K. L. & Shen, L. Cross-presentation: underlying mechanisms and role in immune surveillance. *Immunol Rev* **207,** 166–183 (2005).

108. Heath, W. R. *et al.* Cross-presentation, dendritic cell subsets, and the generation of immunity to cellular antigens. *Immunol. Rev.* **199,** 9–26 (2004).

109. Heit, A. *et al.* CpG-DNA aided cross-priming by cross-presenting B cells. *J. Immunol.* **172,** 1501–1507 (2004).

110. Tvinnereim, A. R., Hamilton, S. E. & Harty, J. T. Neutrophil involvement in cross-priming CD8+ T cell responses to bacterial antigens. *J. Immunol.* **173,** 1994–2002 (2004).

111. Bagai, R. *et al.* Mouse endothelial cells cross-present lymphocyte-derived antigen on class I MHC via a TAP1- and proteasome-dependent pathway. *J. Immunol.* **174,** 7711–7715 (2005).

112. Bevan, M. J. Minor H antigens introduced on H-2 different stimulating cells cross-react at the cytotoxic T cell level during in vivo priming. *J. Immunol.* **117,** 2233–2238 (1976).

113. Cho, J. H., Youn, J. W. & Sung, Y. C. Cross-priming as a predominant mechanism for inducing CD8(+) T cell responses in gene gun DNA immunization. *J. Immunol.* **167,** 5549–5557 (2001).

114. Freigang, S., Egger, D., Bienz, K., Hengartner, H. & Zinkernagel, R. M. Endogenous neosynthesis vs. cross-presentation of viral antigens for cytotoxic T cell priming. *Proc. Natl. Acad. Sci. U. S. A.* **100,** 13477–13482 (2003).

115. Shen, L. & Rock, K. L. Cellular protein is the source of cross-priming antigen in vivo. *Proc. Natl. Acad. Sci. U. S. A.* **101,** 3035–3040 (2004).

116. Norbury, C. C. *et al.* CD8+ T cell cross-priming via transfer of proteasome substrates. *Science* **304,** 1318–1321 (2004).

117. Sigal, L. J., Crotty, S., Andino, R. & Rock, K. L. Cytotoxic T-cell immunity to virus-infected non-haematopoietic cells requires presentation of exogenous antigen. *Nature* **398,** 77–80 (1999).

118. Ramirez, M. C. & Sigal, L. J. Macrophages and dendritic cells use the cytosolic pathway to rapidly cross-present antigen from live, vaccinia-infected cells. *J. Immunol.* **169,** 6733–6742 (2002).

119. Morgan, D. J. *et al.* Ontogeny of T cell tolerance to peripherally expressed antigens. *Proc. Natl. Acad. Sci. U. S. A.* **96,** 3854–3858 (1999).

120. Joffre, O. P., Segura, E., Savina, A. & Amigorena, S. Cross-presentation by dendritic cells. *Nat. Rev. Immunol.* **12,** 557–569 (2012).

121. Fehres, C. M., Unger, W. W. J., Garcia-Vallejo, J. J. & van Kooyk, Y. Understanding the biology of antigen cross-presentation for the design of vaccines against cancer. *Front. Immunol.* **5,** 1–10 (2014).

122. Tacken, P. J. *et al.* Targeting DC-SIGN via its neck region leads to prolonged antigen residence in early endosomes, delayed lysosomal degradation, and cross-presentation. *Blood* **118,** 4111–4119 (2011).

123. Van Kooyk, Y., Unger, W. W. J., Fehres, C. M., Kalay, H. & García-Vallejo, J. J. Glycan-based DC-SIGN targeting vaccines to enhance antigen cross-presentation. *Mol. Immunol.* **55,** 143–145 (2013).

124. Singh, S. K. *et al.* Design of neo-glycoconjugates that target the mannose receptor and enhance TLR-independent cross-presentation and Th1 polarization. *Eur. J. Immunol.* **41,** 916–925 (2011).

125. Chatterjee, B. *et al.* Internalization and endosomal degradation of receptor-bound antigens regulate the efficiency of cross presentation by human dendritic cells. *Blood* **120,** 2011–2020 (2012).

126. Plotkin, S. a. Vaccines: correlates of vaccine-induced immunity. *Clin. Infect. Dis.* **47,** 401–409 (2008).

127. Williams, M. a & Bevan, M. J. Effector and memory CTL differentiation. *Annu. Rev. Immunol.* **25,** 171–192 (2007).

128. Behera, T. & Swain, P. Antigen adsorbed calcium phosphate nanoparticles stimulate both innate and adaptive immune response in fish, Labeo Rohita H. *Cell. Immunol.* **271,** 350–359 (2011).

129. Lebre, F., Bento, D., Jesus, S. & Borges, O. *Chitosan-Based Nanoparticles as a Hepatitis B Antigen Delivery System*. *Methods Enzymol.* **509,** (Elsevier Inc., 2012).

130. Zeng, W. *et al.* A modular approach to assembly of totally synthetic self-adjuvanting lipopeptide-based vaccines allows conformational epitope building. *J. Biol. Chem.* **286,** 12944–12951 (2011).

131. Manolova, V. *et al.* Nanoparticles target distinct dendritic cell populations according to their size. *Eur. J. Immunol.* **38,** 1404–13 (2008).

132. Xiang, S. D. *et al.* Pathogen recognition and development of particulate vaccines: does size matter? *Methods* **40,** 1–9 (2006).

133. Hamdy, S. *et al.* Co-delivery of cancer-associated antigen and Toll-like receptor 4 ligand in PLGA nanoparticles induces potent CD8+ T cell-mediated anti-tumor immunity. *Vaccine* **26,** 5046–5057 (2008).

134. Wilson, J. T. *et al.* PH-responsive nanoparticle vaccines for dual-delivery of antigens and immunostimulatory oligonucleotides. *ACS Nano* **7,** 3912–3925 (2013).

135. Sokolova, V. *et al.* The use of calcium phosphate nanoparticles encapsulating Toll-like receptor ligands and the antigen hemagglutinin to induce dendritic cell maturation and T cell activation. *Biomaterials* **31,** 5627–5633 (2010).

136. Heit, A., Schmitz, F., Haas, T., Busch, D. H. & Wagner, H. Antigen co-encapsulated with adjuvants efficiently drive protective T cell immunity. *Eur. J. Immunol.* **37,** 2063–2074 (2007).

137. Mutwiri, G. K., Nichani, A. K., Babiuk, S. & Babiuk, L. a. Strategies for enhancing the immunostimulatory effects of CpG oligodeoxynucleotides. *J. Control. Release* **97,** 1–17 (2004).

138. Blander, J. M. & Medzhitov, R. Toll-dependent selection of microbial antigens for presentation by dendritic cells. *Nature* **440,** 808–812 (2006).

139. Nakamura, T. *et al.* Octaarginine-modified liposomes enhance cross-presentation by promoting the c-terminal trimming of antigen peptide. *Mol. Pharm.* **11,** 2787–2795 (2014).

140. Brooks, N. a., Pouniotis, D. S., Sheng, K. C., Apostolopoulos, V. & Pietersz, G. a. A membrane penetrating multiple antigen peptide (MAP) incorporating ovalbumin CD8 epitope induces potent immune responses in mice. *Biochim. Biophys. Acta - Biomembr.* **1798,** 2286–2295 (2010).

141. Brooks, N. a., Pouniotis, D. S., Tang, C. K., Apostolopoulos, V. & Pietersz, G. a. Cell-penetrating peptides: Application in vaccine delivery. *Biochim. Biophys. Acta - Rev. Cancer* **1805,** 25–34 (2010).

142. Whitesides, G. M. & Grzybowski, B. Self-Assembly at All Scales. *Science (80-.).* **295,** 2418–2422 (2002).

143. MacPhee, C. E. & Woolfson, D. N. Engineered and designed peptide-based fibrous biomaterials. *Curr. Opin. Solid State Mater. Sci.* **8,** 141–149 (2004).

144. Zhao, Y., Tanaka, M., Kinoshita, T., Higuchi, M. & Tan, T. Nanofibrous scaffold from self-assembly of beta-sheet peptides containing phenylalanine for controlled release. *J. Control. Release* **142,** 354–360 (2010).

145. Hauser, C. a E. *et al.* Natural tri- to hexapeptides self-assemble in water to amyloid beta-type fiber aggregates by unexpected alpha-helical intermediate structures. *Proc. Natl. Acad. Sci. U. S. A.* **108,** 1361–1366 (2011).

146. Wang, W. & Chau, Y. Self-assembled peptide nanorods as building blocks of fractal patterns. *Soft Matter* **5,** 4893 (2009).

147. Gröning, M. Von, Feijter, I. De, Stuart, M. C. a, Voets, K. & Besenius, P. Tuning the aqueous self-assembly of multistimuli- responsive polyanionic peptide nanorods. *J. Mater. Chem. B* **4,** 2008–2012 (2013).

148. Matsui, H., Gologan, B., Pan, S. & Douberly, G. E. Controlled immobilization of peptide nanotubes-templated metallic wires on Au surfaces. *Eur. Phys. J. D* **16,** 403–406 (2001).

149. Trent, A., Marullo, R., Lin, B., Black, M. & Tirrell, M. Structural properties of soluble peptide amphiphile micelles. *Soft Matter* **7,** 9572 (2011).

150. Collins, L. *et al.* Self-assembly of peptides into spherical nanoparticles for delivery of hydrophilic moieties to the cytosol. *ACS Nano* **4,** 2856–2864 (2010).

151. Matsuura, K. *et al.* Spontaneous self-assembly of nanospheres from trigonal conjugate of glutathione in water. *Soft Matter* **5,** 2463 (2009).

152. Frederix, P. W. J. M. *et al.* Exploring the sequence space for (tri-)peptide self-assembly to design and discover new hydrogels. *Nat. Chem.* **7,** 30–37 (2014).

153. Smadbeck, J. *et al.* De Novo Design and Experimental Characterization of Ultrashort Self-Associating Peptides. *PLoS Comput. Biol.* **10,** (2014).

154. Fung, S. Y. *et al.* Amino acid pairing for de novo design of self-assembling peptides and their drug delivery potential. *Adv. Funct. Mater.* **21,** 2456–2464 (2011).

155. Jafari, M., Xu, W., Naahidi, S., Chen, B. & Chen, P. A new amphipathic, amino-acid-pairing (AAP) peptide as sirna delivery carrier: Physicochemical characterization and in vitro uptake. *J. Phys. Chem. B* **116,** 13183–13191 (2012).

156. Kyle, S., Aggeli, A., Ingham, E. & McPherson, M. J. Recombinant self-assembling peptides as biomaterials for tissue engineering. *Biomaterials* **31,** 9395–9405 (2010).

157. Collier, J. H. & Messersmith, P. B. Enzymatic modification of self-assembled peptide structures with tissue transglutaminase. *Bioconjug. Chem.* **14,** 748–55 (2003).

158. Panda, J. J. & Chauhan, V. S. Short peptide based self-assembled nanostructures: implications in drug delivery and tissue engineering. *Polym. Chem.* **5,** 4431 (2014).

159. Tropel, D., Graff, A., Machaidze, G., Burkhard, P. & Genetics, M. Peptide Based Nanoparticles as a Platform for Vaccine Design. *NSTI-Nanotech* **1,** 47–50 (2005).

160. Liu, L. *et al.* Self-assembled cationic peptide nanoparticles as an efficient antimicrobial agent. *Nat. Nanotechnol.* **4,** 457–463 (2009).

161. Wiradharma, N., Tong, Y. W. & Yang, Y. Y. Self-assembled oligopeptide nanostructures for co-delivery of drug and gene with synergistic therapeutic effect. *Biomaterials* **30,** 3100–3109 (2009).

162. Zhao, X. & Zhang, S. Molecular designer self-assembling peptides. *Chem. Soc. Rev.* **35,** 1105–1110 (2006).

163. Li, X. *et al.* Molecular nanofibers of olsalazine form supramolecular hydrogels for reductive release of an anti-inflammatory agent. *J. Am. Chem. Soc.* **132,** 17707–17709 (2010).

164. Naskar, J., Roy, S., Joardar, A., Das, S. & Banerjee, A. Self-assembling dipeptide-based nontoxic vesicles as carriers for drugs and other biologically important molecules. *Org. Biomol. Chem.* **9,** 6610–6615 (2011).

165. Jung, J. P. *et al.* Co-assembling peptides as defined matrices for endothelial cells. *Biomaterials* **30,** 2400–10 (2009).

166. Holmes, T. C. *et al.* Extensive neurite outgrowth and active synapse formation on self-assembling peptide scaffolds. *Proc. Natl. Acad. Sci. U. S. A.* **97,** 6728–33 (2000).

167. Hsieh, P. C. H., Davis, M. E., Gannon, J., MacGillivray, C. & Lee, R. T. Controlled delivery of PDGF-BB for myocardial protection using injectable self-assembling peptide nanofibers. *J. Clin. Invest.* **116,** 237–248 (2006).

168. Davis, M. E. *et al.* Injectable self-assembling peptide nanofibers create intramyocardial microenvironments for endothelial cells. *Circulation* **111,** 442–450 (2005).

169. Boato, F. *et al.* Synthetic virus-like particles from self-assembling coiled-coil lipopeptides and their use in antigen display to the immune system. *Angew. Chemie - Int. Ed.* **46,** 9015–9018 (2007).

170. Collier, J. H. Modular self-assembling biomaterials for directing cellular responses. *Soft Matter* **4,** 2310 (2008).

171. Jung, J. P., Jones, J. L., Cronier, S. a. & Collier, J. H. Modulating the mechanical properties of self-assembled peptide hydrogels via native chemical ligation. *Biomaterials* **29,** 2143–2151 (2008).

172. Rudra, J. S. *et al.* Self-assembled peptide nanofibers raising durable antibody responses against a malaria epitope. *Biomaterials* **33,** 6476–6484 (2012).

173. Rudra, J. S. *et al.* Modulating adaptive immune responses to peptide self-assemblies. *ACS Nano* **6,** 1557–1564 (2012).

174. Zhang, S., Holmes, T., Lockshin, C. & Rich, a. Spontaneous assembly of a self-complementary oligopeptide to form a stable macroscopic membrane. *Proc. Natl. Acad. Sci. U. S. A.* **90,** 3334–8 (1993).

175. Chen, P. Self-assembly of ionic-complementary peptides: A physicochemical viewpoint. *Colloids Surfaces A Physicochem. Eng. Asp.* **261,** 3–24 (2005).

176. Keyes-Baig, C., Duhamel, J., Fung, S. Y., Bezaire, J. & Chen, P. Self-assembling peptide as a potential carrier of hydrophobic compounds. *J. Am. Chem. Soc.* **126,** 7522–7532 (2004).

177. Fung, S. Y., Yang, H. & Chen, P. Formation of colloidal suspension of hydrophobic compounds with an amphiphilic self-assembling peptide. *Colloids Surfaces B Biointerfaces* **55,** 200–211 (2007).

178. Zheng, Y. *et al.* A peptide-based material platform for displaying antibodies to engage T cells. *Biomaterials* **32,** 249–257 (2011).

179. Deng, K. *et al.* Broad CTL response is required to clear latent HIV-1 due to dominance of escape mutations. *Nature* **517,** 381–385 (2015).

180. Lind, A. *et al.* Intradermal vaccination of HIV-infected patients with short HIV Gag p24-like peptides induces CD4 + and CD8 + T cell responses lasting more than seven years. *Scand. J. Infect. Dis.* **44,** 566–572 (2012).

181. Pollard, R. B. *et al.* Safety and efficacy of the peptide-based therapeutic vaccine for HIV-1, Vacc-4x: A phase 2 randomised, double-blind, placebo-controlled trial. *Lancet Infect. Dis.* **14,** 291–300 (2014).

182. Slingluff, C. L. *et al.* Immunologic and clinical outcomes of a randomized phase II trial of two multipeptide vaccines for melanoma in the adjuvant setting. *Clin. Cancer Res.* **13,** 6386–6395 (2007).

183. Vieillard, V., Le Grand, R., Dausset, J. & Debré, P. A vaccine strategy against AIDS: an HIV gp41 peptide immunization prevents NKp44L expression and CD4+ T cell depletion in SHIV-infected macaques. *Proc. Natl. Acad. Sci. U. S. A.* **105,** 2100–2104 (2008).

184. Slingluff, C. L. The present and Furture of peptide vaccines for cancers: single or multiple, long or short, alone or in combination? *Cancer J.* **17,** 343–350 (2011).

185. Lazaro, E. *et al.* Variable HIV peptide stability in human cytosol is critical to epitope presentation and immune escape. *J. Clin. Invest.* **121,** 2480–2492 (2011).

186. Tenzer, S. *et al.* Antigen processing influences HIV-specific cytotoxic T lymphocyte immunodominance. *Nat. Immunol.* **10,** 636–646 (2009).

187. Altunbas, A., Lee, S. J., Rajasekaran, S. a., Schneider, J. P. & Pochan, D. J. Encapsulation of curcumin in self-assembling peptide hydrogels as injectable drug delivery vehicles. *Biomaterials* **32,** 5906–5914 (2011).

188. Fatouros, D. G. *et al.* Lipid-like self-assembling peptide nanovesicles for drug delivery. *ACS Appl. Mater. Interfaces* **6,** 8184–8189 (2014).

189. Chesson, C. B. *et al.* Antigenic peptide nanofibers elicit adjuvant-free CD8+ T cell responses. *Vaccine* **32,** 1174–1180 (2014).

190. Lingnau, K., Riedl, K. & von Gabain, A. IC31 and IC30, novel types of vaccine adjuvant based on peptide delivery systems. *Expert Rev. Vaccines* **6,** 741–746 (2007).

191. Skwarczynski, M. & Toth, I. Peptide-based subunit nanovaccines. *Curr. Drug Deliv.* **8,** 282–289 (2011).

192. Rudra, J. S. *et al.* Modulating Adaptive Immune Response to Peptide Self-assemblies. *acsNano* **6,** 1557–1564 (2012).

193. Huang, Z.-H. *et al.* A totally synthetic, self-assembling, adjuvant-free MUC1 glycopeptide vaccine for cancer therapy. *J. Am. Chem. Soc.* **134,** 8730–3 (2012).

194. Schroeder, U. *et al.* Peptide nanoparticles serve as a powerful platform for the immunogenic display of poorly antigenic actin determinants. *J. Mol. Biol.* **386,** 1368–81 (2009).

195. Zhang, S. Fabrication of novel biomaterials through molecular self-assembly. *Nat. Biotechnol.* **21,** 1171–1178 (2003).

196. Kan-mitchell, J. *et al.* The HIV-1 HLA-A2-SLYNTVATL Is a Help-Independent CTL Epitope. *J. Immunol.* **172,** 5249–5261 (2004).

197. Gray, C. M. *et al.* Frequency of class I HLA-restricted anti-HIV CD8+ T cells in individuals receiving highly active antiretroviral therapy (HAART). *J. Immunol.* **162,** 1780–8 (1999).

198. Whelan, J. A. *et al.* Patterns of Immunodominance in HIV-1 – specific Cytotoxic T Lymphocyte Responses in Two Human Histocompatibility HLA-A * 0201 Are Influenced by Epitope Mutation. *J. Exp. Med* **185,** (1997).

199. Ogg, G. S. Quantitation of HIV-1-Specific Cytotoxic T Lymphocytes and Plasma Load of Viral RNA. *Science (80-.).* **279,** 2103–2106 (1998).

200. Hong, Y., Legge, R. L., Zhang, S. & Chen, P. Effect of amino acid sequence and pH on nanofiber formation of self-assembling peptides EAK16-II and EAK16-IV. *Biomacromolecules* **4,** 1433–42 (2003).

201. Saric, T. *et al.* Major Histocompatibility Complex Class I-presented Antigenic Peptides Are Degraded in Cytosolic Extracts Primarily by Thimet Oligopeptidase. *J. Biol. Chem.* **276,** 36474–36481 (2001).

202. Hong, Y., Pritzker, M. D., Legge, R. L. & Chen, P. Effect of NaCl and peptide concentration on the self-assembly of an ionic-complementary peptide EAK16-II. *Colloids Surf. B. Biointerfaces* **46,** 152–61 (2005).

203. York, I. a. *et al.* The Cytosolic Endopeptidase, Thimet Oligopeptidase, Destroys Antigenic Peptides and Limits the Extent of MHC Class I Antigen Presentation. *Immunity* **18,** 429–440 (2003).

204. Luft, T. *et al.* Exogenous peptides presented by transporter associated with antigen processing (TAP)-deficient and TAP-competent cells: intracellular loading and kinetics of presentation. *J. Immunol.* **167,** 2529–2537 (2001).

205. Ackerman, A. L. & Cresswell, P. Cellular mechanisms governing cross-presentation of exogenous antigens. *Nat. Immunol.* **5,** 678–684 (2004).

206. Marqusee, S. & Baldwin, R. L. Helix stabilization by Glu-...Lys+ salt bridges in short peptides of de novo design. *Proc. Natl. Acad. Sci. U. S. A.* **84,** 8898–8902 (1987).

207. Forood, B., Feliciano, E. J. & Nambiar, K. P. Stabilization of alpha-helical structures in short peptides via end capping. *Proc. Natl. Acad. Sci. U. S. A.* **90,** 838–842 (1993).

208. Parkhurst, M. R. *et al.* Improved induction of melanoma-reactive CTL with peptides from the melanoma antigen gp100 modified at HLA-A*0201-binding residues. *J. Immunol.* **157,** 2539–2548 (1996).

209. Wang, R.-F. & Wang, H. Y. Enhancement of antitumor immunity by prolonging antigen presentation on dendritic cells. *Nat. Biotechnol.* **20,** 149–154 (2002).

210. Van Montfoort, N. *et al.* Antigen storage compartments in mature dendritic cells facilitate prolonged cytotoxic T lymphocyte cross-priming capacity. *Proc. Natl. Acad. Sci. U. S. A.* **106,** 6730–5 (2009).

211. Huang, X., Fan, Z., Colleton, B. & Buchli, R. Processing and presentation of exogenous HLA class I peptides by dendritic cells from human immunodeficiency virus type 1-infected persons. *J. Virol.* **79,** 3052–3062 (2005).

212. Chen, J. *et al.* The use of self-adjuvanting nanofiber vaccines to elicit high-affinity B cell responses to peptide antigens without inflammation. *Biomaterials* **34,** 8776–85 (2013).

213. Ilyinskii, P. O. *et al.* Adjuvant-carrying synthetic vaccine particles augment the immune response to encapsulated antigen and exhibit strong local immune activation without inducing systemic cytokine release. *Vaccine* **32,** 2882–2895 (2014).

214. Lu, S., Wang, H., Sheng, Y., Liu, M. & Chen, P. Molecular binding of self-assembling peptide EAK16-II with anticancer agent EPT and its implication in cancer cell inhibition. *J. Control. Release* **160,** 33–40 (2012).

215. Fung, S. Y. *et al.* Self-Assembling Peptide as a Potential Carrier for Hydrophobic Anticancer Drug Ellipticine: Complexation, Release and In Vitro Delivery. *Adv. Funct. Mater.* **19,** 74–83 (2009).

216. Slavík, J. Anilinonaphthalene sulfonate as a probe of membrane composition and function. *Biochim. Biophys. Acta - Rev. Biomembr.* **694,** 1–25 (1982).

217. Osanai, H. A study of the Interaction of drugs with liposomes with Isothermal titration calorimetry. *J. Biophys. Chem.* **04,** 11–21 (2013).

218. Chodera, J. D. & Mobley, D. L. Entropy-enthalpy compensation: role and ramifications in biomolecular ligand recognition and design. *Annu. Rev. Biophys.* **42,** 121–42 (2013).

219. Schlosser, E. *et al.* TLR ligands and antigen need to be coencapsulated into the same biodegradable microsphere for the generation of potent cytotoxic T lymphocyte responses. *Vaccine* **26,** 1626–1637 (2008).

220. Wu, J., Huang, D. & Tyring, S. Resiquimod: a new immune response modifier with potential as a vaccine adjuvant for Th1 immune responses. *Antiviral Res.* **64,** 79–83 (2004).

221. Almeida, J. R. *et al.* Superior control of HIV-1 replication by CD8+ T cells is reflected by their avidity, polyfunctionality, and clonal turnover. *J. Exp. Med.* **204,** 2473–2485 (2007).

222. Lévy, Y. *et al.* Dendritic cell-based therapeutic vaccine elicits polyfunctional HIV-specific T-cell immunity associated with control of viral load. *Eur. J. Immunol.* 1–28 (2014). doi:10.1002/eji.201344433

223. Buisson, S. *et al.* Monocyte-derived dendritic cells from HIV type 1-infected individuals show reduced ability to stimulate T cells and have altered production of interleukin (IL)-12 and IL-10. *J. Infect. Dis.* **199,** 1862–1871 (2009).

224. Martinson, J. a. *et al.* Dendritic cells from HIV-1 infected individuals are less responsive to toll-like receptor (TLR) ligands. *Cell. Immunol.* **250,** 75–84 (2007).

225. Cardoso, E. C. *et al.* TLR7/TLR8 Activation Restores Defective Cytokine Secretion by Myeloid Dendritic Cells but Not by Plasmacytoid Dendritic Cells in HIV-Infected Pregnant Women and Newborns. *PLoS One* **8,** 1–11 (2013).

226. Kreutz, M., Tacken, P. J. & Figdor, C. G. Targeting dendritic cells - Why bother? *Blood* **121,** 2836–2844 (2013).

227. Knuschke, T. *et al.* Prophylactic and therapeutic vaccination with a nanoparticle-based peptide vaccine induces efficient protective immunity during acute and chronic retroviral infection. *Nanomedicine Nanotechnology, Biol. Med.* **10,** 1787–1798 (2014).

228. Fischer, S. *et al.* Concomitant delivery of a CTL-restricted peptide antigen and CpG ODN by PLGA microparticles induces cellular immune response. *J. Drug Target.* **17,** 652–661 (2009).

229. Engler, O. B. *et al.* A liposomal peptide vaccine inducing CD8+ T cells in HLA-A2.1 transgenic mice, which recognise human cells encoding hepatitis C virus (HCV) proteins. *Vaccine* **23,** 58–68 (2004).

230. Fung, S. Y. *et al.* Self-Assembling Peptide as a Potential Carrier for Hydrophobic Anticancer Drug Ellipticine: Complexation, Release and In Vitro Delivery. *Adv. Funct. Mater.* **19,** 74–83 (2009).

231. Zhao, B., Rong, Y.-Z., Huang, X.-H. & Shen, J.-S. Experimental and theoretical study on the structure and electronic spectra of imiquimod and its synthetic intermediates. *Bioorg. Med. Chem. Lett.* **17,** 4942–4946 (2007).

232. Tanji, H. Structural Reorganization of the Toll-like Receptor 8 Dimer Induced by agonistic ligands. *Science (80-.).* **339,** 1426–1430 (2013).

233. Gentile, F. *et al.* Structure Based Modeling of Small Molecules Binding to the TLR7 by Atomistic Level Simulations. *Molecules* **20,** 8316–8340 (2015).

234. Bevan, M. J. HELPING THE CD8 + T-CELL RESPONSE. *Nat. Rev. Immunol.* **4,** 595 (2004).

235. Schnare, M. *et al.* Toll-like receptors control activation of adaptive immune responses. *Nat. Immunol.* **2,** 947–950 (2001).

236. Rahemtulla, a *et al.* Normal development and function of CD8+ cells but markedly decreased helper cell activity in mice lacking CD4. *Nature* **353,** 180–184 (1991).

237. Novy, P., Quigley, M., Huang, X. & Yang, Y. CD4 T cells are required for CD8 T cell survival during both primary and memory recall responses. *J. Immunol.* **179,** 8243–8251 (2007).

238. Nakanishi, Y., Lu, B., Gerard, C. & Iwasaki, A. CD8(+) T lymphocyte mobilization to virus-infected tissue requires CD4(+) T-cell help. *Nature* **462,** 510–513 (2009).

239. Wang, J.-C. E. & Livingstone, A. M. Cutting edge: CD4+ T cell help can be essential for primary CD8+ T cell responses in vivo. *J. Immunol.* **171,** 6339–6343 (2003).

240. Chen, P., Lahooti, S., Policova, Z., Cabrerizo-Vílchez, M. a. & Neumann, a. W. Concentration dependence of the film pressure of human serum albumin at the water/decane interface. *Colloids Surfaces B Biointerfaces* **6,** 279–289 (1996).

241. Rettig, L. *et al.* Particle size and activation threshold: A new dimension of danger signaling. *Blood* **115,** 4533–4541 (2010).

242. Bachmann, M. F. & Jennings, G. T. Vaccine delivery: a matter of size, geometry, kinetics and molecular patterns. *Nat. Rev. Immunol.* **10,** 787–796 (2010).

243. Diamond, M. S. *et al.* Type I interferon is selectively required by dendritic cells for immune rejection of tumors. *J. Exp. Med.* **208,** 1989–2003 (2011).

244. Hines, J. D., Thomas, R. K., Garrett, P. R., Rennie, G. K. & Penfold, J. Investigation of Mixing in Binary Surfactant Solutions by Surface Tension and Neutron Reflection: Anionic/Nonionic and Zwitterionic/Nonionic Mixtures. *J. Phys. Chem. B* **101,** 9215–9223 (1997).

245. Behrens, G. *et al.* Helper T cells, dendritic cells and CTL Immunity. *Immunol. Cell Biol.* **82,** 84–90 (2004).

246. Ahlers, J. D. & Belyakov, I. M. Memories that last forever: Strategies for optimizing vaccine T-cell memory. *Blood* **115,** 1678–1689 (2010).

247. Baaten, B. J. G. *et al.* CD44 Regulates Survival and Memory Development in Th1 Cells. *Immunity* **32,** 104–115 (2010).

248. Nembrini, C. *et al.* Nanoparticle conjugation of antigen enhances cytotoxic T-cell responses in pulmonary vaccination. *Proc. Natl. Acad. Sci.* **108,** E989–E997 (2011).

249. Kumar, S., Anselmo, A. C., Banerjee, A., Zakrewsky, M. & Mitragotri, S. Shape and size-dependent immune response to antigen-carrying nanoparticles. *J. Control. Release* **220,** 141–148 (2015).

250. Foged, C., Brodin, B., Frokjaer, S. & Sundblad, A. Particle size and surface charge affect particle uptake by human dendritic cells in an in vitro model. *Int. J. Pharm.* **298,** 315–22 (2005).

251. Airen, X. A physical model for the size-dependent cellular uptake of nanoparticles modified with cationic surfactants. *Int. J. Nanomedicine* **7,** 3547–3554 (2012).

252. Stano, A., Nembrini, C., Swartz, M. a, Hubbell, J. a & Simeoni, E. Nanoparticle size influences the magnitude and quality of mucosal immune responses after intranasal immunization. *Vaccine* 6–11 (2012). doi:10.1016/j.vaccine.2012.10.050

253. Tran, K. K. & Shen, H. The role of phagosomal pH on the size-dependent efficiency of cross-presentation by dendritic cells. *Biomaterials* **30,** 1356–62 (2009).

254. Chono, S., Tanino, T., Seki, T. & Morimoto, K. Uptake characteristics of liposomes by rat alveolar macrophages: influence of particle size and surface mannose modification. *J. Pharm. Pharmacol.* **59,** 75–80 (2007).

255. Brewer, J. M., Pollock, K. G. J., Tetley, L. & Russell, D. G. Vesicle Size Infulences the Trafficking, Processing, and Presentation of Antigens in Lipid Vesicles. *J. Immunol.* (2012).

256. Heegaard, P. M. H., Boas, U. & Sorensen, N. S. Dendrimers for vaccine and immunostimulatory uses. A review. *Bioconjug. Chem.* **21,** 405–418 (2010).

257. Diez-Rivero, C. M., Lafuente, E. M. & Reche, P. a. Computational analysis and modeling of cleavage by the immunoproteasome and the constitutive proteasome. *BMC Bioinformatics* **11,** 479 (2010).

258. Arunachalam, B., Phan, U. T., Geuze, H. J. & Cresswell, P. Enzymatic reduction of disulfide bonds in lysosomes: characterization of a gamma-interferon-inducible lysosomal thiol reductase (GILT). *Proc. Natl. Acad. Sci. U. S. A.* **97,** 745–750 (2000).

259. Joshi, M. D., Unger, W. J., Storm, G., Van Kooyk, Y. & Mastrobattista, E. Targeting tumor antigens to dendritic cells using particulate carriers. *J. Control. Release* **161,** 25–37 (2012).